TRANSPORTATION RESEARCH

RECORD

No. 1334

Planning, Administration, and Environment

Maintenance of Pavements, Lane Markings, and Roadsides

A peer-reviewed publication of the Transportation Research Board

TRANSPORTATION RESEARCH BOARD
NATIONAL RESEARCH COUNCIL
WASHINGTON, D.C. 1992

Transportation Research Record 1334
Price: $17.00

Subscriber Category
I planning, administration, and environment

TRB Publications Staff
Director of Publications: Nancy A. Ackerman
Senior Editor: Naomi C. Kassabian
Associate Editor: Alison G. Tobias
Assistant Editors: Luanne Crayton, Norman Solomon
Production Coordinator: Karen W. McClain
Office Manager: Phyllis D. Barber
Production Assistant: Betty L. Hawkins

Printed in the United States of America

Library of Congress Cataloging-in-Publication Data
National Research Council. Transportation Research Board.

Maintenance of pavements and roadsides.
p. cm.—(Transportation research record ISSN 0361-1981 ; no. 1334)
"A peer-reviewed publication of the Transportation Research Board."
ISBN 0-309-05202-5
1. Pavements—Maintenance and repair. 2. Roadside improvement—maintenance and repair. I. National Research Council (U.S.). Transportation Research Board. II. Series: Transportation research record ; 1334.
TE7.H5 no. 1334
[TE220]
388 s—dc20
[625.8] 92-21953
CIP

Sponsorship of Transportation Research Record 1334

GROUP 3—OPERATION, SAFETY, AND MAINTENANCE OF TRANSPORTATION FACILITIES
Chairman: H. Douglas Robertson, University of North Carolina-Charlotte

Maintenance Section
Chairman: Jimmy D. Lee, North Carolina Department of Transportation

Committee on Pavement Maintenance
Chairman: Roger E. Smith, Texas A&M University
Thomas L. Boswell, Kathryn A. Cation, James G. Chehovits, Barry H. Dunn, Robert P. Elliott, Chuck A. Gemayel, David Gieber, Jim W. Hall, Jr., Claus C. Kuehl, Jay K. Lindly, James B. Martin, James S. Moulthrop, Thomas B. Nelson, David E. Newcomb, Frazier Parker, Jr., Michel Ray, Michael M. Ryan, S. C. Shah, Mohamed Y. Shahin, Scott Shuler, James B. Sorenson, Shelly M. Stoffels, Paul E. Theberge

Committee on Roadside Maintenance
Chairman: Wayne G. McCully, Texas A&M University
Dorothy L. Andres, Robert L. Berger, Lonnie M. Cargill, James F. Condron, Joseph M. Di Paola, Ray Dickens, Edward C. Dixon, Dan Flowers, Kurt D. Getsinger, Roy R. Johnson, William D. Johnson, S. Joseph Lesley, Richard C. Moffett, D. James Morre, John E. Rinard, Roy L. Smith, Ronald G. Stahl, Robert E. Tatman, Clifton R. Taylor, Carl B. Wells, Bernard G. Williams, William E. Zitterich

Committee on Coatings, Signing, and Marking Materials
Chairman: Frank D. Shepard, Virginia Transportation Research Council
Secretary: Leo C. Stevens, Jr., Massachusetts Department of Public Works
Robert W. Attaway, Francis J. Bashore, Brian H. Chollar, Robert L. Davidson, Robert D. Finer, John Jewett Henry, Blaine F. Himmelman, James S. Kalchbrenner, Stella L. Marusin, Thomas J. Nettleton, Justin J. Rennilson, Henry A. Ross, Philip O. Russell, J. R. Ryan, Anne-Marie Serres, Lawrence Q. Smith, Martin A. Smith, Robert C. Vanstrum, Raymond Warness, Charles M. Winchester

Committee on Sealants and Fillers for Joints and Cracks
Chairman: John W. Bugler, New York State Department of Transportation
Secretary: Chris Siebel, Jr., Consulting Engineer, Norwood, New Jersey
Michael C. Belangie, Brian T. Bock, Byron B. Brown, Martin P. Burke, Jr., Robert A. Cameron, Robert A. Eaton, Frank D. Gaus, James R. Golden, Donald A. Kaliin, Starr D. Kohn, Kenneth E. Marks, Issam Minkarah, Roger C. Olson, William G. Prince, Guy S. Puccio, Michael W. Roshek, S. C. Shah, Stephen F. Shober, Sherwood Spells, Robert F. Steffes, Ronald J. Watson

Frank Lisle, Transportation Research Board staff

Sponsorship is indicated by a footnote at the end of each paper.The organizational units, officers, and members are as of December 31, 1991.

Transportation Research Record 1334

Contents

Foreword

The introduction of new materials and methods of using them in the maintenance of transportation systems are increasing at an accelerated rate. Selecting the best product and application technique is critical to achieving the highest maintenance level-of-service with the available resources. The eight papers in this Record provide information intended to assist engineers in improving the effectiveness of pavement, lane marking, and roadside maintenance.

The six papers on pavement maintenance provide information on efforts to evaluate and correct concrete slab stepping on runways at the Pearson International Airport in Canada; the formulation and placement of very thin (20 to 25 mm) and ultrathin (10 to 15 mm) asphalt wearing surfaces on French roads; the results of a survey of state DOTs on the use of blade-patching; definitions of pavement maintenance and distress precursors for pavement maintenance measurements developed under the Strategic Highway Research Program; an analysis using Fourier transform infrared spectroscopy to evaluate two-component joint sealant materials; and an analysis using the finite element method to describe the interaction between sealants and joint and crack geometry. The next paper describes a benefit-cost analysis of thermoplastics and paints used in lane markings, and the last paper provides a summary of the benefits and guidelines for establishing and managing roadside wildflower meadows.

Evaluation and Treatment of Slab Stepping on a Major Runway

DAVID K. HEIN, MICHAEL H. MACKAY, AND JOHN J. EMERY

Severe slab-stepping (slab-faulting) problems have been observed during the past 5 years in the takeoff areas of Runway 06R/24L, the main runway at Lester B. Pearson International Airport in Toronto. The magnitude of this slab stepping of the plain portland cement concrete pavement is such that complaints about roughness were being received and airport management was concerned that the functional service life of this critical facility was being reduced. A comprehensive field evaluation of the slab stepping was undertaken to determine its cause, extent, and severity to develop practical rehabilitation alternatives for Transport Canada to consider. This field program included the treatment, on a trial basis, of a short section of the runway using diamond grinding equipment to remove the slab stepping. In 1989 the trial grinding section was resurveyed and no significant slab stepping was observed. In 1991 a contract was let to complete full-scale precision diamond grinding of the concrete in the takeoff areas of Runways 06R and 24L and on Taxiways Bravo and Echo. Postgrinding precision profiling was completed, and pavement roughness was found to be well within commonly accepted standards.

The pavements of Runway 06R/24L at Lester B. Pearson International Airport in Toronto, Canada, were constructed in 1960 using plain portland cement concrete over untreated granular base. The 31-year-old pavement has performed satisfactorily, requiring only routine repairs such as localized slab replacement, joint sealing, and maintenance due to the cumulative effects of age and repeated heavy aircraft loadings. However, in the early 1980s the runway developed a slab-stepping (slab-faulting) problem in the areas of the runway that are subjected to repeated applications of moving, fully loaded heavy aircraft during takeoff (and that generally coincide with the "touchdown" areas of the runway). This slab-stepping problem had progressed to the stage at which most of the slabs in the traveled center portion of the Runway 06R/24L touchdown areas (each about 30.5 m wide and 300 m long) had stepped 6 to 12 mm. Some slabs had stepped as much as 25 to 38 mm; similar slab stepping was also observed on the 24L holding area and adjoining taxiways.

From an operational point of view, Runway 06R/24L is extremely critical to the airport. As the only CAT 2 runway with pavement-inset centerline lighting at that time, Runway 06R/24L was the primary runway at Canada's busiest airport. At about 2900 m, it is the shortest of the three main runways, and its surface has been transversely grooved to improve its skid resistance. The airport runway configuration is shown in Figure 1.

John Emery Geotechnical Engineering Ltd., 52 Ashwarren Road, Downsview, Ontario M3J 1Z5 Canada.

At the request of Transport Canada, an investigation of the runway slab-stepping problem was completed during summer 1987 by John Emery Geotechnical Engineering Limited.

RUNWAY CONSTRUCTION HISTORY AND TRAFFIC ANALYSIS

Transport Canada provided construction history and traffic data for Runway 06R/24L for use during the investigation. This documentation included original construction records (contract documents and construction drawings), pavement construction history sheets, pavement condition survey sheets, skid resistance test results, and aircraft movement data for 1982 through 1986.

The pavement was originally constructed between 1960 and 1962 as 355 mm of plain portland cement concrete (no specified nominal compressive or flexural strength details available) over 150 mm of crushed gravel or crushed stone base and 305 mm of granular subbase. The pavement condition survey data indicated that the runway pavements exhibited moderate corner cracking, slab cracking, and joint sealant failure, and minor edge cracking and joint spalling.

The review and analysis of the aircraft movement records for 1982 through 1986 were particularly relevant to the study. The Runway 06R/24L aircraft movement data are summarized in Table 1. Aircraft movements on Runway 06R have increased by almost 90 percent; movements on Runway 24L have increased by 40 percent (Figure 2). The most significant increase in aircraft movements also occurs in the heavier weight categories—particularly, 90,000 to 136,000 kg. The Runway 24L takeoff area, which also exhibits the most severe slab-stepping problem, has been subjected to the greatest number of and largest increase in heavy aircraft loads. This finding strongly supported the opinion that the stepping problem was related to repetitions of heavy aircraft loads during takeoff and not to impact loads of much-lighter landing aircraft.

FIELD INVESTIGATION PROGRAM

To determine the probable cause of the slab-stepping problem and to assess its overall significance in terms of runway serviceability and rehabilitation, a comprehensive field investigation program was undertaken. The general pavement, subsoil, and groundwater conditions for Runway 06R/24L were determined, and detailed pavement evaluation and geotechnical work was completed in the stepped takeoff areas of the runway and in a small section in the relatively distress-free central portion.

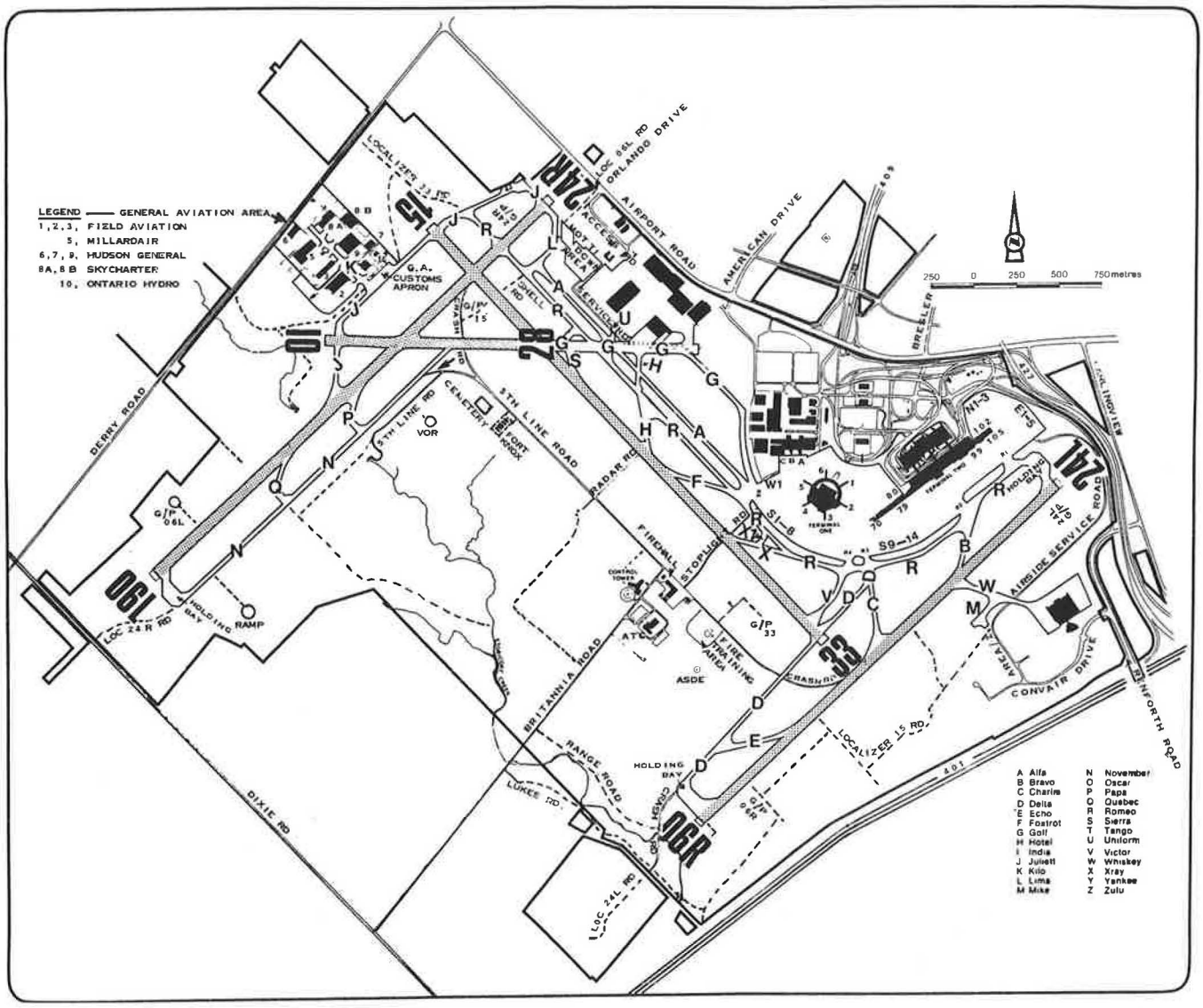

FIGURE 1 Base map of Lester B. Pearson International Airport, 1985.

TABLE 1 RUNWAY TRAFFIC DATA, 1982–1986

Weight Category	Number of Aircraft Movements by Runway and Year									
	1986		1985		1984*		1983		1982	
(kg)	24L	06R	24L	06R	24L	06R	24L	06R	24L	06R
0 to 2000	152	222	208	248	132	202	134	273	130	225
2001 to 4000	1086	1358	1254	1339	983	1198	991	1550	848	1274
4001 to 5670	3574	3564	4269	3098	2519	2210	1745	1984	1241	1174
5671 to 9000	135	271	159	258	209	198	203	356	389	437
9001 to 18000	313	698	211	465	168	274	244	396	214	369
18001 to 35000	4534	3923	4805	2780	2258	1624	1930	1510	2216	1302
35001 to 70000	23195	18414	23444	12800	19321	12515	16847	12487	16748	9365
70001 to 90000	13676	10442	14321	7754	13558	8789	12190	9166	11801	6427
90001 to 136000	4132	3425	3648	1976	2155	1284	949	586	4	2
136000 plus	9994	7051	10639	5272	9692	6059	8976	6034	9916	5582
Total Annual Movements	60791	49368	62955	35990	50995	37963	44209	34342	43509	26157

* Estimated average (one month of data missing)

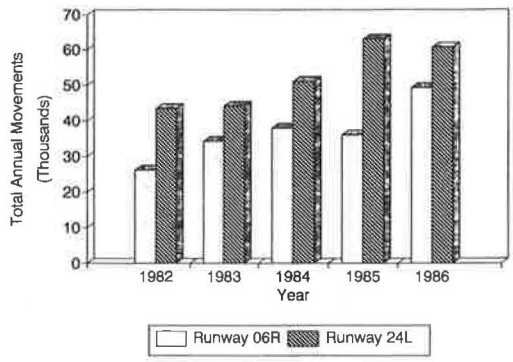

FIGURE 2 Runway traffic data.

The field investigation involved

1. Detailed visual surveying of pavement condition (distress survey);
2. Precise surveying using a precision level and Invar staves to determine the vertical slab orientation;
3. Geotechnical investigation to confirm runway soil and groundwater conditions;
4. Plate load testing of the runway subbase and subgrade;
5. Laboratory testing of the runway slab concrete (flexural strength of concrete prisms and compressive strength of concrete cores);
6. Load transfer determination using the Dynatest falling weight deflectometer (FWD); and
7. Slab deflection testing using a 50-tonne rubber-tired proof roller.

Site Geotechnical Conditions

The geotechnical investigation consisted of 15 boreholes adjacent to the runway and 3 probeholes within repair areas. Subsoil samples were recovered at regular intervals for classification and laboratory testing, and standpipes were installed to allow measurement of the groundwater level.

The principal soil type encountered was dense to very dense sand and silt till. Some compact to dense silty clay fill and sand fill overlying the till (up to 1.5 m deep) were also proven. Groundwater observations confirmed that the groundwater is generally located at depths of 3.0 m at the south end of the runway and 1.5 m at the north end.

To assess the subbase and subgrade support capabilities, nonrepetitive static plate load testing was completed in accordance with Transport Canada procedures. Tests were completed at the top of the granular base course (560 mm of granular base and subbase overlying subgrade at this location) and 150 mm above the subgrade. The testing at the top of the granular base course confirmed a subgrade bearing strength value of 518 kN; testing near the top of subgrade confirmed a bearing strength value of 148 kN.

Pavement Condition

The pavement condition survey was completed in accordance with Transport Canada distress descriptions, supplemented by the American Concrete Institute's *Guide For Making a Distress Survey of Concrete Pavements* and U.S. Army Corps of Engineers' PAVER distress guides. The results of the survey indicated that, with the exception of the slab-stepping problem, the concrete pavement was in good condition. Low-severity pop-outs and joint spalling were observed, as were occasional slab cracking and corner breaks.

The precise surveying confirmed that the joint stepping was confined almost totally to the center two slabs (one on either side of the centerline) for the length of each takeoff area. That of the 24L takeoff area appeared to be the most severe, with stepping on the order of 12 to 15 mm. The stepping had occurred so that the approach side of the joint was higher than the leave side. Stepping of about 10 mm was observed in the 06R takeoff area. The stepping in each takeoff area was noted to end abruptly; virtually no stepping was observed in the central runway area.

Concrete materials testing consisted of flexural strength testing of beams cut from the existing runway concrete slabs and compressive strength testing of 150-mm-diameter cores. The flexural strength of the concrete was determined to be about 6.95 MPa and the compressive strength was determined to be 51.3 MPa.

FWD Testing

To determine rapidly the load transfer between concrete slabs in various thermal curl states and indicate the presence of voids or soft spots for additional testing using a heavy rubber-tired proof roller, deflection testing was undertaken using the Dynatest 8000 FWD. The slab and joint testing was completed under different time and temperature conditions (early morning, very cool; midday, warm; and late evening, cool) to monitor the potential effects of slab curl and thermal expansion and contraction joint "lock up" on load transfer and voids determination. Temperatures ranged from 4°C to 21°C in the most severe testing cycle.

The FWD was used to conduct several tests. Eleven tests were taken per slab to assess representative joint-slab combinations selected on the basis of the pavement condition and precise survey data. The typical testing sequence for each joint-slab combination is illustrated in Figure 3.

Three load levels were employed: 40 kN, 75 kN, and 105 kN. The FWD velocity transducers were positioned such that one was on either side of the joint at distances of 200 and 300

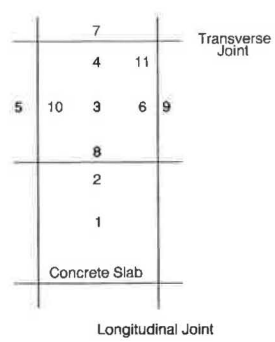

FIGURE 3 FWD testing pattern.

mm from the point of load application. Load transfer and voids detection were indicated using a simple procedure developed for concrete pavements by Shahin et al. (*1*).

The FWD test results for 12 selected joint-slab combinations are given in Table 2. These data indicate that the amount of load transfer across the joints was clearly much less when the slabs were cool because of upward slab curl and unlocking of the joints. In the worst case, the load transfer over a 12-hr period ranged from 2 percent ("unlocked") to 79 percent ("locked"). Slab-rocking potential is indicated by the calculated deflection ratios. As anticipated, there was a very strong indication of rocking in some of the slabs coinciding with the early-morning upward-curl period. However, these same slabs showed virtually no movement once the joints had locked. This strongly suggested not that significant voids were present beneath the slabs but that the "apparent" voids were associated with thermal gradient upward curling of the slabs.

Slab Deflection Testing

Though the FWD testing indicated the load transfer between concrete slabs in various thermal curl states, the relative mass of the concrete slab panels was quite large compared with the maximum FWD loadings (105 kN). Therefore, to replicate the magnitude of load of the heavy loaded aircraft, it was necessary to proof roll selected runway slab panels using a 50-tonne rubber-tired loading cart (a high-capacity FWD has subsequently been developed that simulates an aircraft wheel loading of up to 240 kN). The concrete slab panels were selected on the basis of the FWD testing and degree of slab stepping. The rubber-tired loading cart was pulled across the concrete panel at about 10 m/min using a grader. The slab deflections were continuously measured at the joint using dial gauges attached to a deflection-monitoring beam. The 9.1-m-long beam was anchored outside the influence of the loading cart. The reference frame was rigid enough to be cantilevered across the full width of the slab immediately adjacent to that being tested. Six gauges were located at the joint for each pass. The selected slabs were also measured at different time and temperature periods to monitor the effects of various thermal curl states and to differentiate between slab rocking due to thermal gradient upward curl and voids or soft spots beneath the slabs.

A typical plot of slab deflection versus the loading cart location is shown in Figure 4. Examination of the test results revealed that as the grader moved onto the slab, the leading edge of the slab deflected, causing the gauges at the trailing

TABLE 2 SUMMARY OF FWD LOAD TRANSFER AND VOIDS DETECTION ANALYSIS RESULTS

Slab Number	Time of Test	Temperature Ambient °C	Temperature Surface °C	Load Transfer (%) Approach Slab Approach Joint	Approach Slab Leave Joint	Leave Slab Approach Joint	Leave Slab Leave Joint	Deflection Ratio d centre/ d midslab	Deflection Ratio d corner/ d midslab
32/3	5:17	18	18	95.9	90.1	96.5	85.9	2.4	8.0
	11:06	25	26	87.8	87.0	81.5	89.3	1.5	3.5
	20:55	18	22	96.2	97.8	93.5	96.1	1.5	3.7
44/5	5:35	18	18	6.2	4.9	10.4	5.6	3.5	8.9
	11:26	25	26	19.8	39.8	18.5	24.4	2.5	3.6
	21:10	18	22	68.2	83.2	54.0	65.2	3.0	8.0
50/4	6:01	18	18	3.6	2.0	11.0	6.0	3.4	5.4
	11:44	25	26	19.1	25.3	28.8	41.3	2.3	2.4
	21:25	18	22	62.2	79.4	74.0	83.6	2.7	4.7
55/6	6:17	18	18	97.0	96.1	95.7	98.0	1.6	4.8
	12:05	25	26	93.8	95.1	93.9	97.3	1.2	2.3
	00:05	15	18	72.0	91.5	95.8	95.0	1.2	3.6
75/5	6:33	18	18	22.2	28.2	15.8	18.8	3.1	4.4
	12:54	29	33	62.1	82.2	83.5	85.4	1.3	1.9
	00:23	15	18	72.0	91.5	92.3	95.0	2.0	-
85/4	6:50	18	18	16.9	10.6	14.7	9.4	3.6	7.1
	13:13	29	33	40.6	49.0	77.8	84.1	1.5	2.5
	00:39	15	18	53.2	56.3	59.1	63.9	3.4	-
100/5	7:39	18	18	25.0	14.9	12.8	13.8	2.9	5.3
	13:57	29	33	90.1	78.7	89.9	89.1	1.2	1.3
	00:56	15	18	99.3	93.4	97.7	95.6	1.9	-
110/4	8:00	26	24	17.0	20.1	28.0	31.0	3.8	5.1
	14:15	26	32	97.2	94.4	91.0	89.7	2.9	5.3
	1:14	15	18	98.3	94.2	97.2	96.3	2.7	4.4
226/5	9:48	26	24	24.5	28.1	14.9	18.2	2.1	2.7
	15:53	29	34	37.3	40.3	24.8	32.5	2.2	1.7
	00:28	12	15	26.8	16.9	12.9	28.1	5.4	8.3
234/4	9:28	27	25	12.8	14.5	12.5	13.8	3.4	4.4
	15:38	29	34	21.6	23.6	19.0	22.1	2.5	2.2
	00:13	12	15	4.1	5.8	8.2	5.5	6.5	11.0
430/3	9:05	27	25	95.4	100.0	86.5	88.2	1.4	3.3
	15:18	26	32	96.0	95.4	96.0	94.8	1.0	1.4
	1:51	10	16	94.2	98.0	96.1	93.4	1.4	3.2
440/6	8:24	26	24	94.2	94.9	96.9	94.9	1.5	4.6
	14:42	26	32	97.9	96.7	95.0	96.3	1.0	1.0
	1:35	10	16	97.7	92.8	97.8	97.3	1.4	4.5

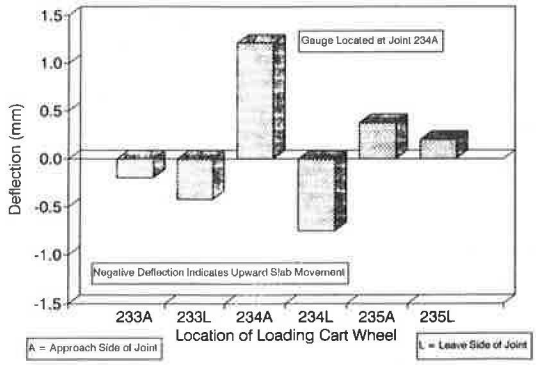

FIGURE 4 Joint deflection profile.

edge of the slab to show an upward movement of the slab. As the loading cart moved across the slab, the deflection became positive, indicating a downward movement of the slab at the joint being monitored. Once the loading cart crossed the joint, there was an abrupt downward movement of the next slab and the first slab returned to its original position. Measurements taken at other temperature conditions indicated that the slab movement (rocking) only took place when the slabs were in an upward-curl position. The loading cart analyses and findings compared quite favorably with theoretical calculations of thermally induced curl for the concrete slab dimensions and temperature gradients.

GRINDING TRIAL EVALUATION

To evaluate possible treatment measures for the slab-stepping problems, Transport Canada also required an evaluation of specialized diamond grinding equipment to restore the runway pavement to a relatively smooth condition. This trial consisted of grinding 14 slab panels (2 panels wide for a distance of 7 panels) using a Target PRM 3800 grinder obtained from Central Atlantic Contractors Inc. of Maryland (Figure 5). This equipment has a 1.0-m-wide grinding head with 60 diamond blades per 300 mm. The resulting concrete surface texture resembles corduroy, and the equipment is capable of very finely controlling the vertical depth of cut (Figure 6).

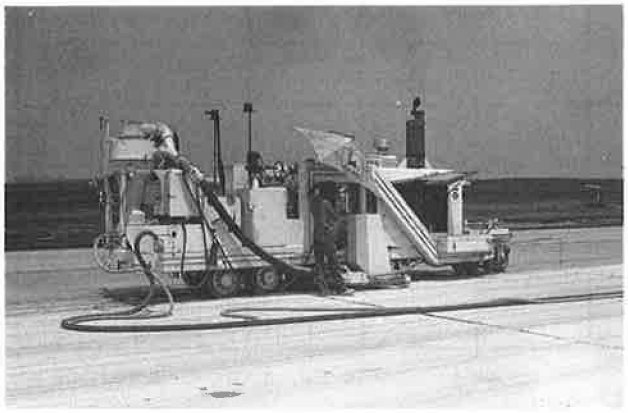

FIGURE 5 Target PRM grinder (Central Atlantic Contractors Inc.).

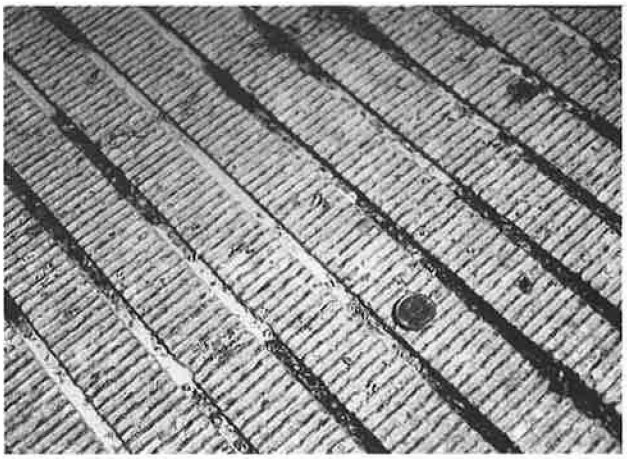

FIGURE 6 Concrete pavement surface texture after grinding.

The longitudinal profile before and after diamond grinding is shown in Figure 7. Clearly, the diamond grinding operation was able to satisfactorily remove the slab stepping and restore the runway pavement to a smooth condition.

On the basis of the results of the postgrinding evaluation, the precision grinding equipment was deemed to have the necessary longitudinal control to remove the stepping problem and produce a relatively flat surface. The grinder was observed to be able to remove only the high spots and neatly feather over the lower areas of the slab. Because of the relatively narrow width of the grinding head, transverse control is somewhat more difficult, relying heavily on the operator.

The trial grinding section was resurveyed immediately after grinding and again after 2 years. Immediately after grinding, the average slab stepping was calculated to be about 1 mm; after 2 years of service, it was about 2 mm. The long-term permanence of this repair technique was not confirmed, but because of the positive trial area performance, it was recommended that the takeoff areas of Runway 06R/24L be diamond-ground using this type of equipment or its equivalent. The apparent absence of significant voids suggested that slab stabilization was not necessary.

FULL-SCALE PAVEMENT GRINDING

In May 1991 full-scale pavement grinding was completed in the takeoff areas of Runway 06R/24L and on Taxiways Bravo

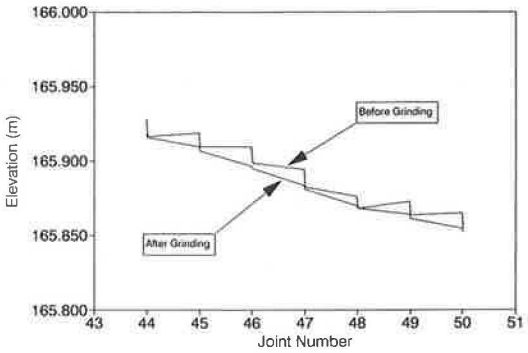

FIGURE 7 Pavement profile: trial grinding area.

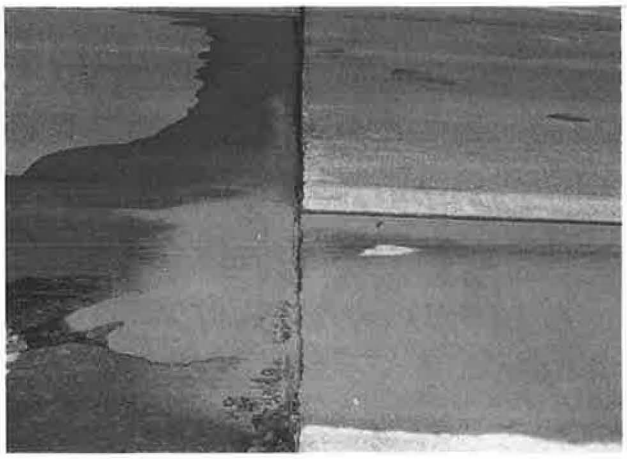

FIGURE 8 Grinding completed on Taxiway Echo.

and Echo. The precision grinding was completed by two Target PRM 3800 grinding machines subcontracted from a U.S. firm. The grinding was completed at about 200 m^2/hr/machine. To restore the pavement profile, up to 15 mm of the concrete was removed (Figure 8). Note the magnitude of the stepping and depth of grinding. Upon completion of the grinding, the transverse grooving of the pavement was reinstated and all of the slab joints were resealed.

To measure and record the actual pavement profile for acceptance purposes after longitudinal grinding was completed, the finished profile was accurately measured using a Digital Incremental Profiler (*3*). The profiler is a relative elevation device that collects pavement profile elevation measurements at 300-mm increments. The data are stored by an on-board computer for later analysis.

The pavement profile was analyzed using the Runway Roughness Analysis Program (RRAP) (*4*). A plot of the postgrinding Runway 24L profile is shown in Figure 9. From the figure, it can be seen that the pavement profile after full-scale diamond grinding is relatively smooth over its entire length.

The pavement surface profiles were processed by the RRAP program to determine several pavement roughness statistics including surface profile/traveling straight edge (SP/TSE), root mean square vertical acceleration (RMSVA), and international roughness index (IRI). The SP/TSE analysis methodology is one of the simplest methods of measuring profile roughness and is the current Transport Canada procedure. The straight edge is basically a simply supported beam with a surface contact sensor at mid-length. The SP/TSE analysis simulates the movement of the straight edge in 300-mm increments with the deviation from the midpoint of the straight edge calculated with each movement. A typical profile detail and deviation plot for a 100-m section on Runway 24L are shown in Figure 10. The relatively straight line on the plots is the actual profile, and the jagged line is the profile deviation from a 3-m straight edge. The highest profile deviation measured is at the slab joints (approximately every 6 m) and measures about 1.0 to 1.5 mm. Transport Canada Publication AK-68-33-199 (*2*) defines the critical deviation (above which corrective action should be taken) as equal to 0.9 times the square root of the straight edge length (SEL) where the SEL is measured in meters and the critical deviation is measured in centimeters. For a 3-m straight edge, the critical deviation is 15.6 mm. The summary roughness statistic for the SP/TSE analysis given in Table 3 is calculated as the sum of absolute deviations per unit length.

RMSVA is defined as the root mean square difference between adjacent profile slopes. A report for the Transportation Development Center and Airports Authority Group Transport Canada (*5*) recommended using the RMSVA statistic to correlate with the current Transport Canada Riding Comfort Index (RCI) statistic. Using the RMSVA, the corresponding RCI values for the postgrinding pavements would be 7 to 8.

The IRI statistic is defined as the average rectified slope of a profile being traversed by a particular reference vehicle at

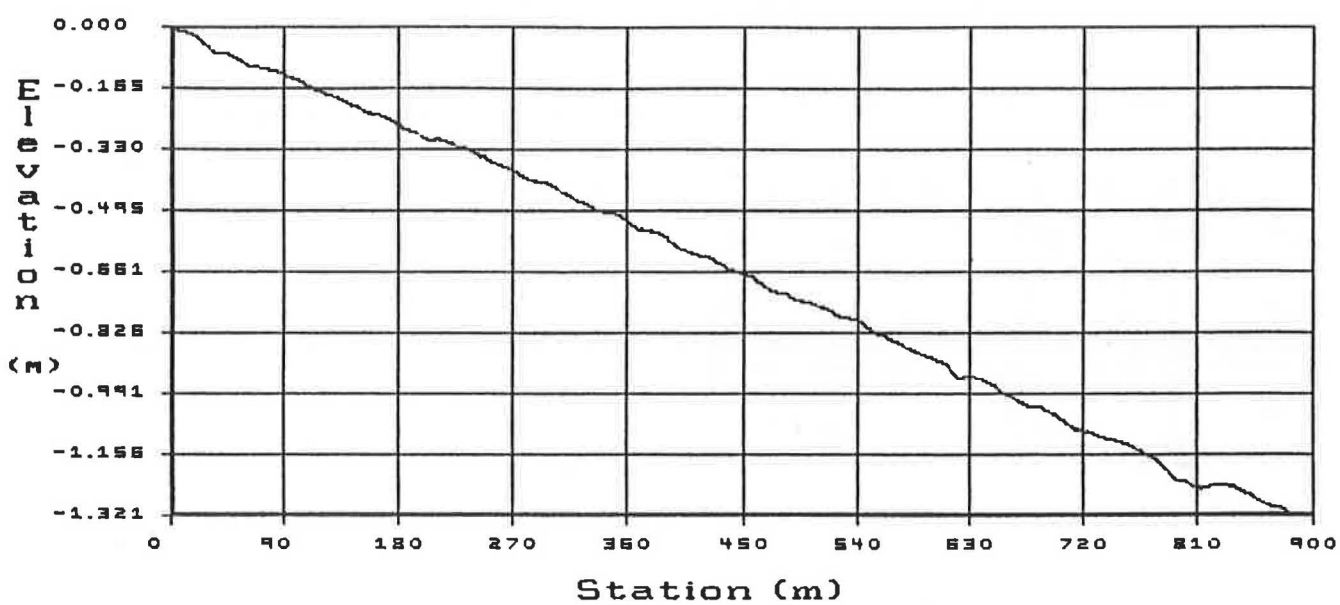

FIGURE 9 Pavement profile after grinding Runway 24L (offset: 3 mL).

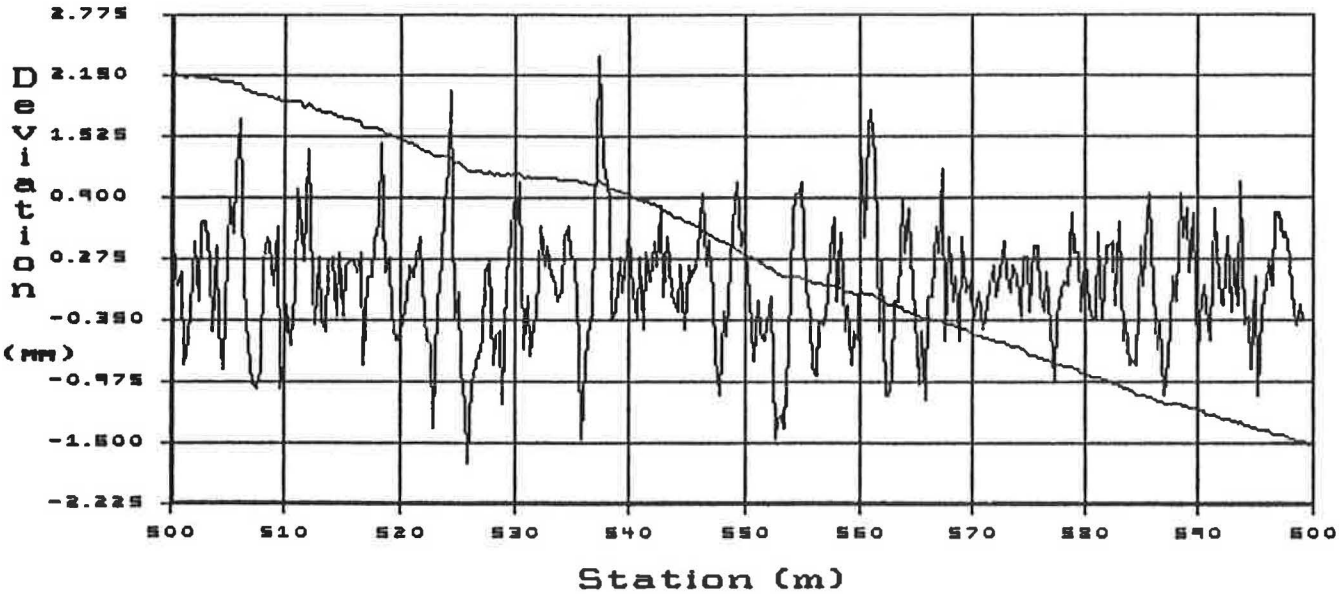

FIGURE 10 Pavement profile detail after grinding showing profile plot and deviation from a 3-m straight edge (critical deviation = 15.59 mm).

80 km/hr. For the facilities analyzed, the IRI values range from 0.93 to 1.3 mm/m. The World Bank (*6*) recommends a maximum IRI value of 2.0 mm/m for runways.

CONCLUDING COMMENTS

The postgrinding profile determination and roughness analysis confirmed the success of the full-scale grinding operation. A relatively smooth pavement surface has been restored (see Figure 11). To assess the long-term effectiveness of precision grinding as a maintenance alternative, it has been recommended that the pavements be resurveyed every 2 to 3 years.

It cannot be overemphasized that precision grinding should be considered only in instances in which the pavement is structurally adequate. Structural testing of the pavement using a high-capacity FWD or its equivalent is strongly recommended. Grinding of structurally inadequate pavements will result in further reduced structural capacity and more rapid pavement deterioration.

TABLE 3 SUMMARY OF PROFILE ANALYSES, POSTGRINDING ROUGHNESS

Facility	Root Mean Square Vertical Acceleration (mm/m2) Base Length 0.6 m	1.2 m	3.0 m	International Roughness Index (mm/m) -->	<--	Profile Deviation Per Unit Length (mm/m) Straight Edge Length 0.6 m	1.8 m	3.0 m
1.Pearson Airport Taxiway Echo OFFSET: 3.0 m R DATE: 05/28/91	2.11	0.81	0.27	0.94	0.93	0.90	1.14	1.67
2.Pearson Airport Runway 24L OFFSET: 3.0 m L DATE: 05/30/91	2.60	0.91	0.28	1.01	1.00	1.01	1.40	1.93
3.Pearson Airport Runway 06R OFFSET: 3.0 m R DATE: 05/28/91	2.86	1.12	0.36	1.15	1.16	1.11	1.65	2.38
4.Pearson Airport Taxiway Bravo OFFSET: 3.0 m L DATE: 05/28/91	3.66	1.16	0.38	1.30	1.33	1.58	1.92	2.42

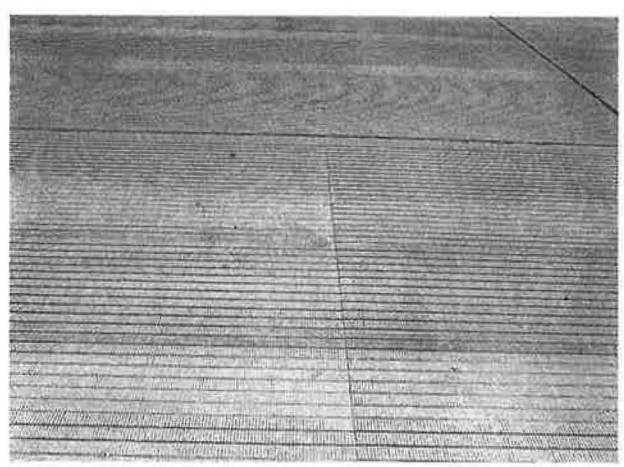

FIGURE 11 Completed pavement surface after grinding and grooving.

REFERENCES

1. M. Y. Shahin, M. I. Darter, and S. D. Kohn. Evaluation of Airfield Pavement Condition and Determination of Rehabilitation Needs. In *Transportation Research Record 700*, TRB, National Research Council, Washington, D.C., 1979.
2. *Pavement Surface Roughness Measurement and Analysis*. AK-68-33-199, Appendix F. Airports and Construction, Airports Facilities Branch, Surface Structures Division, Transport Canada, March 1984.
3. Digital Incremental Profiler. Face Construction Technologies Inc., Norfolk, Va.
4. Runway Roughness Analysis Program. Pavmatec Limited, Downsview, Ontario, Canada.
5. D. K. Hein and M. H. MacKay. *Analysis of Runway Roughness*. Transportation Development Centre of the Policy and Coordination Group and Airports Authority Group, Transport Canada, March 1989.
6. M. W. Sayers et al. *The International Road Roughness Experiment: Establishing a Correlation and a Calibration Standard for Measurements*. Technical Paper No. 45. The World Bank, Washington, D.C., 1986.

The opinions and findings expressed or implied in this paper are those of the authors and not necessarily those of Transport Canada or Public Works Canada.

Publication of this paper sponsored by Committee on Pavement Maintenance.

Thinner and Thinner Asphalt Layers for Maintenance of French Roads

J. BELLANGER, Y. BROSSEAUD, AND J. L. GOURDON

Very thin and ultrathin wearing courses of coated materials have occurred because of changes in pavement construction and maintenance policy; in the ever-higher level of service offered to users; in formulations, following the use of binders modified by adding polymers or mineral or organic fibers; and in the technology of placement.

Thin-layer techniques are used extensively on the French road network. The most widely used by far is the chip seal (CS), of which more than 100 million m^2 is applied every year. Cold mixes are used steadily with limited success; approximately 8 million square meters are applied a year. Some techniques, such as repaving and thermorecycling, have never caught on; others, such as thin hot-mix asphalt with chippings and coated sands with chippings, are in decline. Very thin (20 to 25 mm) and ultrathin (10 to 15 mm) wearing courses of coated materials have experienced very rapid growth in the past few years.

Because of their small or very small thicknesses (less than 40 mm), very thin surface layers (VTSLs) and ultrathin hot-mix asphalt layers (UTHMALs) are normally used on pavements that need neither structural strengthening nor major correction of evenness. They are basically maintenance techniques, but some of them are occasionally used for the wearing courses of new or overlaid pavements.

VTSLs and free-draining surface layers are also used in new wearing courses, preceded by a base course of coated materials 40 to 60 mm thick, when special care must be taken with the surface characteristics of the pavement (comfort and skidding resistance) and when it is judged that one thick layer would not attain the assigned objectives.

COMPARATIVE CHARACTERISTICS OF VTSLs AND UTHMALs

VTSLs and UTHMALs are among the most promising techniques in terms of a compromise among comfort, safety, and inconvenience to users. The UTHMAL technique is a development of the VTSL technique, midway between it and the chip seal. These three techniques will be compared in the following sections.

J. Bellanger, Laboratoire Régional des Ponts et Chaussées d'Angers, Avenue de L'Amiral Chauvin, BP 69, Les Ponts-de-Ce-Cedex 49136, France. Y. Brosseaud and J. L. Gourdon, Laboratoire Central des Ponts et Chaussées, 58 boulevard Lefebvre, F 75732, Paris cedex 15, France.

Formulation

The most common grading is 0/10 mm with a 2/6-mm gap. Gap-graded 0/6-mm formulations are also used in VTSLs and, less often, in UTHMALs. This finer grading is applied mainly in urban settings; the resulting texture is a good compromise between skid resistance and tire-pavement contact noise. There are very few gap-graded 0/14-mm formulations; they are used only in VTSLs because of their tendency to segregate when spread manually. The difference between VTSLs and UTHMALs lies in the percentage of coarse aggregate and the proportion of binder. For example, an intermediate 0/10-mm formulation for VTSL is 65 to 70 percent 6/10-mm and 5.8 to 6.0 weight percent binder; for UTHMAL, it is 75 to 80 percent 6/10 and 5.2 to 5.6 weight percent binder.

The fines content (undersized at 0.080 mm) is generally between 6 and 9 percent for both techniques. The binder is most often a pure distilled 60/70 (occasionally 80/100) penetration grade asphalt.

To improve the mechanical properties and resistance to climatic stresses, additives (polymer or fibers) are often incorporated. These special formulations account for 90 percent of VTSL applications. The criterion generally used in deciding whether to use these formulations is heavy traffic. It is thought that for more than 1,000 trucks/day/direction, it is best to use a modified binder to ensure greater cohesion and a more lasting macrotexture.

The special processes use, in most cases, asphalts modified by synthetic polymers such as styrene butadiene styrene (SBS) or ethylene and vinyl acetate or polymers recovered from recycled rubber powder. These give the binder very good elastomeric properties and make it less sensitive to temperature variations. They also use, to a lesser extent (15 percent of the technique), mineral or organic fibers—from 0.3 to 1.2 percent, according to type. These fibers make it possible to use a larger proportion of asphalt (6.4 to 6.8 weight percent binder) and structure the asphaltic mastic.

Study of Formulation

Existing laboratory tests are poorly suited to products applied in very small thicknesses, because the UTHMAL technique tends toward a monogranular surfacing that is more like a chip seal than a coated material. However, it is possible to characterize trends in the evolution of VTSLs in the laboratory. The tests required by the French standard in the context of formulation studies cover the following:

- Resistance to removal of the coating by water;
- Workability of the VTSL as determined by the density obtained in the Laboratoire Central des Ponts et Chaussées (LCPC) gyratory shear press; and
- Durability of the macrotexture of the surfacing, evaluated by a traffic simulation using the LCPC rutting tester. The change in texture depth by sand patch test (TD) is measured on the sample.

The standard also calls for on-site inspection of the macrotexture, with specific TD values of at least 0.8 mm for a 0/10 and 0.6 mm for a 0/6.

Production

The materials can be produced in all types of coating plants: continuous, batch, or dryer drum mixer. Their preparation requires few special precautions other than observance of the proper aggregate drying temperatures. Contrary to what might be thought, VTSL and UTHMAL are not subject to segregation during transport or spreading because of the low proportion of sand and the large discontinuity. Because their formulations are close to that of porous asphalt, they have a similar appearance after placement. The surfacing is very uniform and the longitudinal joints are practically invisible, giving a very attractive appearance.

Placement

Besides their slightly different formulations, placement is where the VTSL and UTHMAL techniques differ. VTSLs are applied with a normal plant: a conventional paver preceded by a binder spreader. The tack coat is applied, according to the condition of the substrate, at between 0.4 and 0.7 kg/m^2 emulsion, often modified. This cost is essential to the process. It provides the bonding and sealing that the surfacing alone cannot provide because of the overly large percentage of voids (about 10 percent). The spreading speed is 5 to 8 m/min. Compaction is done with steel-wheeled rollers.

Because of the need to spread a substantial tack-sealing coat, 0.8 to 1.0 kg/m^2 emulsion, a special plant must be designed for the simultaneous high-speed spreading of the two layers of the complex in a UTHMAL. This layer consists of an emulsion, modified by latex or an SBS copolymer, giving this layer—the quality of which determines the properties of the surfacing—very good elasticity, cohesion, and adhesion. The plant must include

- A tack coat spreader bar having a flow rate controlled by forward speed and an adjustable width, with associated storage tanks to give the machine adequate capacity between refillings;
- A storage compartment for the coated aggregates to prevent cooling and allow nonstop spreading; and
- A variable-width system for distributing and leveling the coated aggregates.

Its operating characteristics include

- A width of 2.5 to 4.2 m (5.0 m for one of the machines), and
- A working speed always greater than 10 m/min that routinely reaches 20 to 25 m/min.

With this equipment, the three application operations (spreading of binder, coated gravel, smoothing-compaction) follow one another rapidly. This leads to

- Optimal bonding of the coated aggregates to the layer of binder and to one another (no gravel is sprayed when the road is reopened to traffic);
- A clean job;
- Rapid completion of the maintenance work and much less inconvenience to users. The site occupies a length of only 300 to 400 m; traffic resumes immediately after the end of rolling, accomplished by two or three passes of the steel-wheeled roller (one of the contractors recommends using a rubber-tired compactor for finishing). This compaction work in the surfacing is limited to an area of 150 m behind the paver.

COMPARISON OF MAIN PROPERTIES OF CSs, VTSLs, AND UTHMALs

Macrotexture

Assessed by the sand patch method, the ranges of macrotexture measured at sites are given in Table 1. Semigranular (SG) 60 mm thick is included for comparison. The measurements show that macrotexture holds up well in VTSLs and UTHMALs but that in CSs, which have the greatest initial sand height, it deteriorates quickly under high traffic, by indentation into the substrate. However, CSs still have the highest values. Additionally, the type of macrotexture differs according to the placement process;

- CS has a macrotexture "in relief" because of the method of spreading the coarse aggregate and because of compaction by a rubber-tired compactor;
- VTSL has a "flat" macrotexture because of smoothing by a paver screed and compaction by a steel-wheeled roller, which tend to force the coarse aggregate embedded in the asphaltic mortar into a flat position; and
- UTHMAL has an intermediate macrotexture because the smaller quantity of asphaltic mortar leaves the coarse aggregate some freedom of placement, despite light compaction by a smooth roller.

TABLE 1 MACROTEXTURE MEASUREMENTS

	Initial Thickness (mm)	Thickness After 1 Yr of Traffic (mm)
VTSL 0/10	1.0–1.2	0.9–1.0
VTSL 0/6	0.8–1.0	0.8–0.9
UTHMAL 0/10	1.7–2.0	1.3–1.9
CS 0/6	2.5–3.0	1.6–2.2
SG 0/10	0.5–0.7	0.4–0.5

Skid Resistance

Skid resistance is assessed using the coefficient of longitudinal friction (CLF), between 40 and 120 km/hr (smooth tire, locked wheel). The three techniques compared are among the best of all French road surfaces: CLF at 40 km/hr is very good and similar for these three techniques (about 0.5 CLF). It maintains for high speeds (about 0.40 CLF at 120 km/hr), especially for UTHMAL, even though it must be corrected for the younger age of the surfaces tested.

Tire-Pavement Contact Noise

Measurements of tire-pavement contact noise outside the vehicle at 90 km/hr were made on modern thin layers and compared with chip seal noise under comparable conditions. In this way it was shown that a VTSL had a noise level close to that of conventional coated materials, on the order of 74 dB(A), and lower than that of chip seals at the same site [77 to 80 dB(A)]. A recent comparison of a 0/10-mm UTHMAL and a 6/10-mm chip seal using a slightly different measurement method (Franco-German protocol) has also revealed a significant difference [repeatability is 1 dB(A)] in favor of the UTHMAL [77 dB(A) against 80 dB(A) for the chip seal] that can be detected by a human as a doubling of the noise level [+3 dB(A) is equal to a doubling of the noise level].

Impermeability

Impermeability is difficult to measure on site using common means because of the marked macrotexture of very thin layers, which poses problems of tightness around the measurement apparatus. The impermeability of CSs is regarded as very good, thanks to the thick film of binder (1 to 1.7 mm). On VTSLs and UTHMALs, a few measurements of permeability have been made on cores, in the laboratory, at a pressure of 0.3 MPa. For VTSLs, the percentage of voids in the coated materials is high (approximately 12 to 15 percent) and the impermeability is governed by the thickness of the tack coat (0.3 to 0.4 kg/m^2 of residual asphalt). For UTHMALs, laboratory measurements have shown that the tack-sealing coat, at approximately 0.6 kg/m^2 of residual asphalt, ensures good impermeability.

Longitudinal Evenness

By its nature, the chip seal allows no correction of pavement evenness. For VTSLs and UTHMALs, on the other hand, many measurements have been made using the longitudinal profile analyzer (APL). Passes before and after the work show that in most cases, despite the small thickness applied, VTSLs (average thickness 25 mm) and UTHMALs (average thickness 1.5 mm) slightly but really improve the evenness of the pavements on which they are used (improvement is 10 to 25 percent in APL coefficient).

CONCLUSION

In France, VTSL has for 3 or 4 years been an especially powerful and effective maintenance technique that is routinely used to meet the increasingly stringent requirements imposed by growing traffic and higher safety standards. UTHMAL is the ultimate development of the hot-mix technique in the direction of reduced thickness. It is the product of materials and equipment research and of contractors' experience with the tried and tested techniques (CSs and VTSLs) that led up to it. In the surface maintenance of pavements that have suffered little deformation, for all types of traffic, where the use of a layer contributing nothing to the pavement structure is compatible with the long-term maintenance strategy chosen, UTHMAL enables a high level of service at low cost. Its speed of execution and of reopening to traffic, its careful implementation (it does not pollute the environment), its level of comfort and safety, and its very small thickness are its major strengths. The first results meeting a favorable reception by project supervisors and users forecast substantial growth of the UTHMAL technique.

Publication of this paper sponsored by Committee on Pavement Maintenance.

Abridgment

Evaluation of Highway Blade-Patching

DAVID F. ROGGE

A survey of the 50 state highway departments on their use of blade-patching as a maintenance technique is summarized. Blade-patching is defined as cleaning a pavement area, applying tack coat, applying asphalt mix with a motor grader or spreader box, and compacting. On the basis of the information obtained from the survey, a cost analysis comparing blade-patching to a 2-in. overlay was made, illustrating the use of an economic model for decisions between maintenance alternatives. Of the 43 states that responded to the survey, 38 use blade-patching. State highway divisions spend more than $175 million a year on blade-patching, but there is wide disagreement about its usefulness. The best estimate of blade-patch life is 3 years, and economic analysis comparing blade-patching to a 2-in. hot-mix overlay indicates that blade-patching should seldom be used if traffic exceeds 1,500 average daily traffic or if blade-patching required to maintain the pavement exceeds 125 ton/mi/year.

Blade-patching is the application of hot mix, cold mix, or premix to areas of pavement distress, by motor grader or spreader box, without removing existing pavement. Although it is widely used for pavement maintenance, a review of the literature produces little information (*1*). Consequently, a research project was undertaken.

During October 1990, a questionnaire was distributed to the chief maintenance engineer (or similar position) at the highway division of each of the 50 states. The questionnaire requested information about the extent of each state's use of blade-patching as a maintenance technique, appraisals of its usefulness, and suggested alternatives. Forty-three states returned at least partially completed questionnaires.

SURVEY FINDINGS

Highlights of the survey are presented in this paper. For a more detailed discussion, see Rogge (*2*).

Of the 43 states responding to the survey, 5 indicated that they do not use blade-patching and generally do not consider it cost-effective. Six states indicated that they do use blade-patching but provided no information on tons applied or level of budget allocation for this practice.

Table 1 summarizes use, cost, and service life data. The 27 states responding with budget information reported spending a total of about $180 million a year on blade-patching. The top three users account for 50 percent of the tonnage.

The cost figures presented in Columns 5–7 of Table 1 represent what the states believe to be labor, material, and equipment costs for blade-patching. Cost estimates ranged from $28.70/ton to $85.50/ton, with a median value of $44.00/ton. Twenty-one of twenty-nine respondents cited values between $30.00/ton and $50.00/ton.

It is difficult to determine dollars per square yard of blade-patching, because area and thickness of patches vary widely and records of areas covered are not generally kept. Fourteen states attempted to supply this information, however, providing a low of $0.75/yd^2, a high of $11.50/yd^2, and a median value of $2.70/yd^2.

Thirteen states estimated blade-patching costs per lane-mile improved. Values ranged from $1,300/lane-mi to $28,000/lane-mi, with a median value of $7,099/lane-mi.

Estimates for blade-patching life-expectancy ranged from 6 months to 20 years. Most responses were from 2 to 5 years. The average was 3.6 years, and the median, 3 years. These values are of the same magnitude as the average service life value of 3 years for "premix leveling" determined by a 1986 study at Purdue (*3*).

Respondents were asked to estimate the relative distribution of their blade-patching tonnage to various typical applications. More than half the tonnage was estimated to be used to fill ruts or spot depressions. Other uses included repair of surface cracks, bridge approaches, and sunken grades.

Roadway condition before blade-patching was indicated to be evenly distributed between "fair," "poor," and "very poor" pavements. On average, maintenance engineers thought that blade-patching improved the roadway the equivalent of one rating (e.g., "poor" raised to "fair").

Maintenance engineers were asked to agree or disagree with statements about the effectiveness of blade-patching when used for different types of distress and whether blade-patching is a cost-effective substitute for overlays. Significant differences of opinion were expressed on all of these items with one exception: the statement "blade-patching is a temporary measure to maintain the surface until an overlay may be accomplished" drew agreement and strong agreement from all but one respondent.

The survey specifically requested information about cost-effective alternatives to blade-patching that respondents have discovered. These alternatives were milling, leveling with self-propelled AC pavers, 3/8-in. sand mix laid with a paver, slurry seal, microsurfacing, crack sealing, inlay patching, chip seals, small pavers, and resurfacing. Although it was not mentioned by survey respondents, the author knows through other research that Oregon has successfully used cold in-place recycling with a chip seal in lieu of blade-patching on low-volume roads in the high desert environment of central Oregon (*4*). Hot recycling is another process that shows promise.

Department of Civil Engineering, Oregon State University, Corvallis, Oreg. 97331-2302.

TABLE 1 BLADE-PATCHING VOLUME, COST, AND SERVICE LIFE BY STATE

(1)	STATE (2)	ANNUAL BLADE-PATCHING (TONS) (3)	ANNUAL BLADE-PATCHING ($) (4)	ESTIMATED UNIT COST ($/TON) (5)	ESTIMATED UNIT COST ($/SY) (6)	ESTIMATED COST/LANE-MI. ($/LANE-MI) (7)	ESTIMATED SERVICE LIFE (YRS) LOW (8)	AVG (9)	HIGH (10)
1	AL	50,976	$1,244,000	$37.54			5		15
2	AK								
3	AZ								
4	AR	250,000	$9,750,000	$39.00			3		5
5	CA	30,000	$2,000,000	$70.00	$4.00	$28,000		2	
6	CO	200,000	$7,100,000					3	
7	CT	50,000			$0.75	$7,099		3	
8	DE								
9	FL			$54.00				4	
10	GA								
11	HI								
12	ID	157,000	$4,900,000	$31.00	$1.25	$8,000			
13	IL	500			$11.50			2	
14	IN	13,629		$35.69				3	
15	IA	35,000	$1,350,000	$34.00			2		10
16	KS	400,000	$8,800,000			$4,900	1		2
17	KY							5	
18	LA	21,000	$1,200,000	$57.00			3		7
19	ME							3	
20	MD	50,834	$3,002,636	$59.00			1		3
21	MA								
22	MI	6,400		$60.00			3		5
23	MN	8,000		64.59	2.66		1.5		10
24	MS								
25	MO	950,000	$29,000,000	$30.00	$1.18	$1,300	3		4
26	MT								
27	NE	143,000	$4,400,000	$30.64				5	
28	NV	22,000	$3,075,910	$85.50					
29	NH	96,000	$3,557,217	$37.05		$1,872	2		3
30	NJ								
31	NM	216,000	$9,500,000	$44.00	$2.70	$19,000	1		5
32	NY							0.5	
33	NC	150,000	$4,500,000	$30.00	$2.50			3	
34	ND	120,000	$5,500,000	$45.00				20	
35	OH	176,997	$8,173,263	$46.18				3	
36	OK	130,000	$4,300,000	$33.87	$1.87	$13,080	2		3
37	OR	200,000	$7,500,000	$42.50			3		10
38	PA								
39	RI								
40	SC	3,760	$300,000	$50.00	$3.75			2	
41	SD	250,000	$4,000,000	$58.00	$6.00	$3,000	5		10
42	TN						1		2
43	TX	1,339,000	$38,500,000	$28.70	$1.50		5		10
44	UT	125,000	$5,800,000	$46.40	$2.20			3	
45	VT	4,000	$200,000	$50.00			3		5
46	VA			$50.00				8	
47	WA	31,766	$3,904,951					3	
48	WV	146,000	$4,600,000	$31.50	$2.70			5	
49	WI			$34.63				4	
50	WY	70,640	$2,500,000						
	TOTAL	5,447,502	$178,657,977						
	MEAN	136,933	$5,598,319	$44.50	$2.69	$8,136	2.6	3.6	6.1
	MEDIAN	108,000	$4,400,000	$44.00	$2.70	$7,099	3.0	3.0	5.0

NOTE: MEAN VALUES ARE TAKEN AFTER DISREGARDING HIGH AND LOW EXTREME VALUES.

ECONOMIC MODEL

The survey showed a wide disparity in use and perceived usefulness of blade-patching. To aid maintenance managers in comparing blade-patching and other maintenance techniques, an economic model is offered. The model is best explained graphically. Figure 1 shows a plot of equivalent annual cost (EAC) per mile versus average daily traffic (ADT). The cost values for ADT = 0 represent agency costs only, with no consideration of user costs. Therefore, the intersections of the curves with the y-axis show the effects on agency budgets. The area of the graph corresponding to positive ADT values incorporates user costs. The slopes of the lines represent user costs. The steeper the slope, the greater the cost per mile. For a given ADT, the curve with the lowest EAC represents the preferred economic choice. The intersections of curves show ADT values where the preferred economic choice changes.

The example of Figure 1 shows a comparison of blade-patching with a 2-in. overlay applied to a poor pavement where

- 50 ton/mi/year of blade-patching are required to maintain,
- Blade-patching costs $44/ton (median value in survey),
- Blade-patching reduces variable user costs for "medium" cars from $0.162/mi ("poor") to $0.138/mi ("fair"),
- Overlays cost $30/ton and last 10 years, and
- Overlay reduces variable user costs for "medium" cars to $0.119/mi ("very good").

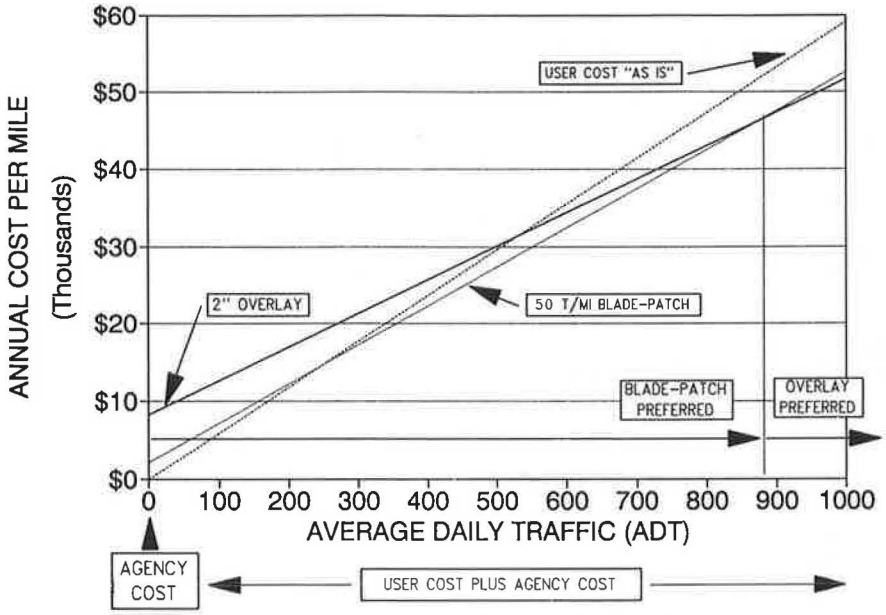

FIGURE 1 Break-even points of user savings and overlay cost for 2-in. overlay or blade-patching applied to "poor" pavement where 50 ton/mi of blade-patching are required.

User costs were taken from a study by Zaniewski (*5*). EACs were calculated using traditional methods of engineering economy with an interest rate of 6 percent. A "do nothing" curve is also included for reference. Below 880 ADT, blade-patching is preferred. Above 880 ADT, the overlay is preferred.

A whole family of lines parallel to the 50 ton/mi curve could be plotted on the graph of Figure 1 to represent blade-patching at different ton-per-mile rates. Lower tonnages of blade-patching required per mile would result in preference for blade-patching at higher ADTs. Higher tonnages would shift the break-even point to lower ADTs. In this example, the maximum allowable blade-patching is 190 ton/m with break-even at ADT = 0. In other words, the cost of blade-patching at 190 ton/mi/year is equal to the annualized cost of the overlay, if user costs are neglected.

The above analysis was repeated for application to "fair" pavement and with a range of overlay prices of $25/ton to $30/ton and lives of 10 to 15 years. The conclusion is that blade-patching is seldom preferred over a 2-in. overlay when ADT exceeds 1,500 or when more than 125 ton/mi of blade-patching are required to maintain the road. Maintenance managers are encouraged to substitute their own values and repeat the analysis. See Rogge (*2*) for a more complete discussion.

CONCLUSIONS

On the basis of the preceding discussions, the following conclusions are warranted:

1. There is a wide divergence of opinion among state highway departments regarding the cost-effectiveness of blade-patching as a maintenance technique. To some it is to be avoided, to some it is a last resort. To others it is a useful technique.
2. The greatest agreement among survey respondents was found to be with the statement "blade-patching is a temporary measure to maintain the surface until an overlay may be accomplished."
3. Costs of blade-patches ranged from $28.70/ton to $85.50/ton with a median value of $44.00/ton.
4. Blade-patches are generally believed to have service lives from 2½ to 6 years; estimates of 3 years were the most common.
5. Respondents collectively estimated that blade-patching raises the condition rating of the pavement approximately one level (e.g., "poor" to "fair").
6. An economic model for comparing blade-patching with other maintenance strategies is presented. When typical values from the survey were incorporated in this model and blade-patching and a 2-in. overlay were compared, blade-patching was seldom preferred if ADT exceeded 1,500 ADT or if more than 125 ton/mi were required to maintain the roadway.
7. Suggested alternatives to blade-patching include milling, leveling with self-propelled AC pavers, 3/8-in. sand mix laid with a paver, slurry seal, microsurfacing, crack sealing, inlay patching, chip seals, small pavers, resurfacing, and recycling.

ACKNOWLEDGMENTS

The author wishes to thank all of the state highway officials who found the time to participate in the survey and contribute a great deal of information. Gratitude is also expressed to the Oregon-Columbia Chapter of the Associated General Contractors of America, which funded this research effort, and

to the Oregon State University Construction Education Foundation for the support provided.

REFERENCES

1. D. F. Rogge. *Literature Review and Economic Analysis of Blade-Patching of Asphalt Roadways*. TRR 88-34. Transportation Research Institute, Oregon State University, Corvallis, April 1988.
2. D. F. Rogge. *Evaluation of Highway Blade-Patching*. TRR 91-3. Transportation Research Institute, Oregon State University, Corvallis, April 1991.
3. K. J. Feighan, E. A. Sharaf, T. D. White, and K. C. Sinha. Estimation of Service Life and Cost of Routine Maintenance Activities. In *Transportation Research Record 1102*, TRB, National Research Council, Washington, D.C., 1986.
4. D. F. Rogge, R. G. Hicks, and T. V. Scholz. *In-Depth Study of Cold In-Place Recycled Pavement Performance, Volume 1—Final Report*. FHWA-OR-RD-91-02A. FHWA, U.S. Department of Transportation, Dec. 1990.
5. J. P. Zaniewski, B. C. Butler, G. Cunningham, G. E. Elkins, and M. S. Paggi. *Vehicle Operating Costs, Fuel Consumption, and Pavement Type and Condition Factor*. Report PL-92-001. FHWA, U.S. Department of Transportation, March 1982.

Publication of this paper sponsored by Committee on Pavement Maintenance.

Abridgment

Defining Pavement Maintenance and Distress Precursors for Pavement Maintenance Measurements

ROGER E. SMITH AND SOHEIL NAZARIAN

An instrument for monitoring conditions indicating pavement deterioration that can be repaired with maintenance treatments has been designed and is being developed at the University of Texas at El Paso as part of a Strategic Highway Research Program (SHRP) project. The measurements made by the device are described. The focus of the SHRP research is to assist with identifying the need for and the effectiveness of maintenance activities, especially preventive maintenance. Considerable effort was directed at distinguishing preventive maintenance from rehabilitation. During this process, the types of damage that lead to the types of distress that are generally addressed with preventive maintenance were postulated. Furthermore, the mechanisms involved in developing different types of distress suitable for maintenance treatments were developed in a conceptual manner. To determine when these mechanisms should be measured, the precursors of the various distress types were hypothesized, and levels that should be considered significant were proposed.

The goal of the Strategic Highway Research Program (SHRP) Project H-104b is to develop equipment that measures the times at which maintenance treatments should be applied and the effectiveness of the treatments, especially preventive maintenance treatments. Part of the first year's work was spent defining the types of damage that could be measured with the equipment and that would be addressed with preventive maintenance. In addition, the level of accuracy required in the proposed measurements had to be determined. These measurements were to identify changes in the pavement layers at early stages of damage to allow preventive maintenance to be applied to prevent—or at least reduce the development rate of—further damage. An instrument has been designed and a prototype built at the University of Texas at El Paso. It is believed that it can make measurements that determine the following conditions: moisture in asphalt concrete pavement (ACP) layers, voids or loss of support in portland cement concrete pavements (PCCPs), fine cracking in ACP, delamination of overlays, and aging of asphalt (*1*).

This paper concentrates on the process used in the SHRP H-104b project to define preventive maintenance, to identify distress types typically addressed with preventive maintenance, to identify damage mechanisms leading to the development of these distress types, and to define accuracy levels needed for measurement. The effort is preliminary in nature; however, it is presented as a first step in defining distress mechanisms and precursors. It is hoped that this will lead to further efforts to define the underlying causes of distress that can be addressed with maintenance in a effort to ensure that the maintenance applied addresses the causes rather than the symptoms of pavement damage. The reader is referred to Nazarian et al. (*1*) for details of the procedures used.

R. E. Smith, Texas Transportation Institute, Texas A&M University, College Station, Tex. 77843. S. Nazarian, Center for Geotechnical and Highway Materials Research, University of Texas, El Paso, Tex. 79968.

DEFINING MAINTENANCE

The first step was to define maintenance types and classifications, because current definitions vary among agencies and over time. The following is presented to develop a coherent set of maintenance terminology.

- Routine Maintenance: This is localized maintenance activity such as pothole patching, spot sealing, and other repairs that are not funded for specific planned treatments for identified pavement segments.
- Programmed Maintenance:
  - —Preventive: Treatments are applied to preserve the existing pavement surface integrity and reduce the rate of deterioration. Examples include programmed joint and crack sealing, chip seals, slurry seals, fog seals, and rejuvenator applications (including minor surface preparation).
  - —Corrective: Treatments are applied to an existing pavement to maintain surface characteristics (surface friction restoration and moisture penetration resistance) and the structural integrity for continued serviceability. Examples include programmed joint sealing with partial depth patching to repair joints, slurry seals, chip seals, friction courses, thin asphalt overlays (1.25 in. and less) (including minor patching and shape correction) applied to correct surface friction problems or repair surface cracking.
- Rehabilitation:
  - —Restoration: New surface layers and repairs are intended to restore the pavement structure to a level approximately equivalent to that which was orignially present. Examples include joint replacement, full-depth slab replacement, full-length overlays with minor repairs to the

existing pavement, and surface treatment with major shape corrections and selective deep patching.

—Major Rehabilitation: Lane-width, full-length layers are added to the existing surface to increase the structural strength to handle increased future traffic loads. Examples include overlays with selective deep patching and recycling one or more pavement layers.

- Reconstruction: This is lane-width, full-length removal and replacement of pavement, mostly on existing alignment, including rehabilitation of associated structures generally to improved standards.

The definition of preventive maintenance in this list was used for the H-104b project.

DAMAGE REPAIRED WITH MAINTENANCE

The next step in the SHRP H-104b study was to determine the types of distress that are generally treated with preventive maintenance and the ways these treatments are programmed. The ultimate goal is to determine the precursors of such distress, but the more advanced stages are discussed before the precursors are postulated. The types considered included

1. Increased moisture in pavement base, subbase, and subgrade layers (ACP) leads to fatigue-type failures that occur because of the decreased strength of these pavement layers (*2*);
2. Moisture under joints (PCCP) leads to a decrease in the strength of base or subgrade materials, increases stresses in the slab, and leads to void development (*2*);
3. Voids or loss of support (PCCP) increase stresses in the slab, increase fatigue-related cracking of the pavement, and lead to faulting (*3*);
4. Overlay delamination allows excessive movement at the bottom of the overlay relative to the top where the wheel load is in contact with the pavement, increasing strains and reducing pavement life;
5. Fine cracking (ACP) is discontinuities in the asphalt concrete structure that reduce the surface modulus and eventually widen to allow moisture infiltration; and
6. Asphalt pavement aging is mostly attributed to progressive oxidation of the in-place asphalt concrete (*4*).

The ability to measure or infer changes in material properties and pavement responses to the test equipment is described in detail by Nazarian et al. (*1*). The different pavement layer properties and changes that can be measured are developed, and their relationships to the distress types are presented.

POSTULATING REQUIRED ACCURACY FOR MEASUREMENTS

The remaining life of a pavement is controlled by the complex interaction of factors such as traffic loadings, pavement structure, drainage, road geometry, climate, material durability, and maintenance actions. Below a certain measurement level, changes in the distress precursors are not significant enough to predict accurately changes in the pavement. If the distress precursors are identified too late, preventive maintenance treatments will not be enough and rehabilitation or reconstruction will be required.

The Texas Flexible Pavement System (TFPS) (*5*) was used to determine how early small changes in the pavement layer properties affect the ultimate pavement life, as defined by fatigue cracking, rutting, and serviceability. This was then used to define the levels of accuracy and precision required for maintenance measuring equipment.

The TFPS model predicts fatigue cracking, rutting, and serviceability as a function of traffic loadings. The impact of changes in base modulus values was used as the primary analysis tool to determine the accuracy needed for changes in base moisture levels. Fatigue cracking was used as the ultimate damage avoided by applying preventive maintenance. Depending on the quantity of cracks, four levels of maintenance or rehabilitation activities were envisioned. Within Level 1, the pavement is in satisfactory condition and no treatment—other than occasional localized maintenance—is needed. In Level 2, maintenance is appropriate for the pavement section. In the more severe cases of Levels 3 and 4, overall rehabilitation or reconstruction is necessary.

To predict the need for preventive maintenance, all measurements were made when the pavement was in Level 1 to predict when the pavement would reach a level at which preventive maintenance was needed or beyond which preventive maintenance would not be appropriate.

TFPS considers the long-term effect of seasonal variation of modulus due to changes in moisture content on the development of fatigue cracks. However, it does not model significant changes that develop partly through the life of the pavement. If the pavement starts with a given set of material parameters and early in its life the material is subjected to an increase in moisture that reduces its stiffness, future deterioration will be influenced by this early change, because it would reduce material stiffness more than would changes due only to seasonal variations in the model.

A conceptual model developed using TFPS allowed the determination of the impact of changes in pavement layers early in the pavement life on the number of load applications, or time, until the pavement reaches established cracking levels. This procedure is considered adequate only for low levels of damage and small quantities of distress (such as those used in this study). By using this approach, early changes in pavement parameters can be used to predict their impact on ultimate life and rate of pavement deterioration to provide the information needed to determine if the preventive maintenance extends the ultimate pavement life or reduces the rate of deterioration.

Accuracy of Measurements Required

The modulus of the base or subgrade and changes in the moduli can be measured within a finite accuracy. Therefore, there is a level of change below which measurements are not accurate enough to detect, and if this change is considered the distress precursor, there is a level below which the distress precursor cannot be detected. Upper limits, or trigger values, for no maintenance, preventive maintenance, and overall

maintenance were set at 2 percent, 5 percent, and 20 percent cracked area based on engineering judgments. Future studies should set these on the economic impact of delaying the maintenance.

Variation in fatigue cracking as a function of number of equivalent single axle loads was calculated for the cases in which the modulus of base was 10 to 50 percent less than a control section. Using the conceptual procedure developed earlier, a damage curve for the situation in which the modulus of base was reduced by 10 to 50 percent because of changes in the equilibrium moisture at a given time. It is conservatively assumed that the change in equilibrium moisture (and as a result the modulus) occurs as soon as the percentage cracking of the control pavement section deviates from zero.

In the next step, the degree of accuracy is determined at which the change in modulus must be measured. It is assumed that the maintenance engineer would like to know within the following 3 years whether maintenance is necessary and, if so, whether it should be localized or overall.

Table 1 shows the degree of accuracy with which the modulus of the base must be measured for different levels of cracking and numbers of years from the date of change in modulus to scheduled treatment. These values are obtained from figures presented by Nazarian et al. (*1*). It can be seen that for a typical pavement, an accuracy of 25 to 30 percent is sufficient. This procedure was repeated for more than one climatic zone, and it was determined that climatic zone had little effect on the accuracy needed.

The advantage of this process is that for each climatic region, each acceptable level of maintenance, and each economically feasible level of deferred maintenance, the required level of measurement accuracy can be determined. Although it is not described in this paper, the same process can be applied to the loss of strength in the subgrade or the subgrade and base combined.

Other Measures

A similar approach was used to determine the accuracy of measurements needed for voids or loss of support in PCCPs, moisture under joints of PCCPs, delamination of overlays, and fine cracking. Aging of asphalt layers was not addressed because adequate precursors had not been defined.

TABLE 1 DEGREE OF ACCURACY NECESSARY FOR DETECTING MOISTURE IN BASE (*1*)

Acceptable Fatigue Cracking (Percent)	Required Accuracy in Measuring Base Modulus (Percent)		
	Year 1	Year 2	Year 3
5	>50	25	10
10	>50	45	30
15	>50	>50	42
20	>50	>50	>50

FUTURE WORK

The equipment under development is programmed to be field tested as this paper is being made final. Considerable field testing of known conditions are planned to define the accuracy level available from the equipment.

SUMMARY

A device is being developed to measure early development of damage in pavements. These measurements are designed to allow the maintenance engineer to determine when maintenance—particularly preventive maintenance—should be applied to the pavement and whether the treatment has been effective. To accomplish this, the project team defined preventive maintenance, the types of damage that can be measured with the equipment that lead to maintenance treatments, and the accuracy needed in the measurements.

This was a first attempt to establish distress precursors and levels of accuracy needed in measurements. More work is needed to define precursors of all types of distress that maintenance activities address. The process needs considerable calibration, but it is hoped that it will be the first step in developing reasonable estimates of the effects of early changes in pavement properties on the pavement's long-term performance.

ACKNOWLEDGMENTS

This research was sponsored by the highway operations portion of the Strategic Highway Research Program. Brian Cox was the project manager.

REFERENCES

1. S. Nazarian, M. Baker, R. E. Smith, *Measurement Concepts and Technical Specifications of Surface Analyzer Device*. Project H-104b, Phase I: Tasks 1 and 2. Strategic Highway Research Program, Washington, D.C., 1991.
2. S. H. Carpenter, M. I. Darter, and B. J. Dempsey. A Pavement Moisture Accelerated Distress Identification System. *Users Manual—Volume 2*. Research Report FHWA/RD-81/080. FHWA, Washington, D.C., 1981.
3. F. Torres and B. F. McCullough. *Void Detection and Grouting Process*. Research Report 249-3. Center for Transportation Research, University of Texas, Austin, 1983.
4. C. A. Bell. *Summary Report on Aging of Asphalt-Aggregate Systems*. Report SR-OSU-A-003A-89-2. Strategic Highway Research Program, Washington D.C., 1989.
5. G. T. Rohde, W. Yang, C. P. Henry, M. Kartsounis, and R. E. Smith. *Users Guide to the Texas Flexible Pavement System (TFPS) Program*. Texas Transportation Institute, Texas A&M University, College Station, 1990.

Publication of this paper sponsored by Committee on Pavement Maintenance.

Quantitative Analysis of Joint Sealants Using FTIR–ATR

LAURAND H. LEWANDOWSKI AND LARRY N. LYNCH

Fourier transform infrared spectroscopy using attenuated total internal reflection (FTIR–ATR) was found to be a reliable analytical method for evaluating a two-component joint sealant material. A calibration curve was developed from measuring the peak heights of infrared absorption bands unique to the different components in the two-component coal-tar modified polymeric joint sealant and relating these to the weight percent of the base component. A nonlinear relationship was found to exist between the ratio of the peak height of Component A over the peak height of Component B versus the weight percent of Component B added to the two-component mixture. FTIR–ATR proved to be a useful and expedient way to evaluate the composition of the joint sealant during or after the mixing and curing process; it may, after appropriate investigation, have potential for use in quality control of joint sealing material installations and forensic investigations of failures in such installations.

Many pavement engineers, contractors, and manufacturers have been less than satisfied with the field performance of some pavement joint sealant materials. Sealant materials that are supposed to perform satisfactorily for 10 years are failing in 1 to 3 years; some user agencies report failure within 6 months after installation (*1,2*). The reasons provided for the premature failure of the sealant often depend on who is providing the explanation. For the pavement engineer or user agency, the cause of failure is normally believed to be an inferior sealant material, poor workmanship, or both. The contractor will cite problems associated with the project specifications, the inspection procedures or requirements used by the user agency, or an inferior product supplied by the manufacturer. The manufacturer will cite project specifications or contractor deficiencies. Any one or all of these reasons could contribute to the unsatisfactory field performance of a pavement joint sealant on a specific project. Regardless of the cause of the failure, corrective action must be taken and lessons must be learned to prevent the failures from reoccurring.

The reason for finding solutions to the poor field performance of joint sealant materials is financial. The user agency specifies a joint sealant material to protect the pavement structure, thereby extending the life of the pavement and reducing the maintenance costs. When the sealant prematurely fails, not only has the protection to the pavement been lost, but the maintenance costs have increased because the sealant must be replaced. The financial loss to both the contractor and manufacturer may be more direct. They may be required to reseal the joints, increasing their labor and materials cost. Their reputations may have been damaged because of what was perceived as a poor job or inferior material. Such perceptions can cause the contractor to lose future projects and the manufacturer to lose sales.

More and more, user agencies, contractors, and manufacturers are trying to work together to provide a high-quality, long-lasting finished product. User agencies have incorporated manufacturers' information about joint preparation requirements and sealant application techniques into the project specifications, and materials testing by an independent laboratory is sometimes required. Inspectors learning the proper procedures for sealing projects and some contractors are striving to instill in all of their personnel that quality control is a high priority. Manufacturers are providing technical support to the contractor, answering questions such as "How clean is clean?" and specifying the environmental conditions under which their material can be successfully installed (i.e., temperature, humidity, etc).

The cooperation between these three groups should eventually help joint sealing projects, but this cooperation is not yet widespread—even when all phases of the project have been conducted well, failures still occur. For example, the personnel on one resealing project conducted at a military base stated that the sealant material was tested and conformed to the appropriate material specification, the joints were "hospital clean," and the sealant was installed properly, but the sealant failed within 3 years. Why did it fail? One can study the contract specifications and conduct field evaluations to determine the joint width, depth, spacing, sealant shape factor, and current sealant condition to speculate with some accuracy about possible causes for the failure. But forensic test methods are not available to determine if some type of contamination was introduced into the sealant to cause the failure. Current conventional joint sealant test methods cannot determine if a hot-applied sealant was overheated, if a two-component sealant was properly mixed, or if the sealant was damaged during shipping. One method that could be useful for such analysis is the Fourier transform infrared spectroscopy–attenuated total internal reflectance (FTIR–ATR).

BACKGROUND

Fourier transform infrared spectroscopy has become a very reliable analytical method for performing quality control of systems containing several different chemical constituents. An especially useful development has been the ATR technique. Using this technique, the sample to be analyzed is pressed against an internal reflectance element (IRE). An infrared beam of light is passed through the IRE, which causes the

U.S. Army Engineer Waterways Experiment Station, 3909 Halls Ferry Road, Vicksburg, Miss. 39180.

beam to undergo multiple internal reflections. These internal reflections create an effect called the evanescent wave, which extends beyond the IRE-sample interface into the sample. The internal reflectance of infrared occurs in the IRE as long as the refractive index of the sample is less than that of the IRE it is touching. For wavelengths at which the sample exhibits absorption, this condition is lost; that is, the complex refractive index of the sample will exceed that of the IRE and light is lost. The spectrum obtained is that of light lost into the sample. This is important: the ATR spectrum represents a dispersive (refractive index) effect and is not based on absorptive processes described by Beer's law. The evanescent wave also decays exponentially as it passes into the sample, making the ATR measurements independent of sample thickness (Figure 1) (*3*).

Considerable work has been done using FTIR–ATR to study the composition and behavior of chemical systems. The research efforts vary from the study of the macromolecular orientation in the polymer surfaces of uniaxially drawn polypropylene sheets (*4*) to the reinforcement mechanism existing between silane coupling agents and glass (*5*). FTIR–ATR was also found to be an ideal method for quantitative analysis of complex mixtures used in carbon-epoxy composite materials. The FTIR–ATR technique has two advantages: spectra obtained using ATR have been shown to provide a more detailed spectrum than those obtained by transmission or reflectance modes for intractable samples (*6*), and samples can be tested in their processed state without time-consuming solvent extraction and film preparation. For pavement joint sealants, this means that it is possible to obtain meaningful analysis of samples obtained from the field. This is not true of conventional joint sealant tests.

The current study is using the FTIR–ATR sampling technique to evaluate joint sealant materials used for pavement sealing projects. The objective is to determine the feasibility of using FTIR–ATR as a quality-control test for measuring the mixing ratios of joint sealant materials after application in the field.

EXPERIMENTAL METHOD

Materials

The material used in this preliminary study was a two-component, cold-applied material manufactured to meet the requirements of Federal Specification SS-S-200E, Type H, Amendment 1 (Table 1). This specification requires the sealant to be both fuel- and blast-resistant. Type H means the sealant is mixed and applied using hand tools instead of sealant application equipment. Originally, a Type M or machine-mixed sealant was to be used for the FTIR–ATR analysis because improper mixing of the Type M material is a common complaint from personnel involved with sealant projects. The Type M material could not be uniformly mixed in different ratios in the laboratory by hand; therefore, the Type H sealant was selected. If different mixing ratios can be determined with the Type H material, it is believed that the method can eventually be transferred to Type M sealants. A second sample of the two-component, cold-applied sealant was obtained for method verification. The second sample was the same product as the first but from a different lot.

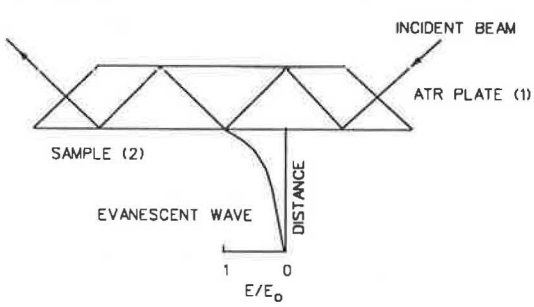

FIGURE 1 Optical diagram of ATR prism showing amplitude decay of evanescent wave (*9*).

Sample Preparation

The two-component, cold-applied sealants were mixed in various ratios by weight and then poured into a mold to produce a sample 2 mm thick, 25 mm wide, and 75 mm long. The weight ratios were determined by measuring each component and then pouring Component A (accelerator) into the container that contained Component B (base). The empty Component A container was reweighed to determine the exact mixing ratio. The mixing ratios are provided in Table 2. The first and last entries in Table 2 represent pure Component A and pure Component B, respectively, which were also analyzed using FTIR–ATR. After the two components were added together, they were mixed manually for approximately 10 min. The mixture was observed under a black light to ensure that it had been uniformly mixed. The samples were then poured into the molds and allowed to cure for a minimum of 24 hr before they were analyzed. Once the samples had cured they were cut out of the mold and were ready for analysis with FTIR–ATR.

The top side of the molded sample—the side that did not come in contact with the mold—was placed on the IRE and then on the ATR accessory. A zinc-selenide (ZnSe) crystal (50 mm × 10 mm × 3 mm) having an incident angle of 45 degrees was selected as the IRE. Before sample placement the crystal was wiped with acetone to remove any residue. A background was run on the ZnSe crystal to eliminate any environmental effects when analyzing the sample spectrum. The cured sealant was pressed against the IRE using a clamping device to maintain a constant path length. All spectra were taken with Nicolet Model 510P Spectrometer using a Michelson Interferometer. Thirty-two scans were used to produce the resulting spectrum, and the resolution was set at 4 cm^{-1}. The system contained a deuterated triglycine sulfate (DTGS) detector, which was purged with dry air to remove moisture and carbon dioxide that might have collected on the optics. All spectra were autobaselined in the absorbance mode before analysis.

The absorbance mode was selected because there is a linear relationship between concentration and the absorption bands. With the bands directly related to concentration, a measure of the area under the band or the band height can be used to measure unknown concentrations.

TABLE 1 FEDERAL SPECIFICATION SS-S-200E TEST REQUIREMENTS

TEST	REQUIREMENT
Accelerated Aging, sealed container, 120°F, 21 days	
Visual	No settling, separation or hardening that will not return to a homogeneous liquid by simple stirring, no skinning greater than 1/16 inch thick
Self-Leveling:	
Level plane	No flow to a variation of the surface greater than 1/8 inch
1.5 percent incline	No flow to a variation of the surface greater than 1/16 inch
Change in Weight by Fuel Immersion, percent	Shall not exceed 2.0 of the initial weight
Change in Volume on Exposure to Elevated Temperature, 158°F, 168 hours, percent	Shall not exceed 5.0 of the initial volume
Resilience:	
Unaged	
Initial indentation, (mm)	0.5 to 2.0
Recovery, percent	Minimum of 75
Aged	
Initial indentation, (mm)	0.5 to 2.0
Recovery, percent	Minimum of 75
Resistance to Artificial Weathering, 140°F, 160 hrs	
Test panels	(a) No breakdown of cure or reversion of the sealant (b) No blistering or deformation greater than "blister size No. 2" and classed as "medium dense" in accordance with ASTM D 714
Volume change, percent	Shall not exceed 5.0 of the initial volume
Bond to Concrete (-20°F) Nonimmersed	None of the specimens shall develop any surface checking, cracks, separation or other opening in the sealant. No hardness or loss of rubber-like characteristics in the sealant.
Fuel-immersed	Same as Nonimmersed
Water-immersed	Same as Nonimmersed
Flame Resistance	Shall not support combustion, flow harden or lose adhesive strength
Flow, cm, 5 hrs, 200°F	No cracking or dimensional change
Type M Sealant	(a) Pressurized mixing and extruding equipment shall be used (b) One to one ratio ± 5 percent by volume of Parts A and B (c) Viscosity, 75 F ± 5°F Part A 200,000 cP max. Part B 200,000 cP max. (d) Working life to allow ample time for filling joints (e) Tack free time 3 hrs max.
Type H Sealant	(a) N/A (b) Ratio Parts A to B supplied by manufacturer (c) Viscosity, 75 F°F ± 5°F Part A 150,000 cP max. Part B 150,000 cP max (d) Same as Type M (e) Tack free time 12 hrs max.

TABLE 2 WEIGHT RATIOS USED TO MIX TWO-COMPONENT JOINT SEALANTS (LOT 1)

Component A (grams)	Component B (grams)	Component B weight (%)
20.00	0.00	0.00
19.05	15.00	44.05
9.60	15.00	60.98
9.70	25.00	72.98
9.16	50.00	84.52
9.74	100.00	91.10
9.49	150.00	94.00
9.49	160.00	94.40
9.64	200.00	95.40
0.00	20.00	100.00

Effect of Depth on Spectra

Because the ATR technique analyzes from the surface only to a depth of approximately 0.5 to 10.0 microns into the sample (*7*), the technique may not be analyzing a representative cross section of the material. To determine the effect of depth on composition, samples from the two-component joint sealant were cut in half and spectra were taken of the exposed surfaces. The effect of depth on composition is presented in Table 3. The ratio of the peak heights was found to be relatively independent of depth or cure time after 1 day. This is consistent with the manufacturer's recommended cure time of 24 hrs.

That the ratio of the peak heights is relatively independent of depth is particularly interesting if field samples are to be analyzed. To analyze a field sample, the surface exposed to the environment would have to be removed to prevent dust and the like from affecting the spectrum.

RESULTS AND DISCUSSION

Spectra Interpretation

The two-component joint sealant is a coal-tar modified polymeric material consisting of an accelerator (Component A) and base (Component B). The bands found to be exclusive to Component A are a broad band from 3600 cm^{-1} to 3200 cm^{-1} from hydrogen bonding of the water and a sharp band at 1736 cm^{-1} from the carbonyl group. Component B contains both the polymer and the coal-tar pitch modifier. Characteristic bands from Component B are observed for the aromatic carbon-carbon double bond at 1599 cm^{-1} and the hydrogen-bonded phenolic (O—H) stretch at 3422 cm^{-1} (*8*). Several sharp peaks appear from 3694 cm^{-1} to 3620 cm^{-1} from hindered phenol groups. A weak band is also observed at 1919 cm^{-1} from overtones of the strong, broad inorganic bands at 900 cm^{-1} and 1000 cm^{-1}.

To develop a calibration curve, nonoverlapping, noninteracting bands must be selected for each component. The changes in these bands with composition will give a measure of the amount of each component in the mix. Because there is some overlap between Component B bands at 3694 cm^{-1} to 3422 cm^{-1} and the broad band of Component A at 3406 cm^{-1}, they were eliminated from consideration. The absorption band at 1599 cm^{-1} from Component B overlaps with several lesser peaks in Component A. The remaining bands available to develop a calibration curve are the strong band at 1736 cm^{-1} for Component A and the weak band at 1919 cm^{-1} for Component B. These two bands were selected for developing a calibration curve.

Developing the Calibration Curve

The calibration curve was produced by measuring the peak heights from the baseline to the peak maximum of the bands displayed in Figures 2 and 3 for Components A and B, respectively. A series of overlaid spectra are displayed in Figure 4, showing the effect of different weight ratios on the absorption of the two bands for Lot 1. A ratio index was then developed to determine the contributions at different weight ratios. The ratio index is defined by the following equation:

$$\text{Index} = A_{\text{Peakmax}}/B_{\text{Peakmax}} \quad (1)$$

where B_{Peakmax} is the peak height of the band at 1919 cm^{-1} extending from 1980 cm^{-1} to 1835 cm^{-1} representing Component B, and A_{Peakmax} is the peak height of the band at 1736 cm^{-1} extending from 1780 cm^{-1} to 1680 cm^{-1} characteristic

TABLE 3 RATIO INDEX VALUES OF VARIOUS 1:10 (A:B) WEIGHTED SAMPLES AT DIFFERENT CURE TIMES AND DEPTHS OF 0 AND 1.5 mm (AVERAGE RATIO = 6.324, STANDARD DEVIATION = .343)

Time (days)	Depth (mm)	Component A (grams)	Component B (grams)	Component B weight (%)	Ratio Index
1	0	9.31	100.00	91.48	5.859
1	1.5	"	"	"	5.875
4	0	9.57	100.00	91.27	6.465
4	1.5	"	"	"	6.662
6	0	9.32	100.00	91.47	6.368
6	1.5	"	"	"	6.716

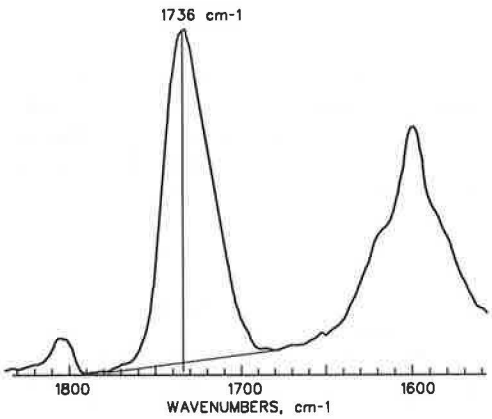

FIGURE 2 FTIR–ATR spectrum of characteristic peak for Component A.

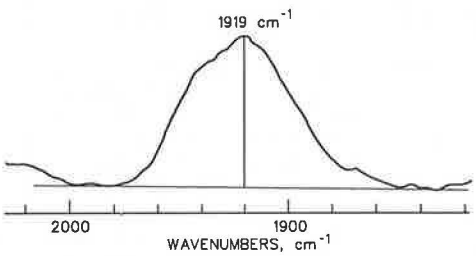

FIGURE 3 FTIR–ATR spectrum of characteristic peak for Component B.

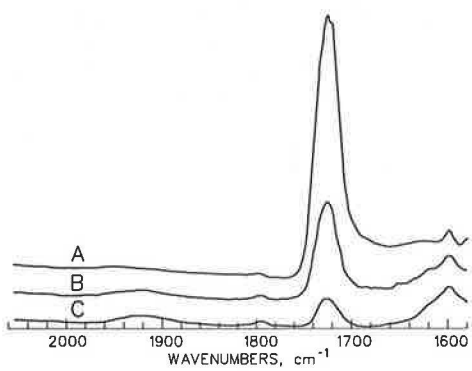

FIGURE 4 FTIR–ATR spectra of two-component joint sealant mixed at following weight percents of Component B: A = 44.05 percent, B = 84.52 percent, and C = 94.40 percent.

of Component A. This ratio index was then plotted against the known weight percent of Component B and is displayed in Figure 5. The resulting curve shows a nonlinear relationship between the ratio index and the weight percent of Component B, suggesting that some interaction is occurring in the two-component system. The different weight ratios will substantially change the degree of cure of the joint sealant, so it is expected that a nonlinear relationship would occur. A second-

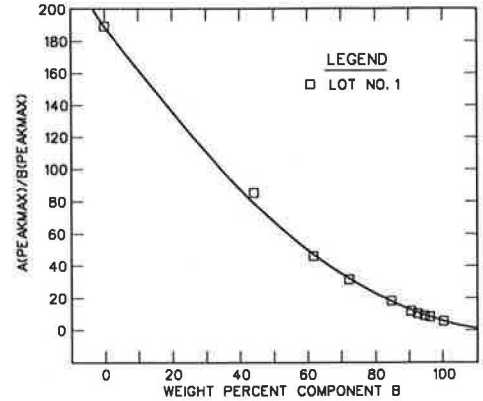

FIGURE 5 Calibration curve for the two-component joint sealant material from Lot 1.

order polynomial was calculated from the data to produce Equation 2.

$$\text{Index} = 6.393 - 0.8119\ (\text{weight percent of Component B}) + 0.01293\ (\text{weight percent of Component B})^2 \quad (2)$$

The second-order polynomial provided an excellent fit with a correlation coefficient of $r = .9989$.

It was first assumed that a linear relationship could be developed between the measured ratio and the actual weight percent of Component B. Because of the curing process in the mixed system, interaction between the components has produced a nonlinear curve. The band used for Component B is from the coal-tar modifier and probably does not change significantly in the presence of Component A; the band selected for Component A is probably directly involved in the curing process. Joint sealant materials are complex chemical systems composed of many different types of chemical compounds. Further research is required to better understand the interactions occurring between these various compounds and how they change with cure time.

Validation of Method

To verify the ability of the calibration curve to determine the mixing ratio of an "unknown" weight percent of Component B sample, another lot number was obtained and mixed in various ratios. The index values calculated from the spectra from Lot 2 were compared to the calibration curve (see Figure 6). It is evident that there is excellent agreement between the ratio index values obtained from the different lot numbers. This suggests that it is possible to develop one calibration curve for each specific joint sealant material.

CONCLUSIONS

1. FTIR–ATR can be a valuable tool for analyzing joint sealant materials with minimal preparation time.

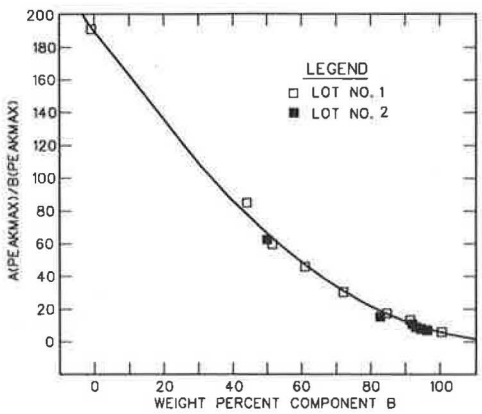

FIGURE 6 Comparison of ratio values measured for known weight percent of Component B for Lot 2 against calibration curve calculated from Lot 1.

2. The work on the coal-tar modified polymeric two-component joint sealant indicates that a calibration curve can be developed to determine the weight percent of an unknown two-component mixed joint sealant sample if a set of known samples exists. This technique could be useful in performing quality control of joint sealant materials mixed at the construction site or in a postconstruction evaluation to determine whether the manufacturer's specified mixing ratio was met.

3. Although the absorption bands selected for the calibration curve were nonoverlapping, there was significant interaction between the two components during the curing process. The interactions produced a nonlinear calibration curve. Joint sealant materials are a very complex system composed of polymers, plasticizers, fillers, pigments, activators, extenders, and base resins. The interaction between the components makes spectrum interpretation very difficult; further work is required to better understand these interactions.

ACKNOWLEDGMENTS

The support of the U.S. Army Engineer Waterways Experiment Station in collecting and preparing material for this paper is gratefully acknowledged. The review and comments of Timothy Vollor, George Hammitt II, Raymond Rollings, and Paul Hadala are greatly appreciated.

REFERENCES

1. L. N. Lynch. *Joint Sealant and Field Performance Survey*. Miscellaneous Paper GL-89-3. U.S. Army Engineer Waterways Experiment Station, Vicksburg, Miss., March 1989.
2. L. N. Lynch. *Pavement Crack and Joint Sealant Evaluation for FY 89 and FY 90*. Miscellaneous Paper GL-91-9. U.S. Army Engineer Waterways Experiment Station, Vicksburg, Miss., March 1991.
3. Introduction to ATR Spectroscopy. Nicolet Fact Sheet.
4. N. J. Harrick. *Internal Reflection Spectroscopy*. Wiley-Interscience, New York, N.Y., 1967.
5. F. M. Mirabella, Jr. A Critical Evaluation of Internal Reflection Spectroscopic Methods for Determining Macromolecular Orientation in Polymer Surfaces. *Applied Spectroscopy*, Vol. 42, No. 7, 1988, pp. 1258–1265.
6. E. Nishio et al. Fourier Transform Near-Infrared Attenuated Total Reflectance Spectroscopy of Silane Coupling Agents on Glass IRE. *Applied Spectroscopy*, Vol. 44, No. 4, 1990, pp. 614–617.
7. K. C. Cole et al. Comparison of Infrared Spectroscopic Methods for the Quantitative Analysis of Epoxy Resins Used in Carbon-Epoxy Composite Materials. *Applied Spectroscopy*, Vol. 42, No. 5, 1988, pp. 761–769.
8. T. F. Yen. *Chemistry and Structure of Coal-Derived Asphaltenes and Preasphaltenes*. Contract EX-76-C-01-2051. U.S. Department of Energy, Sept. 1980.
9. I. Ishida. Quantitative Surface FT-IR Spectroscopic Analysis of Polymers. *Rubber Chemistry and Technology, Rubber Review*, Vol. 60, No. 3, 1987, pp. 497–554.

Publication of this paper sponsored by Committee on Sealants and Fillers for Joints and Cracks.

Comparing Rectangular and Trapezoidal Seals Using the Finite Element Method

MICHEL F. KHURI AND EGONS TONS

To design proper seals, it is important to understand seal behavior and joint and crack geometry. Different seal cross sections are compared, namely, rectangular, trapezoidal, and trapezoidal-rectangular shapes. After a closed-form solution could not be achieved using the theory of elasticity, the plane strain, nonlinear, incompressible, hyperelastic (Mooney-Rivlin) finite element formulation of the software ABAQUS was used to evaluate different seal cross-sections in tension and compression with emphasis on bulge and sag and on shear strain (e_{12}). Laboratory measurements using Silicone Dow Corning 888 were taken to determine bulge and sag. It was concluded that the most desirable cross section of the three shapes is the rectangular. Axial strains (e_{11}) at the surface of the seal were compared with Tons' parabolic deformation calculations. There was good agreement all along the seal surface except near the joint walls because of a singularity. With continued research, the structural response calculations at the joint wall interface should be improved.

To make the pavement adjust to climatic conditions, joints are usually sawed or formed and a sealant material is poured or installed in the resulting groove to form a rectangular seal cross section such as the one shown in Figure 1*a*. *Wt* stands for top width; *Wb*, for bottom width; *D*, for total depth; *Dt*, for trapezoidal depth in a rectangular seal; and *Dr*, for rectangular depth in a trapezoidal-rectangular seal.

The cracking problem, however, is generally attributed to localized weakness of the pavement. These cracks are due to weather conditions (freeze-thaw cycles, large changes in temperature, shrinkage, etc.) and to loading caused by traffic.

To keep a highway in good condition and prolong its life, the cracks are sometimes grooved by a router, cleaned, then sealed. It is important to note that the resulting groove tends to have a trapezoidal shape, whether routed or not, because the top edges of a crack are exposed to weather and traffic and tend to spall because of lack of support. When a sealant material is poured into such a groove, the resulting shape of the seal may also end up being trapezoidal (Figure 1*b*), or it could be trapezoidal-rectangular (trap-rec) if there is no backup material to protect the sealant from flowing (Figure 1*c*). The problem is that cracks are sealed without trapezoidal or trap-rec cross sections being considered.

The objectives of this paper are to investigate the deformations and strains in different rubber seal cross sections (rectangular, trapezoidal, and trap-rec) using the finite element method (FEM) implemented on incompressible rubberlike materials and to compare the obtained results with laboratory measurements of top (*Ht*) and bottom (*Hb*) maximum displacements (Figure 2) with Tons' parabolic model (*1*).

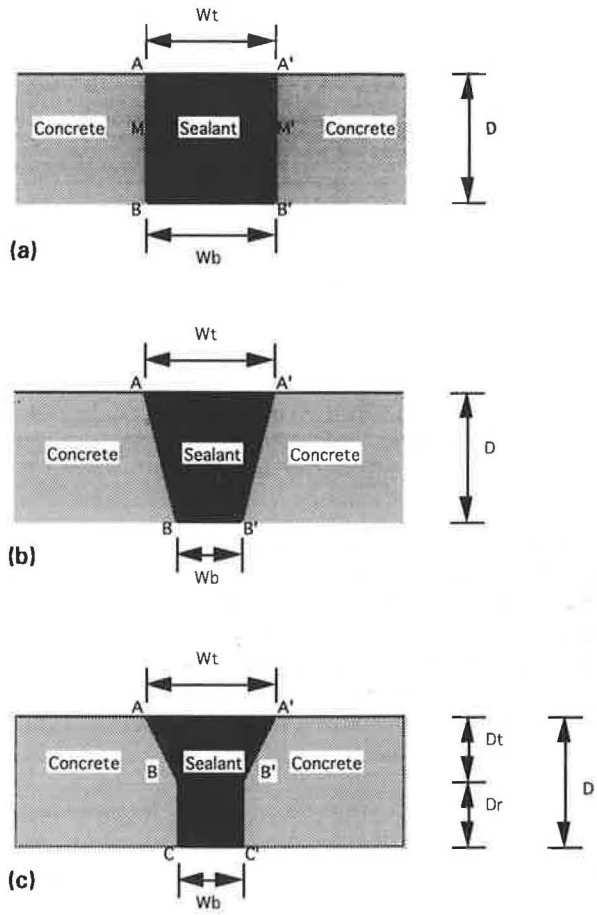

FIGURE 1 Cross sections: *a*, rectangular seal; *b*, trapezoidal seal; and *c*, trapezoidal-rectangular seal.

BACKGROUND

Rectangular Seals

The cross section of a joint is usually made rectangular. This shape is encouraged because of its simplicity (*1*).

The tools used to prepare joints for sealing and resealing are usually designed to make the joint walls vertical. The

M. F. Khuri, Modern Engineering Service Company, 2410 Darrow Drive, Ann Arbor, Mich. 48104. E. Tons, Department of Civil Engineering, University of Michigan, Ann Arbor, Mich. 48109.

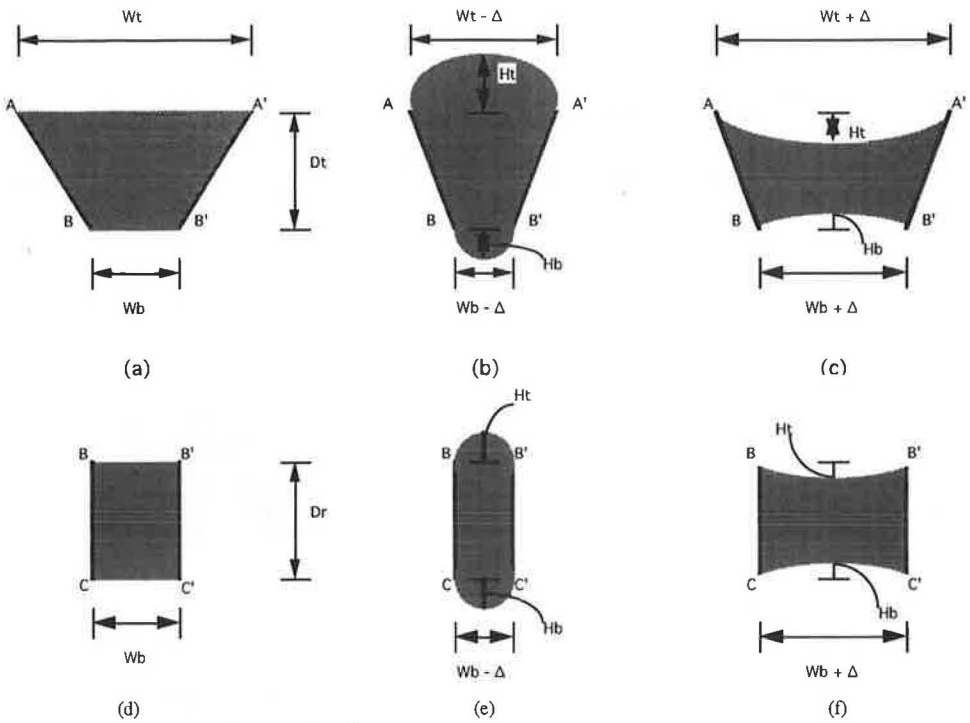

FIGURE 2 Trapezoidal seal: *a*, in its undeformed state; *b*, under compressive development; and *c*, under tensile displacement; rectangular seal: *d*, in its undeformed state; *e*, under compressive development; and *f*, under tensile displacement.

depth of the joint groove is usually controlled. Schutz (*2*) coined the term "shape factor," which has been attributed to Tons' work (*1,3*), to describe the depth-to-width ratio (D/W) of a treated joint.

A variety of sealant cross sections has been studied. Chong and Phang have experimented with a ¾- × ¾-inch cross section for transverse cracks in asphalt pavements in Canada. They also experimented with seals of dimensions 1.6 × 0.4 in. (D/W = 1/4) (*4*).

The shape factor concept for a rectangular cross section that has a D/W ratio of about 1 is generally used for sealing joints and cracks.

Trapezoidal Seals

As mentioned, trapezoidal cross sections tend to form in highway cracks because of weather and traffic. A trapezoidal cross section will also result if the crack is widened by a conical tool. Cook (*5*) mentioned that trapezoidal cross-section seals would help eliminate spalling failure in a pavement. Boot (*6*) stated that cracks do not have parallel walls like joints do, and when routed, the shape of the cross section becomes trapezoidal. Leigh (*7*), on the other hand, used trapezoidal extruded neoprene sponge rubber for cracks. The dimensions were 1- or ½-in. deep and ⅜-in. thick at the base, tapering to ¼-in. at the top.

Trapezoidal-Rectangular Seals

Trap-rec seals may exist if a crack is widened with a conical tool and not closed at the bottom by a backup rod, causing the sealant material to flow to a deeper level and making the seal cross section trapezoidal, as shown in Figure 1*c*. This cross section, as will be explained, tends to give high strains at the bottom of a seal, thereby increasing the probability of failure.

Finite Element Application

Applying the finite element method to the analysis of joint seals is a promising idea, but obtaining reliable results may be complicated. This is because rubber material used in this analysis is assumed to be incompressible, and enforcing the incompressibility condition, as far as mathematical aspects are concerned, requires special computational methods. Also, because of the large deformation encountered with sealants and the existence of a singularity, predicting the response using the classical finite element method is not very accurate. But with the use of special techniques, results can be substantially improved.

The only significant work found to have applied the finite element method to highway rubber seals was done by Wong (*8*), who used viscoelastic models. Such application is considered to be complicated, because finding the material properties and a model that predicts the behavior of the seal structure are two tedious tasks and may not be accurate. Also, the singularity at the joint-wall interface cannot be eliminated.

To analyze the response of rubberlike material, one must find the law that the material under consideration obeys. Different material laws have been suggested, such as Ogden material, Neo-Hookean material, and Mooney-Rivlin material.

The Mooney-Rivlin strain energy formulation has been used by many investigators to analyze rubberlike material (*9–15*).

The process involves determining the strain energy function of the material. Different procedures have been used to determine the strain energy function, but what is important is to fit the function to the obtained experimental data (*16–18*).

In this study the Mooney-Rivlin strain energy function was used, where material and geometric nonlinearity were assumed.

ASSUMPTIONS

Besides the fact that FEM by itself is an approximate method used in various types of structural analysis, other assumptions were made. These assumptions are as follows:

1. The material is hyperelastic, perfectly incompressible; that is, Poisson's ratio as viewed from the compressible field is equal to 0.5. This is a simplified assumption, because rubber materials in general are viscoelastic and Poisson's ratio is not exactly equal to 0.5.
2. A perfect bond is assumed between the sealant and the concrete.
3. The side at which the sealant is in contact with the concrete is assumed to be rigid or fixed in all degrees of freedom. Assumptions 2 and 3 are justified especially if the seal is handled properly (sawed, cleaned, primer is applied, and workmanship is good).
4. The sealant is assumed to be free at the bottom surface.

EXPERIMENTAL WORK

Strain Energy Function and Stress-Strain Equations

To determine the strain energy function, the use of one or more homogeneous deformations is recommended. Two homogeneous tests were used in this work, namely, simple tension and pure shear.

Specimens were prepared only with Silicone Dow Corning 888 for two main reasons:

1. Silicone Dow 888 properties do not change significantly with temperature (*19*), so it can be assumed that one strain energy function may well define the material properties at various temperature conditions—unlike rubber asphalt, for example, where one must determine the material properties at different temperatures.
2. For the same cross-sectional dimensions, FEM results for strains and displacements are the same regardless of the material type and modulus of elasticity, so it is unnecessary to do the analysis for different material properties. This is so, keeping in mind that the stresses are different but they can be normalized over the initial modulus of elasticity to give similar results for different materials.

Using the method provided in ABAQUS (*20*), which is based on minimizing the error of the function that fits both simple tension and pure shear tests, the following form of the strain energy function (U) was obtained for Silicone Dow 888:

$$U = C_1(I_1 - 3) + C_2(I_2 - 3)$$

where

$C_1 = 7.132$,
$C_2 = 7.878$,
I_1 and I_2 = first and second principal strain invariants of the left Cauchy-Green strain tensor B_{ij}, and
I_3 = third strain invariant unity (because imcompressibility condition is assumed) (*14,17*).

For a Mooney-Rivlin first-order deformation strain energy function, the stresses τ^{ij} can be obtained using the following:

$$\tau^{ij} = (2C_1 g^{ij}) + (2C_2 B^{ij}) + (PG^{ij})$$

$$g^{ij} = (g_{ij})^{-1}$$

$$G^{ij} = (G_{ij})^{-1}$$

where

$B^{ij} = (I_1 g^{ij} - g^{ir} g^{js} G_{rs})$;
g_{ij} and G_{ij} = metric tensors in undeformed and deformed configurations, respectively;
$B^{ij} = (B_{ij})^{-1}$; and
P = pressurelike variable that is calculated for every element, just like the displacement.

On the other hand, the strains ε_{ij} are of the form

$$\varepsilon_{ij} = \tfrac{1}{2}(B_{ij} - I)$$

where I is the identity matrix.

For additional and detailed explanation of the mathematical formulation and the experimental determination of the strain energy function, the reader is referred to the work by Khuri (*21*).

Determination of Top and Bottom Displacements (*Ht* and *Hb*)

Silicone Dow 888 was poured between two wood blocks that were cut to the desired dimensions. The sealant material was cast and left to cure under room temperature, then tested in the lab in tension and compression using an INSTRON machine. For a detailed description of the experimental methods, the reader is referred to the work by Khuri (*21*).

FINITE ELEMENT MODELING

Type of Element Used

Eight node elements were used throughout this study. A plane strain element called CPE8H in ABAQUS consists of eight nodes; four lie at the corners and four lie at the midpoint of each side. CPE8H is a stable element and may be best suited to model rubberlike material (*20*). The mathematical formulation of this element is explained in detail in ABAQUS (*20*) and by Khuri (*21*) and Bathe (*22*).

Number of Elements Chosen

In determining the stresses and strains in a typical seal cross section, it was observed that the response near the points A,

A', B, and B' in Figure 1*a* does not stay constant as the number of elements changes in that area (Figure 3*a*). This is because the material is fully supported at sides AB and $A'B'$ and imposing large deformation creates a discontinuity (non-Lipschitzian domain) between the material and the fixed end. This means that as one approaches the corner, the deformation tends to become tangent to the vertical axis, causing the response to increase, because the gradient tends to infinity. This means that the finite element method used is not accurate in the vicinity of the corner. However, because the objective is to compare the behavior of different seal cross sections, a model that can give values useful for comparison is needed.

It was decided to perform analyses using ABAQUS on 2-×-2, 6-×-6, 10-×-10, 20-×-20, and 80-×-80 elements. By studying the behavior of the shear strains at the integration points (Figure 3*a*), it can be observed that values are the same until the last integration point closest to the corner is reached, at which point the output of the strain is higher. Values of shear strain at the corner node versus number of elements are shown in Figure 3*b*, which shows that the value is higher for a higher number of elements and goes to infinity for an infinitely large number of elements. This again emphasizes that the finite element method does not evaluate the response accurately at the corner. However, if one finds the area under the curve in Figure 3*a* for each of the number of elements for a rectangular cross section (2 × 2, 6 × 6, 10 × 10, 20 × 20, and 80 × 80), it can be observed in Figure 3*c* that after a 10-×-10 element mesh, the area under the curve tends to be about the same regardless of the number of elements used. Because of this, it was decided to use the response that corresponds to 10-×-10 elements. These ideas were suggested by Kikuchi (*23*) and personal communications with ABAQUS consultants.

As can be observed in Figure 3*a*, if a 2-×-2 mesh is used, the shear strain obtained at the corner node may be about half of what is obtained if a 10-×-10 mesh is used. However, as the number of elements is increased, the response keeps increasing, and the upper limit tends to infinity where the $1/r$ singularity is in effect, where r is a radius that describes a domain in which, as one approaches the corner from the sealant material point of view, the stress goes to infinity.

Boundary Conditions

Modeling rectangular seals was done on the basis of 10-×-10 element mesh. After using two-directional symmetry, with respect to both x- and y-axes, a 5-×-5 element structure is obtained. All rectangular cross sections used were modeled by 5-×-5 elements regardless of the depth-to-width ratio of the seal cross section (Figure 4*a*).

Although somewhat different, both trapezoidal and trap-rec seal models may be considered under the same category and were modeled on the basis of 10-×-10 elements. After one-directional symmetry with respect to the vertical y-axis, a 10-×-5 structure was obtained. The loads and boundary conditions for trapezoidal and trap-rec cross sections are shown in Figures 4*b* and 4*c*, respectively.

RESULTS AND DISCUSSION

Comparison of Results

For the rectangular seals, laboratory results, FEM results, and the parabolic deformation model suggested by Tons (*1*) were compared. In Figure 5, *Ht* or *Hb* (*Ht* = *Hb* for rectangular sections) is plotted versus extension and contraction, respectively. The legend with subscript (FE) stands for FEM results; the legend with subscript (P) stands for parabolic model results. The legend with subscript (L) stands for laboratory results. Note that laboratory results for each specimen size are based on the average of results obtained from three specimens. Similar results were obtained when comparing laboratory results and FEM results for trapezoidal and trap-rec cross sections. Figure 5 shows that the experimental measurements are close to FEM results (range between 2 to 10 percent difference), and Tons' calculations tend to overestimate the measurements (range up to about 20 percent difference).

Comparisons Based on FEM Only

It is important to note that using the finite element method, the top and bottom displacements obtained from similar specimen dimensions gave the same top and bottom displacements and strains regardless of the material properties. This behavior is expected, because the material is considered incompressible (it deforms with no change in volume); the deformation should be the same, regardless of the modulus of elasticity of the material. This is true, even though the force required to stretch different materials to the same amount of displacement may be different, but the force can be normalized over the modulus of elasticity to give similar results.

In the following subsections, the behavior of rectangular, trapezoidal, and trap-rec seal cross sections under tensile and compressive displacements was investigated for typical selected specimens. Variations of strains and displacements in the seal structures are reported.

Comparison of Displacement (Ht *and* Hb)

In comparing rectangular, trapezoidal, and trap-rec rubber seal cross sections, it is important to understand the mechanism of deflection, in tension and in compression. In this paper, tensile displacements are emphasized. For a more detailed description of the performance under compressive displacements, see Khuri (*21*).

A trapezoidal cross section, which is the top portion of a trap-rec section, is shown in Figure 2*a* in its undeformed state; in Figure 2*c*, it is shown under tensile displacement. A rectangular cross section, which is the bottom portion of a trap-rec seal, is shown in Figure 2*d* in its undeformed condition; in Figure 2*f*, it is shown under tensile displacement. Note that *Ht* and *Hb* are identical because of symmetry. However, in Figure 2*c*, which shows a trapezoidal seal under tensile displacement, *Ht* is always greater than *Hb*. For trap-rec cross sections, behavior can not be predicted without calculations (*Ht* may be larger or smaller than *Hb*, as will be explained

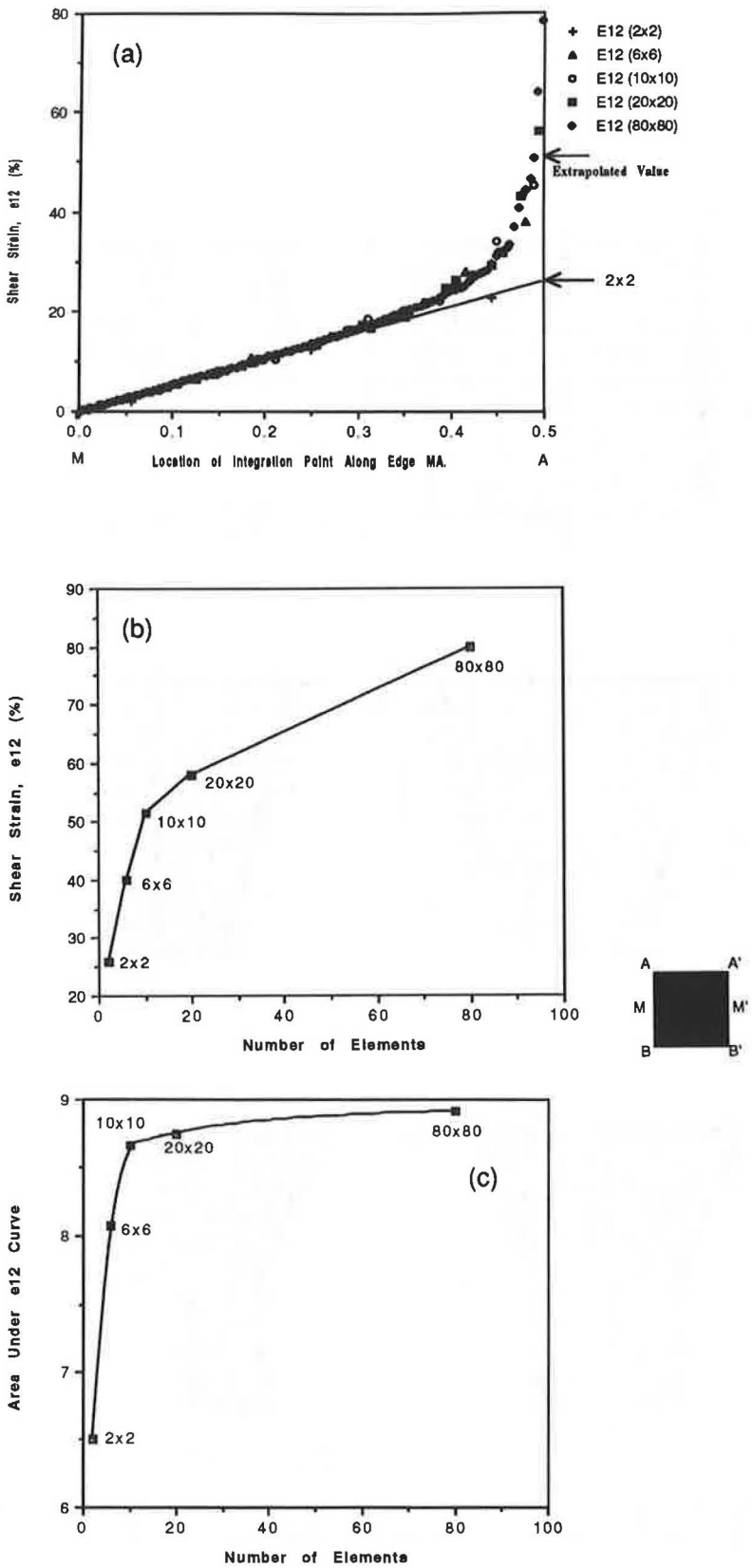

FIGURE 3 Evaluation of finite element model: *a*, shear strain versus location of corresponding integration points between *M* and *A* at 20 percent *Wb* tensile displacement; *b*, shear strain at corner node versus number of elements; and *c*, area under shear strain curve versus number of elements in FEM model.

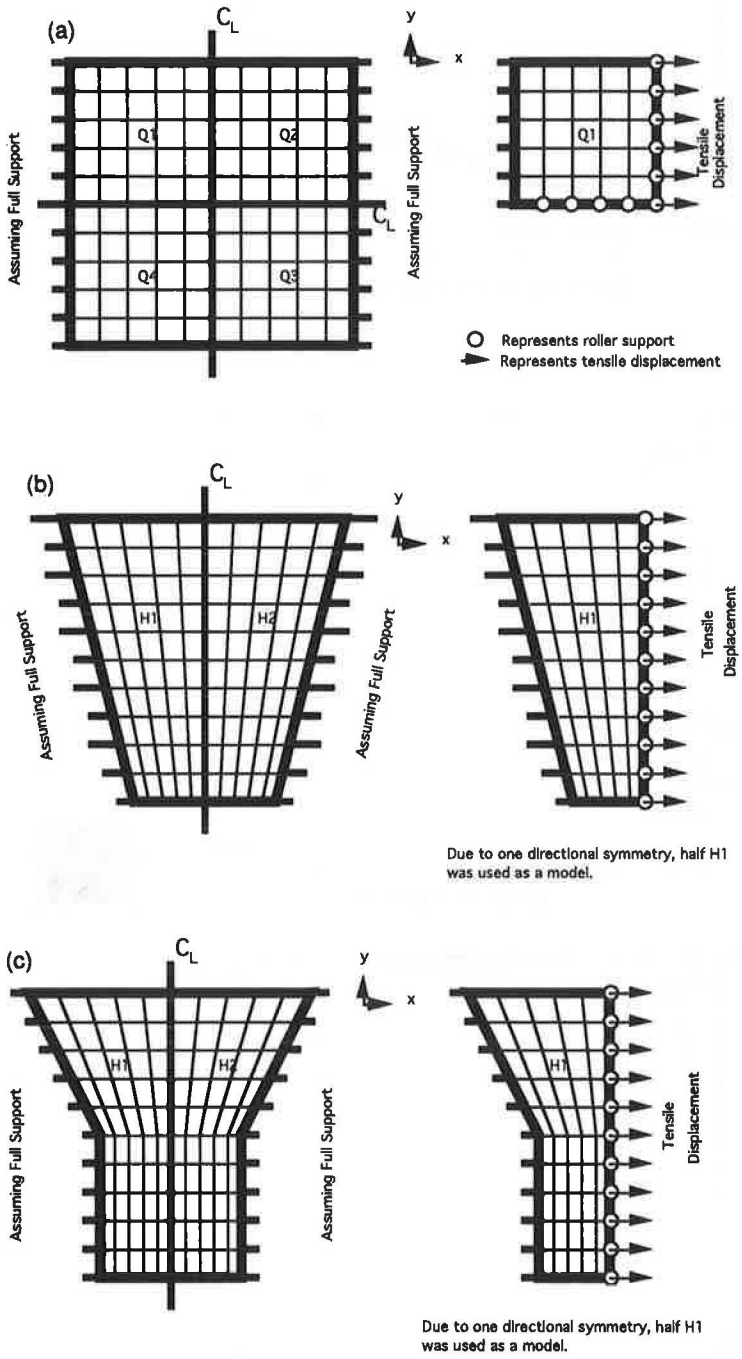

FIGURE 4 Finite element model: *a*, rectangular cross section; *b*, trapezoidal cross section; and *c*, trapezoidal-rectangular cross section.

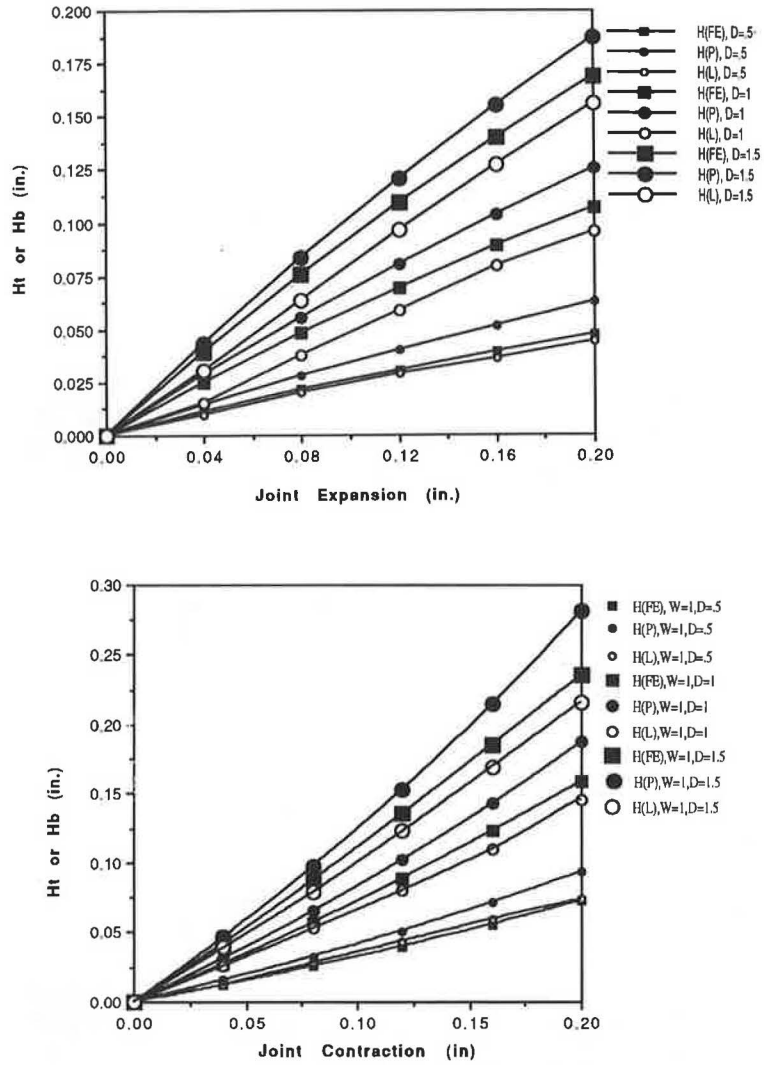

FIGURE 5 Comparison between lab, parabolic, and FEM results for Ht or Hb versus extension (*top*) and contraction (*bottom*) for different rectangular cross sections.

later). The same principle applies to seals under compressive displacement shown in Figures 2*b* and 2*e*.

Comparisons Based on Strains

In this section, strains in the x-direction (e_{11}), strains in the y-direction (e_{22}), and shear strains (e_{12}) are evaluated for all three cross sections.

Edge Conditions For all seal cross sections, edge conditions along Line ABC in Figure 1*c* yielded the highest shear strains. This is due to stress concentration near the corner. In this region, only the shear strain was considered because all other strains are zero at a fixed edge. Some values were obtained for e_{11} and e_{22} at the corners and along the edge, because in finite element analysis, response is calculated at integration points and then extrapolated to the nodes.

Shear strain (e_{12}) versus location along the depth as shown in Figure 6 is drawn at the edge for rectangular, trapezoidal, and trap-rec cross sections.

Figure 6*c* shows the shear strain behavior in a trap-rec cross section under 20 percent of Wb tensile displacement. It starts from depth equal zero at the bottom to depth equal one at the top. Shear strain (e_{12}) is highest at the bottom corner. Going up from the bottom corner, e_{12} decreases until the midline is reached, which is the point at which the rectangular cross section ends and the trapezoidal cross section starts. At this point there is a strain concentration, and on the way up toward the trapezoidal portion, the strains decrease because the imposed displacement on the seal is only 20 percent of Wb, which is 5 percent of Wt.

Figure 6*b* is plotted for e_{12} at the edge from bottom to top for a trapezoidal cross section. Shear strains are highest at the bottom, decrease to zero at about quarter of the depth going up, then increase again at the top, because of the corner.

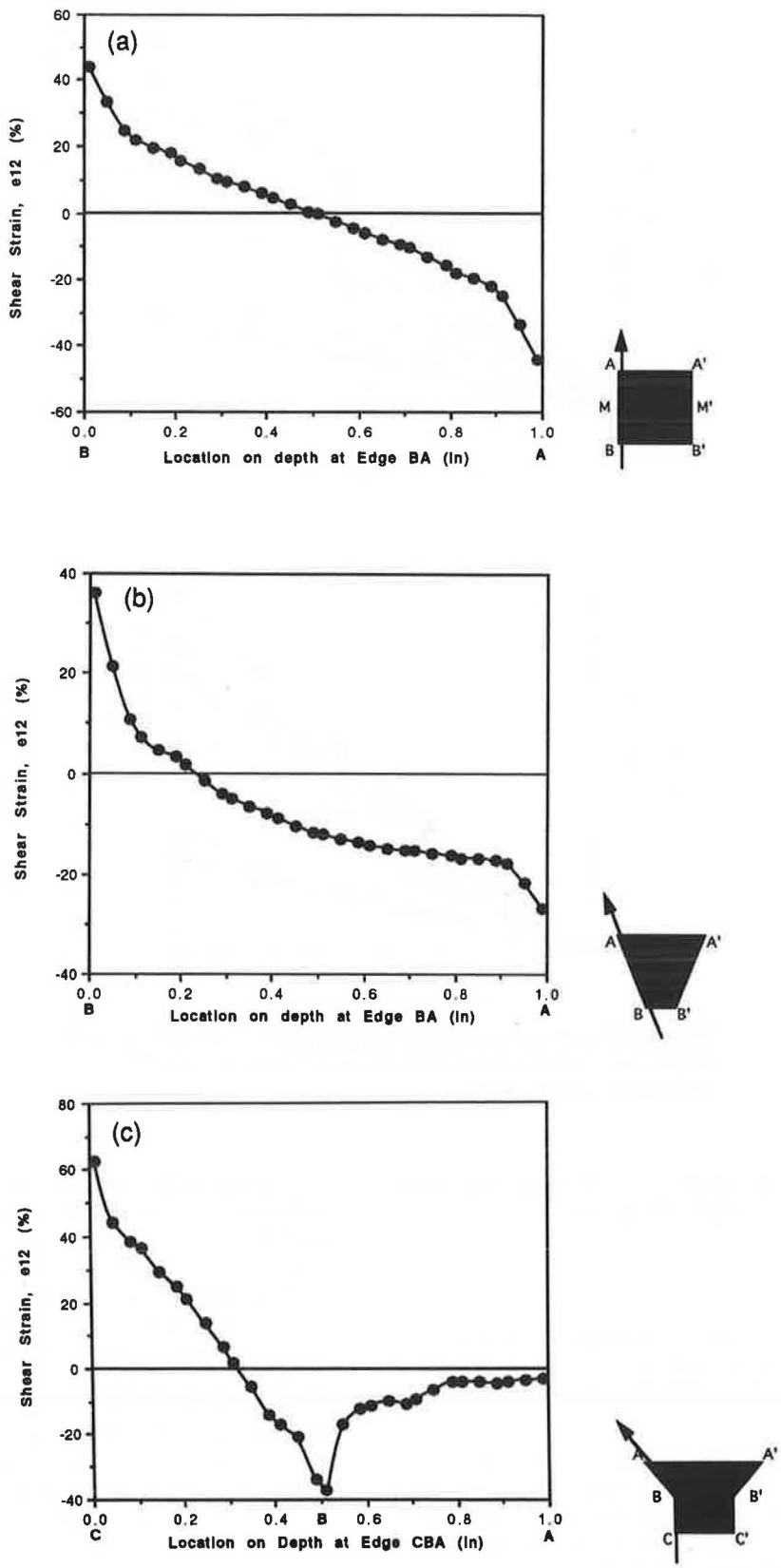

FIGURE 6 Shear strain versus location of integration points at 20 percent *Wb* tensile displacement for $D = 1$ and $Wt = 1$: *a*, shear strain along Line *BA* for seal cross section $Wb = 1$; *b*, shear strain along Line *BA* for seal cross section $Wb = 0.5$; and *c*, shear strain along Line *CBA* for seal cross section $Wb = 0.25$ and $Dr = 0.5$.

In Figure 6*a*, e_{12} is highest at the bottom or top corner, decreasing to zero at the center, and then increasing to a maximum at the other corner. Note that values at both corners are equal due to symmetry.

Centerline Conditions In Figure 7, e_{11}, e_{22}, and e_{12} are plotted at the centerline of symmetry with respect to the *y*-axis. Very consistent results are observed where e_{11} and e_{22} are equal and opposite in magnitude because the volumetric strain is zero. That is to say, since the total volumetric strain, $e_{11} + e_{22} + e_{33} = 0$, and $e_{33} = 0$, $e_{11} = -e_{22}$. On the other hand, e_{12} is always about zero at the center.

Comparison of e_{11} with Parabolic Model Figure 8 shows axial strain (e_{11}) comparison between FEM results and the results obtained by Tons' parabolic model for a rectangular cross section along Line *AA'* and *BB'* (*1*). It can be observed that e_{11} is uniform in magnitude in the interior portion of the seal, and there is an agreement in results between Tons' model and FEM all along the seal surface except at the corners of the joint-wall interface.

Effects of Variations in Cross-Section Dimensions

In the following analysis and discussion, a typical trap-rec cross section was used as the starting point with varied dimensions. Rectangular and trapezoidal cross sections were covered in the analyses of these variations.

Effects of Variations in Bottom Width (Wb)

A trap-rec cross section was analyzed for different values of *Wb*, keeping *Wt*, *Dt*, and *Dr* constant. *Wb* was varied between ⅛ and 1 in. at $Wt = 1$, $Dt = 0.5$, and $Dr = 0.5$ in. Graphs for the shear strains and maximum displacements versus *Wb* are shown in Figure 9.

It can be noticed from Figure 9 (*top*) that there is a significant increase in shear strain between values at $Wb = 1$ and values at $Wb = ⅛$ in. At 20 percent of *Wb* displacement, e_{12} at $Wb = 0.125$ is about 1.6 e_{12} at $Wb = 1$.

In Figure 9 (*bottom*), *Ht* and *Hb* are plotted against *Wb*. Note that the maximum *Ht* at $Wb = 1$ is about 3 times higher than the maximum *Ht* when $Wb = ⅛$ in. This may be because the structure is being displaced to 20 percent of *Wb*. When $Wb = ⅛$ in., the total imposed 20 percent *Wb* displacement is 0.025; when $Wb = 1$ in. the total displacement is 0.2, which is eight times larger.

Note also that *Ht* is less than *Hb* at values of $Wb < 0.35$ in. and becomes greater between values of $0.35 \leq Wb < 1$. At $Wb = 1$, the section is rectangular or square and $Ht = Hb$. This behavior might be explained as follows: when the seal is very narrow at the bottom rectangular portion, the 20 percent extension of *Wb* is small compared with *Wt* and does not have a significant effect on the trapezoidal portion.

Effects of Variations in Rectangular Depth (Dr)

The same trap-rec cross section was analyzed for different values of *Dr*, keeping *Wt*, *Wb*, and *Dt* constant. *Dr* was varied between 0 and 1.5 in. Graphs for the shear strains and maximum displacements versus *Dr* are shown in Figure 10.

It can be observed in Figure 10 (*top*) that as *Dr* increases, maximum shear strain increases significantly. That is, e_{12} for $Dr = 1.5$ is about seven times e_{12} for $Dr = 0$. This means that if the crack were closed at the bottom of the trapezoidal section, the strain concentration could be decreased seven times.

Figure 10 (*bottom*) shows *Ht* and *Hb* at 20 percent of *Wb* displacement. *Hb* at $Dr = 1.5$ is about 20 times higher than when $Dr = 0$, that is, when the section is only trapezoidal.

It is important to observe that although the top width is wider than the bottom width, it can be seen that *Hb* at high $Dr > 0.35$ tends to be larger than *Ht*, making $Ht/Hb < 1$. As the rectangular depth *Dr* increases, both displacements increase. As *Dr* reaches about 0.35, *Hb* becomes greater than *Ht*.

Effects of Variations in Trapezoidal Depth (Dt)

Again, the same trap-rec cross section was analyzed for different values of *Dt*, keeping *Wt*, *Wb*, and *Dr* constant. *Dt* was varied between 0 and 1.5 in. at constant $Wt = 1$, $Wb = 0.25$, and $Dr = 0.5$ in. Results show that *Dt*, when compared with *Dr* or *Wb*, does not have a significant effect on the change in response. For detail explanations, the reader is referred to the work by Khuri (*21*).

GENERAL OBSERVATIONS

The discussion shows that as *Dr* of a trap-rec section increases, strains, *Ht*, and *Hb* increase significantly and that as *Wb* decreases, the response increases accordingly.

In comparing Figures 9 and 10, it can be observed that an increase in *Dr*, as seen in Figure 10, has a significantly larger effect on the increase in shear strain (e_{12}) and displacements (*Ht* and *Hb*) than that of a decrease in *Wb* in Figure 9. This is because an increase in the depth of a narrow joint ($Wb = 0.25$) will increase the strains, because when $Dr = 1.5$, larger deformations will occur in the material near the bottom corner.

Also, the displacement imposed on the sealant is 20 percent of *Wb* throughout. If this crack were actually designed or assumed to be larger than the actual *Wb*, then a 20 percent displacement would give much higher values because it is not 20 percent anymore, but actually it could be 50 or 100 percent. If a crack is assumed to be ½-in. at the bottom and was designed or expected to be such, then 20 percent of *Wb* is equal to 0.1 in. However, if the crack is not closed at the bottom, the material will flow into a much smaller *Wb* than was calculated for—say, ⅛ in. This means that a 0.1-in. displacement is not 20 percent of *Wb* anymore but 80 percent of *Wb*. A displacement of 80 percent of *Wb* would cause very large strains in a seal.

As can be seen from these results, closing the bottom of the joint may improve the performance and life expectancy of crack sealants. This can be done by installing a special backup rod at the desired depth.

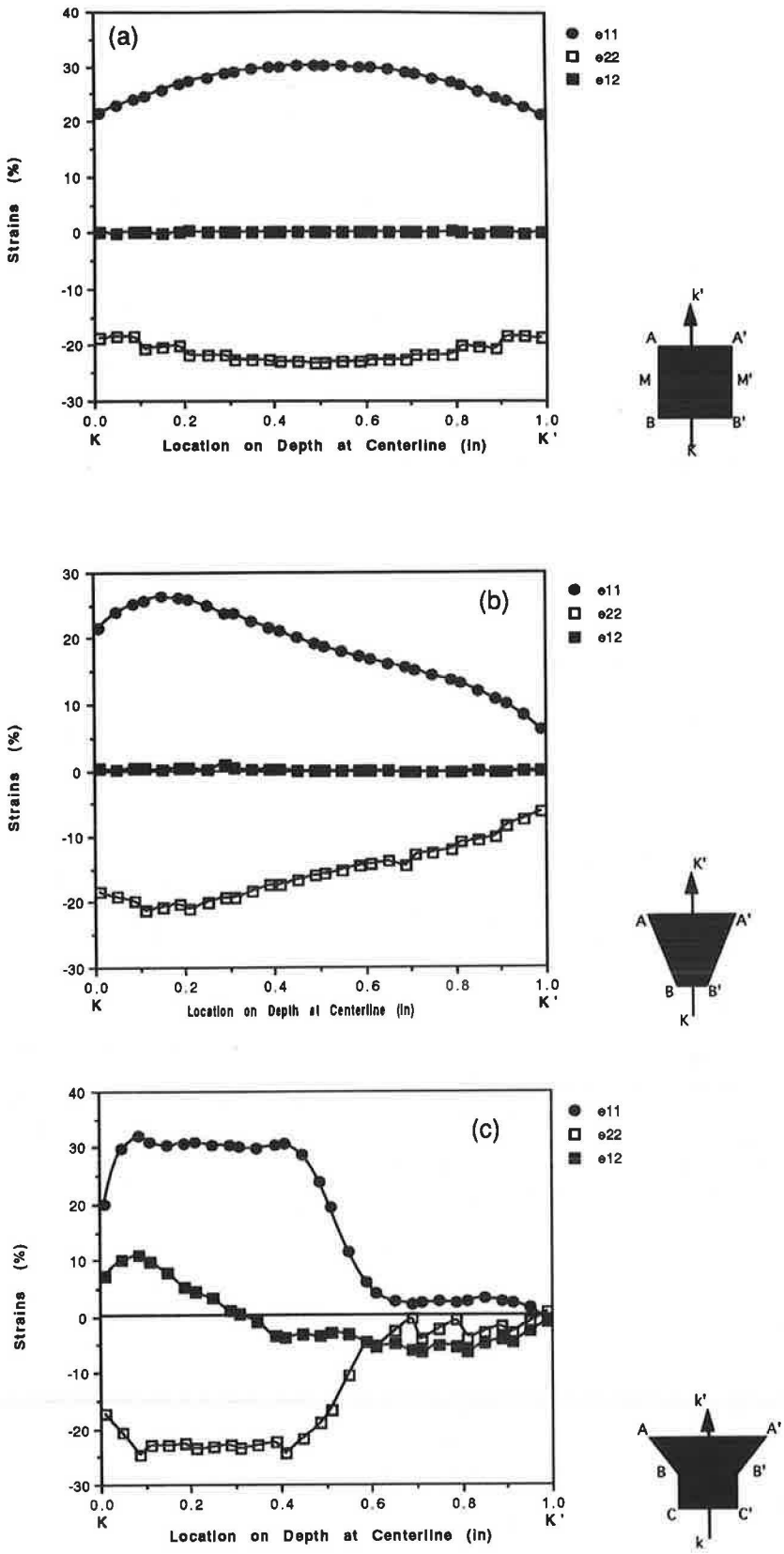

FIGURE 7 Strains versus location of integration points at 20 percent *Wb* tensile displacement for *D* = 1 and *Wt* = 1: *a*, strains along Line *KK'* for seal cross section *Wb* = 1; *b*, strains along Line *KK'* for seal cross section *Wb* = 0.5; and *c*, strains along Line *KK'* for seal cross section *Wb* = 0.25, *Dt* = 0.5, and *Dr* = 0.5.

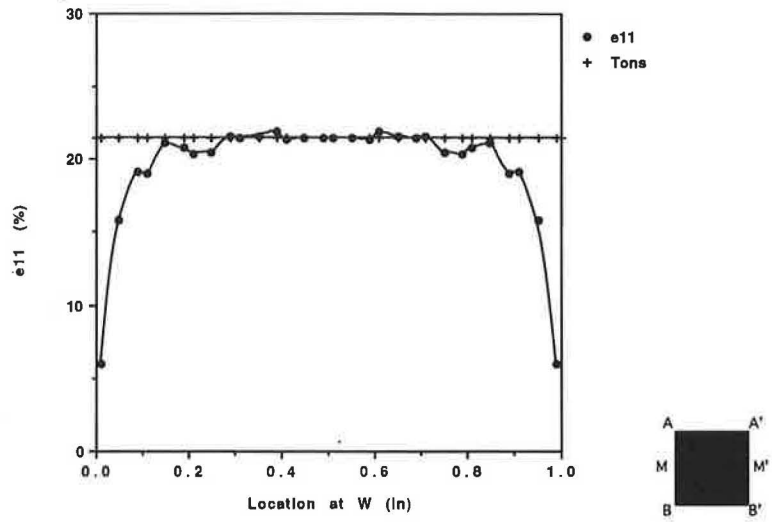

FIGURE 8 Surface strain (e_{11}) comparison between FEM results and Tons' parabolic model calculations along line *AA'* or *BB'* for a rectangular seal.

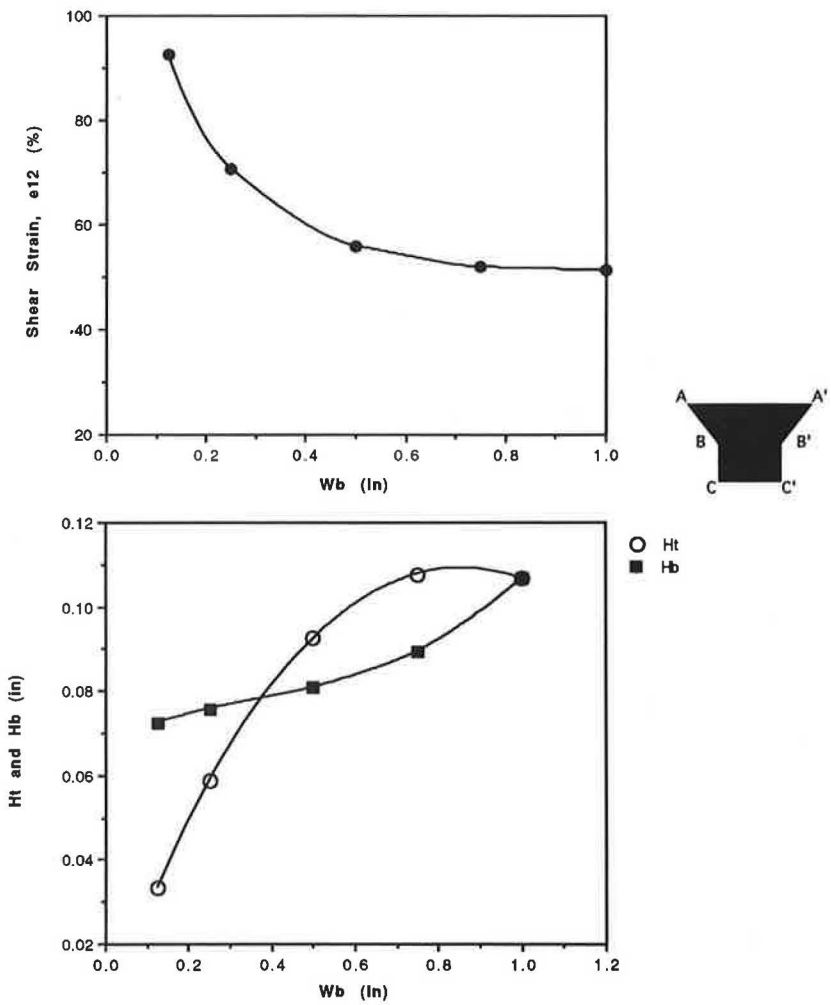

FIGURE 9 Evaluation of shear strains (e_{12}) and *Ht* and *Hb* versus changes in bottom width *CC'* for trap-rec seal at 20 percent *Wb* tensile displacement for constant *Wt* = 1, *Dt* = 0.5, and *Dr* = 0.5: *top*, shear strain versus *Wb*; *bottom*, *Ht* and *Hb* versus *Wb*.

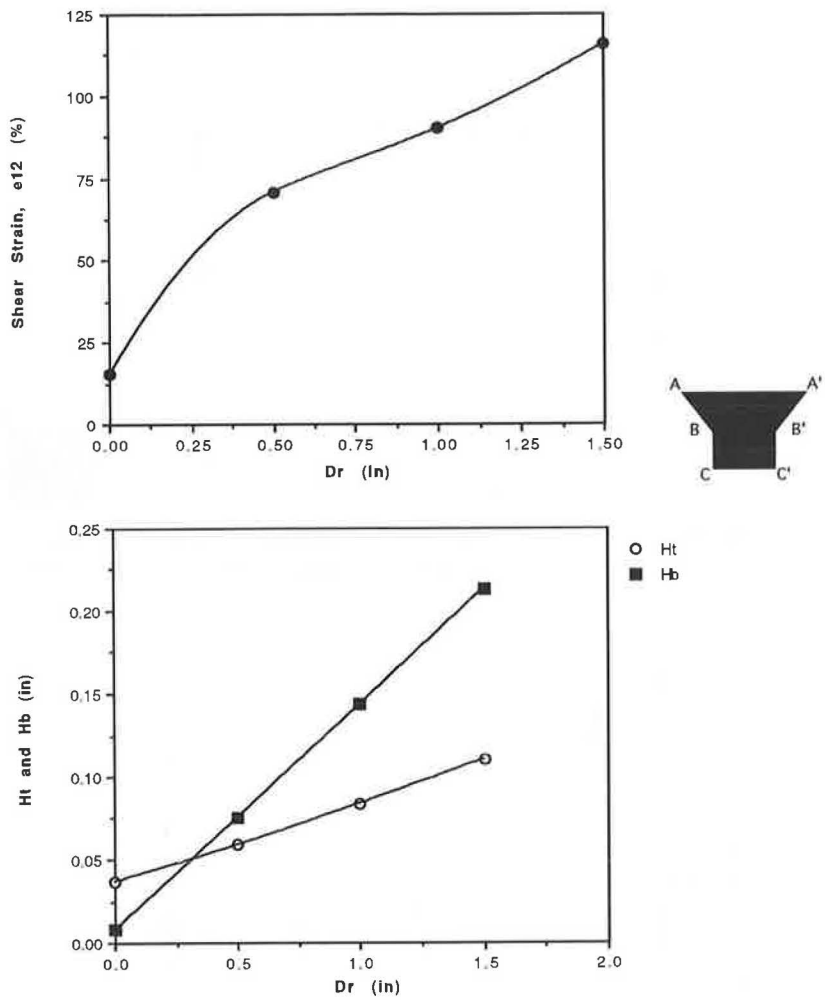

FIGURE 10 Evaluation of shear strains (e_{12}) and *Ht* and *Hb* versus changes in bottom width *CC'* for a trap-rec seal at 20 percent *Wb* tensile displacement for constant *Wt* = 1, *Wb* = 0.5, and *Dt* = 0.5: *top*, shear strain versus *Dr*; *bottom*, *Ht* and *Hb* versus *Dr*.

CONCLUSIONS

Laboratory measurements and nonlinear incompressible hyperelastic (Mooney-Rivlin) finite element formulations were used to compare different seal cross sections. Silicone Dow 888 was used for laboratory determination of the strain energy function and bulge and sag measurements. Using certain assumptions, finite element analysis was used to calculate strains and displacements. Comparisons between all cross sections were made on the basis of strains and displacements and cross-sectional variations in dimensions.

It was concluded that

1. The most desirable cross section is rectangular, because trapezoidal and trap-rec cross sections can cause high strains if not properly designed and implemented.
2. Wide and shallow seals are highly recommended; seals with a high *W/D* ratio (> 1.5) provide lower strains than those with a low *W/D* ratio.
3. *Ht* = *Hb* for rectangular cross sections and *Ht* > *Hb* for trapezoidal cross sections, but *Ht* and *Hb* for a trap-rec cross section are not predictable without calculations and depend mostly on *Dr* and *Wb*.
4. As the bottom width (*Wb*) in a trapezoidal seal is decreased and the depth is increased, strains are increased; as the material is allowed to flow deeper into a crack, it creates a point of high stress concentration. This leads to the conclusion that cracks should be closed at the bottom by a backup rod to eliminate the possibility of creating a trap-rec cross section.
5. Tons' parabolic calculations (for rectangular seals) and the finite element analysis appear to be in close agreement for the maximum displacements, bulge and sag. For the axial strain (e_{11}), results show that there is a good agreement all along the sealant surface except at the corners, where the sealant meets the joint walls. Tons' method does not apply to trapezoidal or trap-rec cross sections.
6. The FEM method used in this research seems to be promising, but it did not accurately predict the response at the corners because of a discontinuity. However, with continued research and development in this area, improvements may be expected, including new seal design procedures.

RECOMMENDATIONS

Recommendations for future research are summarized as follows:

1. Experimentally determine failure strain limit inside the seal by implanting strain gauges at the corners and throughout the seal structure and simulating environmental conditions; using these values, comparison with FEM results can be made.
2. Apply the theory of fracture mechanics to determine bond failure criteria, then use the polynomial version of the finite element method, which may be more stable at the discontinuity.

ACKNOWLEDGMENT

This paper is part of a Ph.D. thesis written by M. F. Khuri at the University of Michigan, Ann Arbor.

REFERENCES

1. E. Tons. A Theoretical Approach to the Design of a Road Joint Seal. *Bulletin 229*, HRB, National Research Council, Washington, D.C., 1959, pp. 20–53.
2. R. J. Schutz. Shape Factor in Joint Design. *Civil Engineering*, Vol. 32, No. 10, 1962, pp. 32–36.
3. E. Tons. Field Molded Joint Seal in Tension and Compression. *Joint Sealing and Bearing Systems for Concrete Structures*. Special Publication 94. American Concrete Institute, 1986.
4. G. J. Chong and W. A. Phang. *Improved Preventive Maintenance: Flexible Pavements in Cold Regions*. Research Report 8. Research and Development Branch, Ministry of Transportation and Communications, Ontario, Canada, 1988.
5. J. P. Cook. A Study of Polysulfide Sealants for Joints in Bridges. In *Highway Research Record 80*, HRB, National Research Council, Washington, D.C., 1965, pp. 11–35.
6. R. J. Boot. Sealants. *Silicone Sealants* (A. Damusis, ed.), Reinhold Publishing Co., New York, N.Y., 1967, Chapter 4.
7. J. V. Leigh. Repairing Cracked Concrete Road Slabs. *Road and Road Construction*, Jan. 13, 1965.
8. C. J. Wong. *A Finite Element Analysis of Viscoelastic Sealants*. Ph.D. thesis. University of Cincinnati, Ohio, 1984.
9. M. Mooney. The Theory of Large Elastic Deformations. *Journal of Applied Physics*, Vol. 11, 1940, pp. 522–530.
10. R. S. Rivlin and D. W. Saunders. Large Elastic Deformations of Isotropic Materials: VII. Experiments on the Deformation of Rubber. *Philosophical Transactions*, Series A, No. 243, 1950, pp. 251–288.
11. L. R. G. Treloar. *The Physics of Rubber Elasticity*. Oxford University Press, London, England, 1958.
12. A. E. Green and J. E. Atkins. *Large Elastic Deformations (and Non-linear Continuum Mechanics)*. Oxford University Press, London, England, 1960.
13. C. Truesdell and W. Noll. The Non-linear Field Theories of Mechanics. *Encylopedia of Physics* (S. Fluegge, ed.), Vol. 3. Springer-Verlag, Berlin, Germany, 1965.
14. A. E. Green and W. Zerna. *Theoretical Elasticity*, 2nd ed. Oxford University Press, London, England, 1968.
15. R. W. Ogden. Large Deformation Isotropic Elasticity—On the Correlation of Theory and Experiment for Incompressible Rubber-like Solids. *Proc., Royal Society of London*, Series A, No. 326, 1972, pp. 565–585.
16. B. G. Kao and L. Razgunas. *On the Determination of Strain Energy Function of Rubbers*. Ford Motor Company, 1987.
17. R. E. Marusak. *Determining the Parameters of Elastic Strain Energy Equations*. Report 88–04. The Texas Institute for Computational Mechanics, University of Texas, Austin, May 1988.
18. T. Scharnhorst and H. H. Pian. Finite Element Analysis of Rubber-like Materials by a Mixed Model. *International Journal of Numerical Methods for Engineering*, Vol. 12, 1978, pp. 665–676.
19. S. Spells and J. M. Klosowski. *The Importance of Sealant Modulus to the Long-Term Performance of Concrete Highway Joint Sealants*. Dow Corning Corp.
20. *ABAQUS (Finite Element Program)*, Version 4. Hibbitt, Karlsson and Sorensen, Inc., Providence, R.I., 1987.
21. M. F. Khuri. *Analysis and Design of Incompressible Rubber Seals Using Experimental and Finite Element Methods*. Ph.D. thesis. Department of Civil Engineering, University of Michigan, Ann Arbor, Dec. 1989.
22. K. J. Bathe. *Finite Element Procedures in Engineering Analysis*. Prentice-Hall, Englewood Cliffs, N.J., 1982.
23. N. Kikuchi. *Finite Element Methods in Mechanics*. Cambridge University Press, New York, N.Y., 1986.

Publication of this paper sponsored by Committee on Sealants and Fillers for Joints and Cracks.

Benefit-Cost Analysis of Lane Marking

TED R. MILLER

Pavement markings save lives and reduce congestion. A benefit-cost analysis of edgelines, centerlines, and lane lines is presented. The analysis considers marking applied with fast-drying paint or thermoplastic, the most frequently used marking materials in the United States. A literature review and telephone survey suggested striping with fast-drying paint costs $0.035/linear-ft in rural areas and $0.07/linear-ft in urban areas. Thermoplastic lines cost more than painted ones, but they can have lower life-cycle costs; in areas where snowplowing is unnecessary, they have longer lives. Published literature suggests that existing longitudinal pavement markings reduce crashes by 21 percent and edgelines on rural two-lane highways reduce crashes by 8 percent. Applying these percentages to published aggregate crash costs by roadway type yields the safety benefits. The analysis assumes markings improve traffic flow from 6:00 a.m. to 7:00 p.m. on arterials, freeways, and Interstate highways, increasing average speeds by 2 mph. On average, each dollar currently spent on pavement striping yields $60 in benefits. The benefit-cost ratio rises with traffic volume. The urban ratio is twice the rural ratio. The sensitivity analysis shows the benefit-cost ratios are robust. Where striping reduces congestion, the travel time savings alone yield a positive benefit-cost ratio for striping. Most highways already have a full complement of lines; rural two-lane highways, however, sometimes lack edgelines. Edgelines on these roads will yield benefits exceeding their costs if an average of one nonintersection crash occurs annually every 15.5 mi of roadway.

Driving down a dark road on a misty night is never pleasant. The only comfort comes from centerlines and edgelines. These pavement marking, along with lane lines, are important driving aids. The driver's manual advises watching the edgeline when blinded by oncoming headlights. Lane lines organize vehicles into efficient lanes on multilane roads. Centerlines help oncoming vehicles to avoid collisions. Even in daylight, pavement markings make it possible for vehicles to travel more safely and quickly. They reduce congestion and raise roadway capacity.

This paper probes the costs and benefits of roadway pavement markings. It restricts itself to edgelines, centerlines, and lane lines, the longitudinal lines that run parallel to traffic. It shows that existing markings on different classes of roads have benefit-cost ratios ranging from 21 to 103. Most roads already have a full complement of lines. Some rural two-lane highways, however, lack edgelines; a few even lack centerlines. Edgelines would be cost-effective on a mile of rural two-lane highway if one crash a year occurred outside the roadway every 15.5 mi.

MARKING MEDIA

Longitudinal pavement markings typically are applied using a liquid marking medium or binder that is visible during the day. The medium binds glass beads that make the lines visible when headlights shine on them at night. The principle underlying night visibility is retroreflectivity. Retroreflection means light reflects off the binder-coated backs of the beads and is returned to its source. Because the beads are almost perfectly round, the retroreflected light is concentrated in a small angle of return, making the marking conspicuous.

Existing binders include fast-drying high-solvent paint, latex paint, thermoplastic, epoxy, and polyester. Some markings are also applied using preformed tape. This paper computes benefit-cost ratios for the marking media that historically captured the largest market shares: high-solvent paint and thermoplastic. Other media, especially latex paint, have gained market share recently.

Fast-drying high-solvent paint has dominated the U.S. market for many years. It is inexpensive to buy and apply. Because it dries quickly, a trailing vehicle moving at 10 to 15 mph can prevent traffic from tracking the newly applied paint. High-solvent paint has two drawbacks: a short life, often as little as 6 to 12 months, and environmentally damaging emissions during application. The newer latex paints are waterborne rather than solvent-borne. Thus, they avoid emission problems. Most latex formulations dry more slowly than high-solvent paint; typically, application proceeds at 5 mph.

Thermoplastic has captured roughly an eighth of the U.S. striping market. Although costly to buy and apply, it has a long life—4 to 7 years. Thermoplastic lines are much thicker than painted lines, which makes them more vulnerable to snowplow damage. Contractors apply most thermoplastic in most states.

BENEFIT-COST EQUATION

The benefit-cost ratio (BCR) computed in this paper equals the monetized benefits from pavement marking divided by the marking costs. Let B equal the benefits expected per year from pavement marking and C equal the annualized marking costs. Then the benefit-cost ratio is

$$\mathrm{BCR} = B/C \tag{1}$$

The benefits include increased safety and reduced travel time.

UNIT COSTS OF MARKING

Pavement markings rarely require maintenance between applications. Their useful life ranges from 6 months to 7 years depending on the marking medium, traffic volume, location (lane lines and centerlines require more frequent replacement

The Urban Institute, 2100 M Street N.W., Washington, D.C. 20037.

than edgelines), and snowplowing (plowing bare road causes rapid deterioration). The annualized application costs are

$$C = M + P + E + \text{ADMIN} \quad (2)$$

where

M = annualized materials costs, including binder, beads, and fuel;
P = annualized personnel costs, including wages, fringe benefits, and per diem when striping crews are away from home overnight;
E = annualized costs of equipment and storage facilities; and
ADMIN = annualized contract letting, monitoring, and other administrative costs.

The annualized costs include multiple applications for which the useful life is less than a year. The annualization multipliers used were capital recovery factors computed using the formula by Winfrey (*1*). The analysis used a discount rate (present value factor) of 4 percent. That rate is recommended for use in analyzing highway safety countermeasures with lives less than 5 years (*2*). The sensitivity analysis examined the benefit-cost ratio at a 10 percent discount rate.

Data on marking costs were drawn from a literature review and a telephone survey. Table 1 summarizes the cost estimates per application. The top panel in the table shows published estimates; the bottom panel shows the estimates from the telephone survey. Typically, the installed cost of high-solvent paint, in 1991 dollars, is $0.035/linear-ft of 4-in. stripe in rural areas and $0.07/linear-ft in urban areas.

Thermoplastic costs vary widely, ranging from $0.15 to $0.40/linear-ft. The average is $0.32/linear-ft. Reasons that the telephone survey suggested for the wide variation include

- Thermoplastic lines range from 60 to 120 mils in thickness (with corresponding differences in materials cost and useful life).
- The war-related surge in oil prices at least temporarily raised materials costs.
- Contractor availability varies—prices are higher where contractors are scarce.
- Thermoplastic is produced primarily in southern and western factories, and shipping it elsewhere is costly.
- Thermoplastic costs are sensitive to propane costs, which vary regionally (propane is used to heat and agitate the thermoplastic).

Rural-Urban Variation

Most published costs are state averages. They mask substantial variability. Costs are low in suburban and rural areas where daylong striping will not disrupt traffic significantly. Urban striping costs often are higher. Reasons that the telephone survey suggested for higher urban costs are

- The striping day is short to avoid delaying rush-hour traffic.
- Striping roads with daylong congestion requires extra staff and equipment to control traffic.
- More time and care are required because the longitudinal pavement markings must mesh with many crosswalks, stop lines, and other special markings.

TABLE 1 PAVEMENT MARKING COSTS

Source	Year	High VOC Paint Avg ($/ft)	High VOC Paint Range ($/ft)	Thermoplastic Avg ($/ft)	Thermoplastic Range ($/ft)
Henry et al. (*14*); 14 states	1988	.035	.02-.055	.35	.17-.60
Aurand et al. (*11*); 9 states, 6 manufacturers	1988	.035		.17	
Hughes et al. (*15*); state survey	1983	.035	.02-.07		
Attaway et al. (*16*); N.C.	1988		.03-.045		.28-.40
Mendola (*17*); N.J.	1988				.15-.28
DePaulo (*18*); Ohio	1988	.035	.035-.04		
SASHTO (*19*); 14 states	1991	.035	.02-.05	.24	.12-.40
California	1990	.035	.10contr	.26	
Colorado	1991	.04	.055contr	.40	
Florida	1991	.04	.08contr		.25-.35
Illinois	1991	.02		.37	
Los Angeles, Calif.	1991	.06		.28	
Maine	1991	.035			
Md./Va. contractor	1991			.32	.30-.50
Montana contractor	1991		.04-.045		
North Carolina	1991	.03	.09contr	.35	
Phoenix, Ariz.	1991	.07	.085contr	.29	
Texas	1991	.035rur, .07urb		.35	.22-.45

NOTE: All items inflated to December 1990 dollars using the Consumer Price Index.

Comparing costs between striping media requires caution. The costs for high-solvent paint in Table 1 assume lines will retrace existing lines. Such restriping generally is done by state forces. Striping after repaving or chip sealing requires premarking to establish line locations. This costs perhaps $0.005 to $0.01/linear-ft. The paving contract generally includes premarking and striping. Because striping usually is subcontracted, contract costs include two tiers of administrative expenses and profits. Unlike painting contracts, thermoplastic contracts are often first-tier contracts.

The contract paint and thermoplastic costs in Table 1 exclude the costs of contract letting and monitoring. The Texas Department of Transportation (DOT) estimated these costs at 5 percent of the contract price. The North Caroline DOT, which inspects more extensively than most, estimated the costs at 7 percent.

Values Used

The analysis used the following marking costs and material lives:

- $0.035/linear-ft rural and $0.07/linear-ft urban for high-solvent paint, with restriping every 6 months on Interstates, other freeways, and major urban arterials, and every 12 months on other roads. At a 4 percent discount rate, the annualized costs per mile are $381 for rural Interstates, $192 for other rural roads, $762 for urban freeways and major arterials, and $385 for other urban roads. For striping and premarking by contractors every seventh year, $0.09/linear-ft, implying an annualized premarking premium of $49/mi rural and $18/mi urban. Including the premarking cost, for example, the annualized cost per mile on most rural roads total $241. These costs assume all lines are solid, single stripes. The sensitivity analysis examines an alternative assumption.
- $0.26/linear-ft rural and $0.33/linear-ft urban for thermoplastic, with restriping every 5 years. Where climate is appropriate for thermoplastic, state materials choices suggest its life-cycle costs are competitive with high-solvent paint if average daily traffic (ADT) exceeds roughly 2,500. The annualized costs per mile are $308 rural and $391 urban.

Miles Striped

The miles striped by roadway type and land use were computed using data on number of lanes by roadway mileage from FHWA's 1988 highway statistics (*3*). Undivided highways require one edge or lane line per lane and a centerline. For example, a four-lane highway requires two edgelines, two lane lines, and a centerline; a six-lane highway requires two more lane lines. Each side of a divided highway requires one edge or lane line per lane and an additional edgeline. Line mileage was computed using the following assumptions:

- Divided Interstate highways with more than four lanes have an average of seven lanes in urban areas and six lanes in rural areas.
- Other divided urban freeways with four or more lanes average five lanes. Divided major arterials average 4.5 lanes.
- Other divided roads with four or more lanes average four lanes.
- Undivided roads with more than two lanes average four lanes.

The first column of data of Table 2 shows the line miles by roadway functional class (excluding local streets, which are rarely wide or heavily traveled enough to stripe) and rural-urban land use. Rural roads, primarily major collectors, account for more than 75 percent of the line miles.

BENEFITS OF MARKING

The benefits of marking, B in Equation 1, are the present value of the sum of the annual benefits. The benefits for a 1-mi road segment are

$$B = A * R * CS + V * T(1/S_O - 1/S) \quad (3)$$

where

A = crashes per year on road segment,
R = fractional reduction in crashes expected due to marking,
CS = cost savings per crash prevented,
V = annual traffic volume on road segment,

TABLE 2 LINE MILES AND CRASH COSTS BY ROADWAY FUNCTIONAL CLASS AND LAND USE, EXCLUDING LOCAL STREETS

Road Type	Urban Line Miles	Urban Costs	Rural Line Miles	Rural Costs
Interstate	84,520	$12,230	201,525	$10,489
Other freeway	51,187	6,602	0	0
Major arterial	238,852	58,260	303,499	23,102
Minor arterial	270,822	41,963	460,750	23,094
Major collector	245,512	17,136	1,321,942	30,330
Minor collector	0	0	886,192	14,642
Total	890,893	$136,191	3,173,908	$101,657

NOTE: Costs in millions of December 1990 dollars.

T = value of 1 vehicle-hr of travel time,
S_O = average speed on road segment before marking, and
S = average speed on road segment after marking.

Cost Savings of Crash Prevention

Safety benefits—the crash cost savings—were adapted from data from Miller et al. (*4*). They include medical, emergency services, workplace, legal, property damage, travel delay, and administrative costs, as well as lost wages and household production; and pain, suffering, and lost quality of life. The benefit values were derived using the method dictated by FHWA (*5*) and the U.S. Office of Management and Budget (OMB) (*6*) for valuing life-saving benefits.

The analysis by roadway functional class (e.g., rural Interstate, urban arterial) uses total crash costs by road type and land use from Miller et al. (*4*). Total crash costs equal $A_i * CS$. The second data column in Table 2 summarizes the costs. The cost savings equal these costs times R.

To analyze striping benefits for rural two-lane roads in more detail, the nonfatal injury benefits were tailored to the injury distribution for related crashes. These include crashes with first harmful events outside the roadway and head-on crashes. The injury distribution was computed using 1984 National Accident Sampling System data.

The related crashes are costly. The average benefit per related crash prevented, including fatal crashes and property-damage-only crashes, is $95,000 (in December 1990 dollars). The benefits are $3,079,000 per fatal crash prevented and $154,000 per injury crash prevented. By comparison, Miller et al. (*4*) find that the average benefits of crash prevention are $48,000 for a police-reported crash and $79,000 for a police-reported injury crash.

The safety benefits given by Miller et al. (*4*) are for a 4 percent discount rate. For the sensitivity analysis, benefits at 10 percent were taken from unpublished tables supporting Miller et al.

Table 3 compares the costs per injury by police-reported severity at 4 percent and 10 percent discount rates. The nonfatal injury costs with a 10 percent discount rate are higher, an apparent anomaly. This occurs for two reasons. First, the value placed on the sum of lifetime earnings and quality of life is computed independent of the discount rate by Miller et al. (*4*) [using the method prescribed by OMB (*6*)]. The sum equals $2.5 million (in December 1990 dollars). Although earnings losses are less at a higher discount rate, because the sum is a constant, the value placed on lost quality of life rises by an offsetting amount. Second, to value the lost quality of life resulting from nonfatal injury, Miller et al. (*4*) apply the discount rate to compute a value per life year for lost quality of life. At a 4 percent discount rate, the loss per year equals the total loss divided by 20.8; at 10 percent, it equals the total divided by 10.2. Because nonfatal injuries affect quality of life predominantly in the year of the injury, the much higher value for a year of lost quality of life yields a higher average injury cost, even though costs in future years have a lower present value at the higher discount rate.

Percentage Reduction in Crashes Attributable to Pavement Markings

A literature review of the percentage of crashes prevented by longitudinal pavement markings revealed several studies that used treatment and control groups. It also revealed some studies without well-matched controls and values from some studies without proper bibliographic references. Table 4 summarizes all the percentages. Most studies supplemented existing centerlines with edgelines.

Average effectiveness was computed for all the studies and for several subsets. The subsets included

- Studies of edgelines only,
- Studies of edgelines excluding the highest and lowest effectiveness estimates, and
- Studies that were examined and judged sound.

The averages ranged from 20 to 21 percent. The average for sound studies examined was 21 percent. This paper assumes that roads already are marked, meaning the present crash levels are 21 percent lower than the levels without markings. Expressed in terms of current crash rates, the percentage reduction in crashes due to striping is $100 * .21/(1 - 0.21) = 26.5$ percent.

The best U.S. effectiveness study is that by Bali et al. (*7*), who examine rural two-lane roads. This 10-state study includes more than 500 sites. Each site had either a significant and adequately maintained, nonexperimental change in delineation 2 or 3 years before the study or an undelineated,

TABLE 3 COSTS OF AN INJURY BY POLICE-REPORTED SEVERITY AND DISCOUNT RATE

Police-Reported Severity	Cost by Discount Rate 4%	10%
K - Fatal Injury	$2,392,742	$2,360,330
A - Incapacitating Injury	169,506	190,069
B - Evident Injury	33,227	43,770
C - Possible Injury	17,029	27,757
O - Property Damage Only	1,734	1,734

SOURCE: Miller et al. (*4*) and unpublished supporting materials, inflated to December 1990 dollars.

TABLE 4 REDUCTION IN CRASHES DUE TO LONG LINES

	Reduction (%)
Edgelines	
United States	
Nationwide (*7*)	8
Kansas (*21*)	16.5
Kansas (*22*)	14.5
Ohio (*23*)	19
Illinois (*22*)	21
Idaho (*22*)	16
Utah (*22,24*)	38
Arizona (*22*)	60
Michigan (*22*)	3
England (*25*)	
East Sussex	18
South Yorkshire	30
Cornwall	26
Northamptonshire	12
Hertfordshire	22
France (*26*)	
Lorraine	27
Germany (*20*)	
Hesse	20
Lower Saxony	25
Centerlines	
United States (*7*)	29
Bavaria (*20*)	10

matched control site. Data were obtained on crash experience for 2 to 3 years at each site (at least 2 years before and 2 years after delineation for the sites with delineation added). The study finds that adding edgelines and centerlines reduces crashes by 36 percent. Adding edgelines to a centerline yields an 8 percent reduction. These percentages were used in the more detailed analysis of marking rural two-lane roads.

Using the percentage reduction in crashes to compute safety benefits should yield conservative estimates. Several published studies suggest the percentage of injuries and fatalities reduced is greater than the percentage of crashes reduced.

Travel Time Savings

The benefit-cost ratios by roadway type include travel time saved because edgelines and centerlines let traffic go faster on busy roads. The analysis assumes

- Travel time was saved during the peak period of 6:00 a.m. to 7:00 p.m. Eighty percent of vehicle miles of travel (VMT) occur during this period (*8*,Table 5-5). Weekend and weekday travel generate roughly the same percentage of travel miles per day (8, Table 5-9). Furthermore, trips are heavy in all hours from 6:00 a.m. to 7:00 p.m., ranging from 5.4 to 6.3 percent of all trips in each peak hour before 4:00 p.m. and after 6:00 p.m. and 8.1 percent between 4:00 and 6:00 p.m. (*8*,Table 5-5).
- Pavement markings raised speeds, thus saving travel time, only on Interstate highways, other freeways, and arterials.
- The average 56-mph speed on these roads (*3*) would fall to 54 mph during the peak travel period if the roads were lacking lane lines, edgelines, and centerlines.

The analysis uses travel time values of 60 percent of the wage rate for the driver and 45 percent for passengers. These values are recommended by Miller (*9*), who critically reviews the literature. They also are used in FHWA's Highway Economics Requirements System model. The average vehicle has 0.7 passengers (*8*,Table 8-1). Time of day and day of week do not unduly affect occupancy (*8*,Figure 8-6), so it is reasonable to use this occupancy for peak-hour trips.

The value of travel time saved per vehicle is 60 percent + 45 percent * 0.7 = 91.5 percent of the wage rate. The average nonsupervisory wage in 1990 was $9.66/hr (*10*). Thus, a vehicle hour of travel time (T in Equation 3) is worth $8.84.

Table 5 shows the annual VMT by roadway class (V in Equation 3).

BENEFIT-COST RATIOS BY ROADWAY TYPE AND LAND USE

Applying Equation 3 to the data given above yields benefit-cost ratios by roadway type and land use. Table 5 shows the benefit-cost ratios for high-solvent paint (as well as VMT).

TABLE 5 ANNUAL VMT (IN MILLIONS) AND BENEFIT-COST RATIO FOR LONGITUDINAL PAVEMENT MARKINGS BY ROADWAY FUNCTIONAL CLASS AND LAND USE, EXCLUDING LOCAL STREETS

Roadway Class	Urban		Rural		All
	VMT	BCR	VMT	BCR	BCR
Interstate	258,662	74.1	181,284	46.3	58.3
Other freeway	116,965	63.4	0	--	63.4
Major arterial	319,286	102.0	160,253	105.2	102.9
Minor arterial	231,786	125.8	151,783	68.9	97.1
Major collector	99,245	52.2	183,507	28.6	34.2
Minor collector	0	--	46,985	20.6	20.6
Total	1,025,944	90.6	723,812	40.1	60.0

SOURCE (VMT): FHWA (*3*)

Nationally, pavement striping has a benefit-cost ratio of 60. On average, each dollar spent on longitudinal pavement markings yields $60 in increased safety and reduced congestion benefits. The benefit-cost ratio is highest on arterial roads. The urban ratio is more than twice the rural ratio. Annual benefits average $19,226/line-mi.

The sensitivity analysis showed that the benefit-cost ratios were robust. The ratios by land use were not greatly affected by choice of marking medium, changed assumptions, or introduction of additional cost considerations. Table 6 summarizes the ratios.

Varying the paint cost affects the benefit-cost ratios, but it does not change their order of magnitude. Assuming a uniform restriping frequency of 9 months lowers the rural benefit-cost ratio but raises the urban ratio. Wear and tear, especially in the winter, probably reduces nighttime marking effectiveness to 9 months except on lightly traveled minor rural collectors. Because the effectiveness studies involved annual restriping, the effectiveness estimates already should incorporate this temporal decline. Assuming that they do not would reduce the benefit-cost ratio by 15 percent.

Typically, high-solvent paint releases 69 lb of volatile organic compounds (VOCs) per mile of solid 4-in. stripe (*11*). VOCs oxidize, creating ozone that can cause respiratory distress for sensitive people. They also are suspected carcinogens. Krupnick and Kurland (*12*) suggest valuing the short-term health effects of VOCs at $620/ton (inflated to December 1990 dollars). Each restriping, the cost is $21/mi of solid stripe. This value is primarily for the northeastern United States, but it is suspected to be a reasonable national average (personal communication, 1991). The value does not consider the long-term cancer risk or any effect on plants and animals.

The environmental costs suggest latex paint would be more cost-effective than high-solvent paint if its applied cost were another $0.004/linear-ft ($1.30/gal). The better durability of some latex paints might justify an even greater cost. These conclusions apply only to latex paints with fast drying times.

In climates where thermoplastic markings are practical, their long life makes their life-cycle cost competitive with painted markings. They are especially competitive on high-volume urban roads. For ease of comparison, the ratios for thermoplastic were computed as if it could be used nationwide.

The benefit-cost ratios presented so far assumed all longitudinal pavement markings are single, solid lines. In reality, centerlines often are doubled, then dashed in passing zones. The industry rule of thumb is that a centerline on a two-lane road takes 1.3 times as much paint as a solid line. Conversely, lane lines are dashed. Typical lane lines are 10-ft stripes separated by 30-ft gaps in rural areas and 9-ft stripes with 12-ft gaps elsewhere. Applying these ratios to the estimated line miles marked yields paint miles. Costing with paint miles raises the benefit-cost ratio slightly. Table 6 shows the revised ratios both excluding and including environmental damage.

The benefit-cost ratio of 59 with environmental damage and paint miles may be more accurate than the ratio for 60 for the base case. Considering these additional costs raises the urban benefit-cost ratio but lowers the rural ratio.

Another possible model refinement would assume that longitudinal pavement markings prevent unreported crashes as effectively as they prevent reported crashes. Applying the underreporting estimates from Miller et al. (*4*) yields substantially higher benefits. It raises the benefit-cost ratio for all roads to 76.

Omitting the travel time savings affects the benefit-cost ratios only for congested roads. On these roads, savings in travel time alone would justify longitudinal pavement markings. On major rural roads, the benefit-cost ratios for these markings range from 6.4 to 10.2 if only reduced congestion is considered. On major urban roads, they range from 8.0 to 18.3. Where pavement markings will ease congestion, they almost surely will be cost-beneficial.

Ignoring the extra cost of contract pavement markings at repaving would raise the benefit-cost ratio. Using a 10 percent discount rate would affect the benefit-cost ratio minimally.

EDGELINES ON RURAL TWO-LANE ROADS

The lowest benefit-cost ratios for longitudinal pavement markings are for edgelines on rural two-lane highways. This section examines the benefit-cost ratio for these lines in more detail. It again uses Equations 1 through 3. The analysis is by average daily traffic volume. It ignores any travel time savings.

TABLE 6 BENEFIT-COST RATIOS BY RURAL-URBAN LAND USE, SHOWING EFFECTS OF ALTERNATIVE ASSUMPTIONS AND MARKING MEDIA

	Rural	Urban	Combined
Using High-Solvent Paint (Base Case)	40.1	90.6	60.0
Using a Paint Cost That Is $.005			
Higher	36.2	82.6	54.4
Lower	45.0	100.5	67.1
Uniform 9-Month Striping Cycle	33.4	96.3	54.6
Effective Only for 9 Months Except on Minor Rural Collectors	31.6	80.1	50.7
Costing VOC Damage To Environment	36.7	85.7	55.6
Using Thermoplastic			
$.26/ft rural	32.9	130.0	58.9
$.22/ft rural	38.8	130.0	66.4
Adjusting Paint Use for Unpainted Parts of Lane Lines and Double/Skip Parts of Centerlines	41.6	99.3	63.6
Costing VOC Damage and Adjusting Paint Use	38.1	94.0	58.9
Including Crashes Not Reported to Police	51.2	114.5	76.0
Omitting Travel Time Savings	38.1	81.9	54.9
Ignoring Higher Cost At Repaving	49.7	93.5	69.1
Applying a 10% Discount Rate	38.8	93.5	59.9

Bali et al. (*7*) find edgelines prevent 0.72 crashes per million VMT on rural two-lane roads. Multiplying this value times the ratio of fatal crash rates per million VMT on rural federal-aid secondary roads in 1988 and 1978 [from FHWA (*13*)] suggests 0.48 crashes would be prevented today. This estimate is conservative, because nonfatal injury rates probably fell less than fatality rates (*13*). The low quality of the nonfatal injury data precludes their use in adjusting to present crash rates.

Figure 1 shows the benefit-cost ratios. Even at 500 ADT, edgelines on rural two-lane roads yield $17 in safety benefits for every dollar invested.

Bali et al. (*7*) find that edgelines reduce crashes by 7.9 percent on rural two-lane roads with lane widths of 11 ft or more. Using that estimate, the number of crashes per year needed to justify striping (A) can be computed as

$$A = C/(CS * R)$$

$$= 2 \text{ edgelines} * \$240/\text{mi}/(\$95{,}074/\text{crash} * .079)$$

$$= .064 \qquad (4)$$

Edgelines are justified on a rural two-lane highway with .064 or more crashes per mile per year. Interpreting this number conservatively, edgelines are justified if an average of one nonintersection crash occurs annually every 15.5 mi. Bali et al. (*7*) recommend against edgelines, however, if lane widths are less than 11 ft.

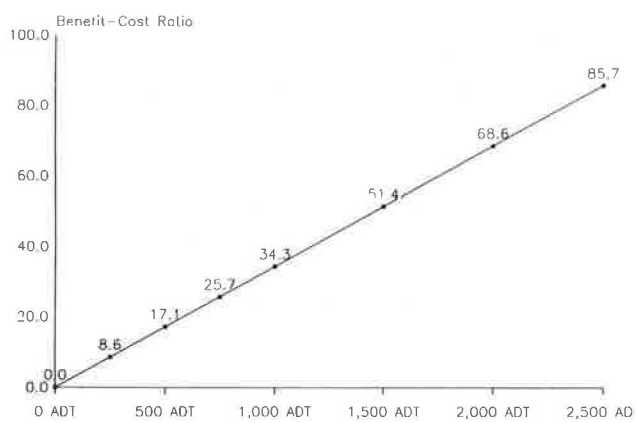

FIGURE 1 Benefit-cost ratio by ADT for edgelines on rural two-lane roads.

CONCLUSION

Existing longitudinal pavement markings yield benefits far greater than their costs. They increase safety and reduce congestion. Much of the safety benefit is achieved during periods of poor visibility. That suggests checking roadway retroreflectivity regularly and restriping promptly when retroreflectivity drops below recommended levels.

Edgelines may not be used often enough on rural two-lane roads in some states. The number of nonintersection crashes needed to justify edgelines is quite small. Rural collectors have far higher crash costs per million VMT than other roads (*4*). Wider use of edgelines on these roads may be a cost-effective way to cut the crash toll.

ACKNOWLEDGMENTS

The American Glass Bead Manufacturers Association funded this study. Study liaison Dave Mastro of Potters Industries provided many helpful insights. Thanks to the many government agencies and AASHTO affiliates that provided data on striping costs and useful lives.

REFERENCES

1. R. Winfrey. *Economic Analysis for Highways*. International Textbook Company, New York, N.Y., 1968.
2. T. R. Miller, B. E. Whiting, B. C. Kragh, and C. Zegeer. Sensitivity of a Highway Safety Resource Allocation Model to Variations in Benefit Computation Parameters. In *Transportation Research Record 1124*, TRB, National Research Council, Washington, D.C., 1987, pp. 58–65.
3. FHWA. *Highway Statistics 1988*. Report FHWA-PL-89-003. U.S. Government Printing Office, Washington, D.C., 1989.
4. T. R. Miller, J. G. Viner, S. Rossman, N. Pindus, W. Gellert, J. Douglass, A. Dillingham, and G. Blomquist. *The Costs of Highway Crashes*. Report FHWA-RD-91-055. The Urban Institute, Washington, D.C., June 1991.
5. *Motor Vehicle Accident Costs*. Technical Advisory T7570.1. FHWA, U.S. Department of Transportation, June 1988.
6. U.S. Office of Management and Budget. *Regulatory Program of the United States*. U.S. Government Printing Office, Washington, D.C., 1989.
7. S. Bali, R. Potts, J. A. Fee, J. I. Taylor, and J. Glennon. *Cost-Effectiveness and Safety of Alternative Roadway Delineation Treatments for Rural Two-Lane Highways*. Report FHWA-RD-78-50. National Technical Information Service, Springfield, Va., April 1978.
8. D. Klinger and R. Kuzmyak. *Personal Travel in the U.S.: 1983–1984 Nationwide Personal Transportation Survey*. National Technical Information Service, Springfield, Va., 1986.
9. T. R. Miller. *The Value of Time and the Benefits of Time-Saving*. The Urban Institute, Washington, D.C., and Transit New Zealand, Wellington, 1989.
10. *Economic Report of the President, Transmitted to the Congress February 1991*. U.S. Government Printing Office, Washington, D.C., 1991.
11. G. A. Aurand, M. B. Turner, C. J. Athey, and R. M. Neulicht. *Reduction of Volatile Organic Compound Emissions from the Application of Traffic Markings*. Midwest Research Institute Report EPA-450/3-88-007. Office of Air Quality Planning and Standards, Environmental Protection Agency, Research Triangle Park, N.C., Aug. 1988.
12. A. J. Krupnick and J. Kurland. *An Analysis of Selected Health Benefits from Reductions in Photochemical Oxidants in the Northeastern United States*. Final Report to Environmental Protection Agency. Resources for the Future, Washington, D.C., Sept. 1988.
13. *Fatal and Injury Accident Rates on Public Roads in the United States*. Report FHWA-SA-90-29. FHWA, U.S. Department of Transportation, June 1990.
14. J. J. Henry, C. A. Antle, and J. L. Carroll. *Service Life and Cost of Pavement Marking Materials*. Unpublished Final Report to NCHRP. The Pennsylvania Transportation Institute, University Park, March 1990.
15. W. E. Hughes, H. W. McGee, S. Hussain, and J. Keegel. *Field Evaluation of Edgeline Widths*. Report FHWA-RD-89-111. National Technical Information Service, Springfield, Va., Dec. 1989.
16. R. W. Attaway and P. O. Adeleke-Sheidun. *Pavement Marking Materials Program*. Report FHWA/NC/89-005. University of North Carolina Institute for Transportation Research and Education, Research Triangle Park, Jan. 1990.
17. A. A. Mendola. *Comparative Study of the Performance and Cost Effectiveness of Large Glass Beads and NJ DOT Standard Glass Beads in Epoxy Traffic Paint*. New Jersey Department of Transportation, Trenton, Sept. 1990.
18. D. C. DePaulo. Ohio Tests Larger Glass Striping Beads. *Better Roads*, April 1990, pp. 42–43.
19. *SASHTO Pavement Marking Information*. Southeastern Association of State Highways and Transportation Officials, July 1991.
20. F. Bitzl et al. *Wirksamkeit von Leiteinrichtungen*. Der Beratater fur Schadenverhutung, Huk-Verband, Cologne, West Germany, 1961.
21. A. J. Basile. Effect of Pavement Markings on Traffic Accidents in Kansas. In *HRB Bulletin 308*, HRB, National Research Council, Washington, D.C., 1962, pp. 80–86.
22. P. R. Macy, N. D. Nedas, and G. P. Balcar. *Road Markings as an Alcohol Countermeasure in Traffic Safety: A Field Test of Standard and Wide Edgelines*. Final Report to FHWA. Potters Industries, Inc., Hasbrouck, N.J., June 1980.
23. J. V. Musick. Effect of Pavement Edge Markings on Two-Lane Rural State Highways in Ohio. In *HRB Bulletin 266*, HRB, National Research Council, Washington, D.C., 1960, pp. 1–7.
24. J. Jackson. Reflectorised Road Markings: Their Contribution to Traffic Safety. *Proc., Symposium on Visual Aspects of Road Markings*, Paris, France, May 1983.
25. *The Road Safety Benefits of Edgelining*. Road Marking Industry Group, United Kingdom, May 1981.
26. J. Jackson and J. Fournier. *The Lorraine Edgelining Study*. Potters-Ballotini, Ltd., South Yorkshire, England, March 1983.

Publication of this paper sponsored by Committee on Coatings, Signing, and Marking Materials.

Roadside Wildflower Meadows: Summary of Benefits and Guidelines to Successful Establishment and Management

JACK AHERN, CINDY ANN NIEDNER, AND ALLEN BARKER

For the past 4 years, research has been conducted to refine the state of knowledge about the establishment and management of herbaceous meadows for highway landscapes in Massachusetts. As alternatives to turfgrass, meadows can provide three principal types of benefits: (a) ecological benefits derived from a more diverse self-sustaining planting without a reliance on agrichemicals and mowing, (b) economic benefits through dramatic reductions in mowing, and (c) aesthetic improvements resulting from a diverse planting of indigenous flowers and grasses. A split-block replicate experimental planting was installed in 1989 to test the effects of three tillage treatments, three fertilizer treatments, and two postemergent herbicide treatments. Two years of field observations on species diversity and plant density found that tilling permitted better establishment of wildflowers than not tilling; preemergent treatments showed a significant decrease in invasive grasses and an increase in wildflowers; fertilization did not improve the growth of wildflowers, grasses, or broadleaved weeds; and the monocot-specific herbicide was effective in controlling invasive grasses. The research documented that the primary obstacle to successful wildflower establishment is the spread of opportunistic turf-forming grasses and broadleaved weeds. This experiment has led to revised site preparation and establishment specifications to help maintain successful, self-sustaining meadows for highway landscapes.

Wildflower meadows enhance the aesthetic and ecological value of the landscape and reduce the time, money, and resources spent on conventionally mowed turfgrass areas (*1*). Highway meadows provide seasonal color changes along roadsides and expose surrounding vistas. Meadows of native vegetation also provide habitat and food for wildlife. Once the wildflower meadow becomes a well-established plant community, it is less susceptible to weed invasions and less in need of maintenance (*2,3*). However, proper site-preparation and management techniques are essential to establishing a stable plant community and aesthetic wildflower meadow planting. Proper site preparation will permit the establishment of wildflowers while reducing undesirable opportunistic grasses and weeds. Opportunistic grasses are defined as turf-forming species (fescues, bluegrasses, perennial ryes) that successfully invade and displace desirable wildflowers and clump-forming grasses (bluestem, side-oats grama, Indian grass, switch grass). Weeds are defined as annual or perennial forbs that exhibit undesirable invasive behavior (spotted knapweed, some goldenrods), that are noxious or allergenic (ragweed, nettle), or that are visually unacceptable (burdock, dock). Proper management can sustain a desirable species mix and an attractive appearance.

J. Ahern, C. A. Niedner, Department of Landscape Architecture and Regional Planning, 109 Hills North, University of Massachusetts, Amherst, Mass. 01003. A. Barker, Department of Plant and Soil Sciences, Bowditch Hall, University of Massachusetts, Amherst, Mass. 01003.

BENEFITS OF WILDFLOWER MEADOWS

The principal advantages of wildflower meadows are ecological, economic, and aesthetic. The extent to which these benefits are achieved depends on many factors, including species selection, planting site location, establishment cost and success, and management. The following sections will elaborate on these potential benefits.

Ecological Benefits

The value of maintaining a diversity of habitat types has long been recognized as being important to environmental health and quality. The plant community is substantially more diverse when highway rights-of-way are managed as meadows than they are when managed as turfgrass landscapes. In addition, highway meadows may provide habitat for wildlife and insects. These meadows may provide a vegetational buffer between the highway and the adjacent forest—a common landscape context for highways in New England. If implemented on a large scale, highway meadows can provide a network of linked corridors that supports a diversity of plant and animal life.

Another form of ecological benefit is the reduced environmental effects of maintaining highway meadows when compared with maintaining turfgrasses. The management of turfed highway rights-of-way affects water quality because pesticides, oil, gasoline, lead, and sediments are contributed to the runoff (*4*). Wildflower meadow maintenance does not entail using pesticides, so this form of pollution can be reduced or eliminated. Other pollutants can be reduced by the wildflowers themselves, which trap and filter airborne pollutants on their leaves and stems. The efficiency of this pollutant trapping increases directly in proportion to a plant's total surface area (*5*). Thus, a growth of wildflowers 2 to 3 ft high will be more efficient at trapping pollutants than a growth of turfgrasses 6 in. high. Furthermore, once these pollutants are trapped by the vegetation, they are more likely to leach into the soil than to run off into surface waters. This is because there is less runoff with wildflower vegetation than with turf

(*6*). Because soil is an effective sink for these pollutants, water quality can be improved substantially.

Economic Benefits

The primary and most obvious economic benefit of managing a highway with meadows is the reduction in mowing requirements. Turfgrasses require 6 to 20 mowings a year (depending on the weather and desired appearance), but typical roadside meadows need only one mowing a year. In Massachusetts the Department of Public Works manages roughly 3,300 acres of roadside turf at a 1987 cost of approximately $1.1 million, or $337/acre, for six mowings (Evans, unpublished data, 1987). It can then be assumed that for every acre managed as wildflowers, a cost savings of 83 percent, or $280/acre/year, can be realized. The actual figure may vary considerably when wildflowers are planted in small areas where the time and effort to mow around them eliminates any cost savings; this is an important consideration in planning and designing highway wildflower meadows.

Aesthetic Benefits

Wildflowers are often praised for their aesthetic benefits, which include increased color, more interesting textures, and greater awareness of seasonal change. Research on environmental preference has found that although nature is often considered synonymous with the open landscape (such as a highway right-of-way), these wide, open spaces are not universally preferred (*7*). In fact, scenes that lack particular characteristics of spatial definition tend to be disliked. Only when these areas include elements that help to differentiate the openness, such as groupings of trees and shrubs, are they preferred. These landscapes, often described as being like parks or savannah, have invoked high preference in a number of studies. This suggests that to make highway landscapes more aesthetically appealing, elements that articulate and differentiate the highway's visual space should be incorporated. Wildflowers and masses of native woody plants are a means of achieving this vegetative diversity while attaining the ecological and economic benefits discussed earlier. Wildflower meadows are increasingly used as transitions between formally maintained landscapes and relatively unmanaged areas, even in urban contexts (*8*).

WILDFLOWER ESTABLISHMENT

There are many opinions about what constitutes appropriate site-preparation and management techniques and about which of these techniques are the most cost-effective (*1–3,9–12*). Interested in developing locally relevant procedures, the Massachusetts Department of Public Works commissioned a study to determine the effects of tillage, fertilizer, and herbicide preparation techniques on the growth and establishment of a wildflower meadow planting. This study has given the department suggestions for cost-effective and successful preparation techniques for roadside wildflower meadows. Following is a discussion of the results from the second season of the wildflower meadow establishment in this experiment. The results from the first year were reported by Barker and Ahern (unpublished data).

Research Procedure

Site Description

The site selected for this study was a parcel of land in the right-of-way of State Route 116 at the intersection of Sunderland Road in Amherst, Massachusetts. Within this site a study area 45 × 300 ft was staked out (Figure 1). The study area was approximately 100 ft from Route 116 and 50 ft from the tree line on the south end of the site. The study area was divided into four blocks, each 45 × 75 ft, to allow for replication of treatments. Each block was further divided into nine plots, which received a different preparation treatment. The nine preparation treatments consisted of three tillage treatments combined with three fertilizer treatments. Each of these preparation treatments occurred once in a random position in each of the four blocks, yielding four replicates of each of nine preparation techniques. Randomizing the treatment position ensured that location in the study area did not influence growth and establishment trends. Each plot was further divided into two equal subplots and received one of two postemergent herbicide treatments. Plant density data was collected in 1-m^2 quadrants at random locations within each of the subplots.

Wildflower Seed Installation

The seed mix and seed rate used were the standards used by the Massachusetts Department of Public Works for all wildflower plantings done statewide in 1989. Wildflower seeds were installed with a wildflower seed drill capable of high precision in seed dispersal and planting depth. All plots were seeded on June 29, 1989. Species and seed rates are shown in Table 1.

Fertilizer Treatments

Fertilizers are commonly recommended in the establishment of lawns and tree and shrub plantings. Wildflower planting guidebooks either are silent on the topic or recommend against it (*1–3,9,10*). These recommendations are rarely referenced to empirical studies. In the interest of challenging these recommendations, this study included three fertilizer treatments that were broadcast by hand and watered immediately after application.

Unfertilized No fertilizer was applied.

Urea A nitrogen-only fertilizer was applied. The urea was applied at a rate of 1.75 lb/1,000 ft^2 (75 lb/acre) of nitrogen. The urea was applied on June 30, 1989.

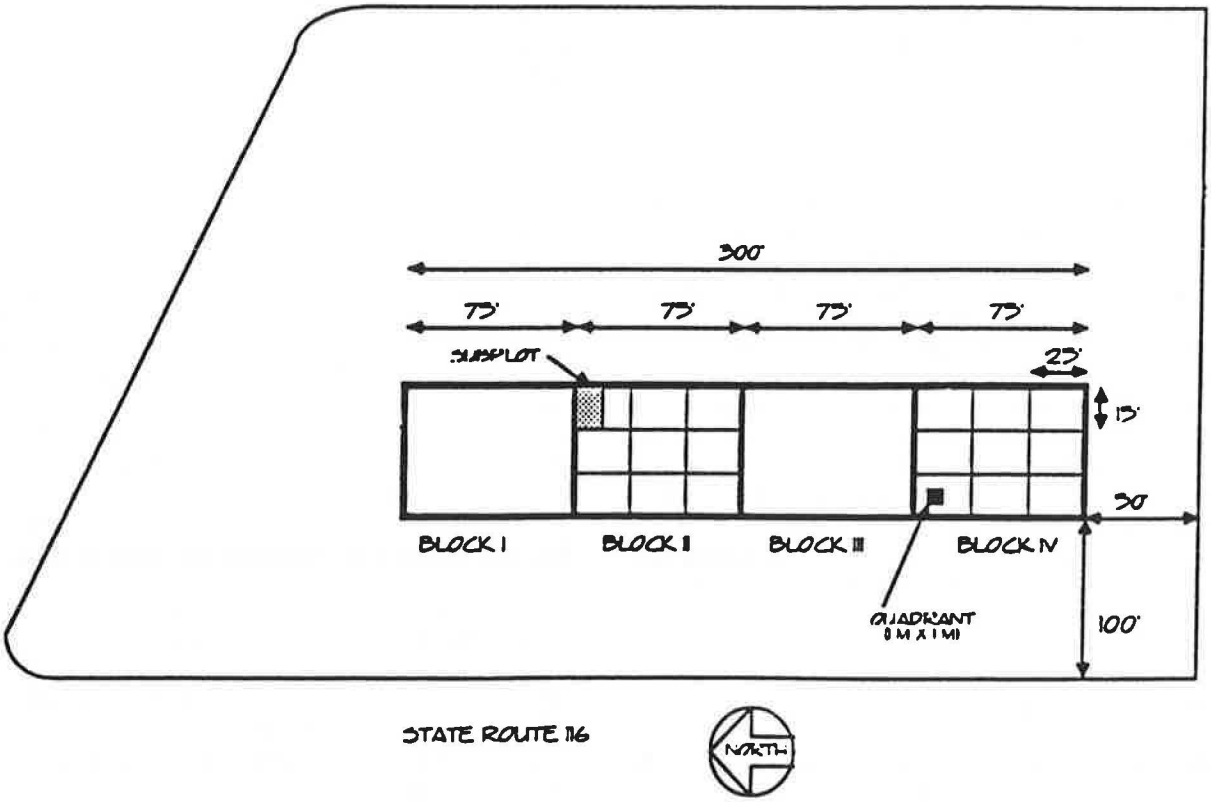

FIGURE 1 Arrangement of site.

TABLE 1 WILDFLOWER SEED MIX AND SEEDING RATES (SEED INSTALLATION: JUNE 29, 1989)

	Rate (lb/acre)
Annuals	
Baby's breath (*Gypsophilia elegans*)	0.56
Chinese houses (*Collinsia heterophylla*)	0.24
Perennials and Biennials	
Yarrow (*Achillea millefolium*)	0.56
New England aster (*Aster novae-angliae*)	0.22
Oxeye daisy (*Chrysanthemum leucanthemum*)	1.48
Coreopsis (*Coreopsis lanceolata*)	1.48
Queen Anne's lace (*Daucus carota*)	0.89
Dame's rocket (*Hesperis matronalis*)	0.92
Chicory (*Cichorium intybus*)	0.93
Black-eyed Susan (*Rudbeckia hirta*)	1.11
Showy goldenrod (*Solidago speciosa*)	0.09
Yellow coneflower (*Ratibida pinnata*)	0.31
Purple coneflower (*Echinacea purpurea*)	0.56
Total seed	9.35

10-10-10 Fertilizer A 10-10-10 fertilizer was applied at a rate of 1.75 lb/1,000 ft^2 (75 lb/acre) of nitrogen, 0.75 lb/1,000 ft^2 (30 lb/acre) of phosphorus, and 1.45 lb/1,000 ft^2 (60 lb/acre) of potassium. The 10-10-10 fertilizer was applied on June 30, 1989.

Tillage Treatments

Three tillage treatments were tested to evaluate a wide range of potential site-preparation techniques. Site preparation is one of the more expensive parts of wildflower establishment, so it has the potential for cost savings if labor can be reduced. In addition, the Massachusetts Department of Public Works was interested in developing planting methods that could be implemented by its staff rather than by outside contractors.

No Till The existing vegetation was killed with glyphosphate (Round-Up) applied at 1 oz active ingredient/100 ft^2 (2.5 lb/acre). After about 2 weeks the treated area was mowed. This treatment involved the least expense in terms of labor, equipment hours, and material cost. The initial treatment occurred on May 26, 1989.

Tilled Only The plots were cultivated with two passes of a tractor-mounted rototiller and then York-raked. Plant debris was raked and removed from the site. The tilling was performed on May 31, 1989.

Tilled Followed with Preemergent Herbicide The plots were cultivated with two passes of a tractor-mounted rototiller and then York-raked. Plant debris was raked and removed from the site. A preemergent herbicide, Diphenamid (Enide 90W), was applied over the germinating seedlings. The herbicide was applied at 2.6 oz active ingredient/1,000 ft^2 (6.6 lb/acre). To prevent any detrimental effect on wildflower establishment, the Diphenamid was applied when the wildflower seedlings had an average of three true leaves. This treatment is the most expensive in terms of labor, equipment hours, and materials. The tilling was performed on May 31, 1989, the seeding was done on June 29, 1989, and the herbicide was applied on July 28, 1989.

Postemergent Herbicide Treatment

Half of each plot (subplot) was treated with the postemergent herbicide Fluazifop-butyl (Fusilade 4E), which is known to be monocot-specific. The other half of each plot was left untreated. This was done to determine the effect of reducing invasive grasses on the establishment of the desired wildflowers. Wildflower meadows often contain grasses, but many times turf-forming species are overly aggressive in the meadow (*13*).

Fluazifop-Butyl (Fusilade 4E) The Fusilade was applied at the rate of .02 oz active ingredient/1,000 ft^2 (0.5 lb/acre). The Fusilade was applied on August 4, 1989.

No Fusilade Herbicide was not applied to the adjacent subplot.

Treatment Position

Each one of 18 combinations of treatments within each block was numbered (Figure 2). These treatments were in a random position in each of the four blocks (Figure 3).

Data Collection

First Year (1989) The chronology of treatment dates was important to the collection of data in the first year, because treatments were performed concurrently with data collection. When the July data were collected, the study site had not been treated with the postemergent herbicide, Fluazifop-butyl (Fusilade), or the preemergent herbicide, Diphenamid (Enide). Quadrants 1 m^2 were sampled on July 11 and 18 and on

1: TILLED & NO FERTILIZER & NO FUSILADE
1A: TILLED & NO FERTILIZER & FUSILADE
2: TILLED & 10-10-10 & NO FUSILADE
2A: TILLED & 10-10-10 & FUSILADE
3: TILLED & UREA & NO FUSILADE
3A: TILLED & UREA & FUSILADE
4: TILLED/HERBICIDE & NO FERTILIZER & NO FUSILADE
4A: TILLED/HERBICIDE & NO FERTILIZER & FUSILADE
5: TILLED/HERBICIDE & 10-10-10 & NO FUSILADE
5A: TILLED/HERBICIDE & 10-10-10 & FUSILADE
6: TILLED/HERBICIDE & UREA & NO FUSILADE
6A: TILLED/HERBICIDE & UREA & FUSILADE
7: NO TILL & NO FERTILIZER & NO FUSILADE
7A: NO TILL & NO FERTILIZER & FUSILADE
8: NO TILL & 10-10-10 & NO FUSILADE
8A: NO TILL & 10-10-10 & FUSILADE
9: NO TILL & UREA & NO FUSILADE
9A: NO TILL & UREA & FUSILADE

FIGURE 2 Numbering of treatment combinations.

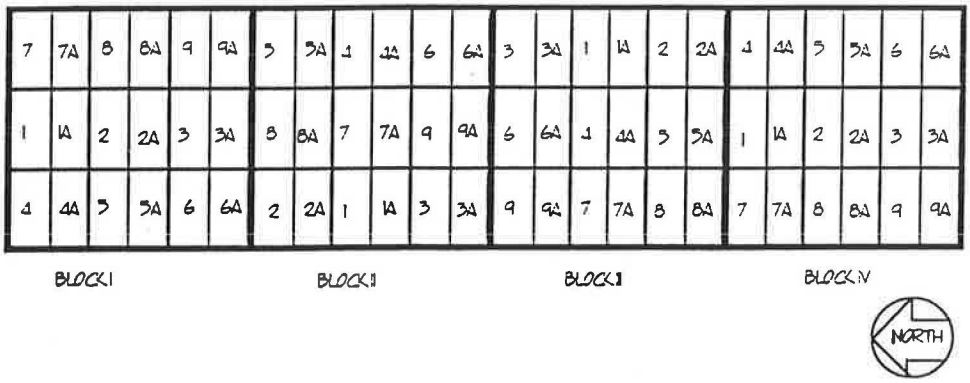

FIGURE 3 Arrangement of treatment subplots in study area.

August 1, 22, 23, and 24. Information about densities and maximum height of wildflower seedlings, broadleaved weeds, and grasses present were recorded. Wildflowers were considered to be those plants that occurred in the seed mix used by the Massachusetts Department of Public Works in 1989 (see Table 1). Grass weeds were considered to be monocots including opportunistic grasses, sedges, and rushes. Broadleaved weeds were considered to be dicot plants that were not part of the wildflower seed mix.

Second Year (1990) Between the first and second years of data collection the site was not mowed. No new treatments to the study area were performed during the second year. Data measurements were recorded the last weeks of June, July, and August. Data from a random sampling of a 1-m^2 quadrant within each subplot were recorded for each month (Figure 4). For each of the species of wildflowers that were seeded, the number present in each quadrant was recorded. The total number of grasses and broadleaved weeds present, the type of broadleaved weeds present, and the maximum height of wildflower plants, broadleaved weeds, and grasses were also recorded.

RESULTS

The results from the first year of data collection have been reported (Barker and Ahern, unpublished data). The data from the second year of collection were averaged across the replicates for each month. The effects of fertilizer, Fusilade, and tillage are summarized.

Fertilizer Effects

There was no significant difference between wildflower populations in untreated quadrants and those in quadrants treated with urea or 10-10-10 fertilizer (Table 2). The number of grasses and broadleaved weeds in the quadrants did not demonstrate an increase or decline with respect to fertilizer treatment (Tables 3 and 4). This finding supports the recommendations often made by the wildflower seed industry that fertilizers are not necessary in new wildflower establishment.

Fusilade Effects

There was a significant increase in the wildflower plants in the subplots treated with Fusilade (Table 2). The subplots treated with Fusilade had far fewer grasses (Table 3). This was particularly notable in August, when the number of grasses in the subplots not treated with Fusilade reached the highest densities recorded over this study.

This finding is important because highway wildflower meadows are often planted in a matrix of turfgrasses. These turfgrasses have been observed to be invasive in Massachusetts wildflower meadows, particularly during the establishment period: the first 2 years after planting (Ahern, unpublished data). Fusilade has been shown to control invasive turf-forming

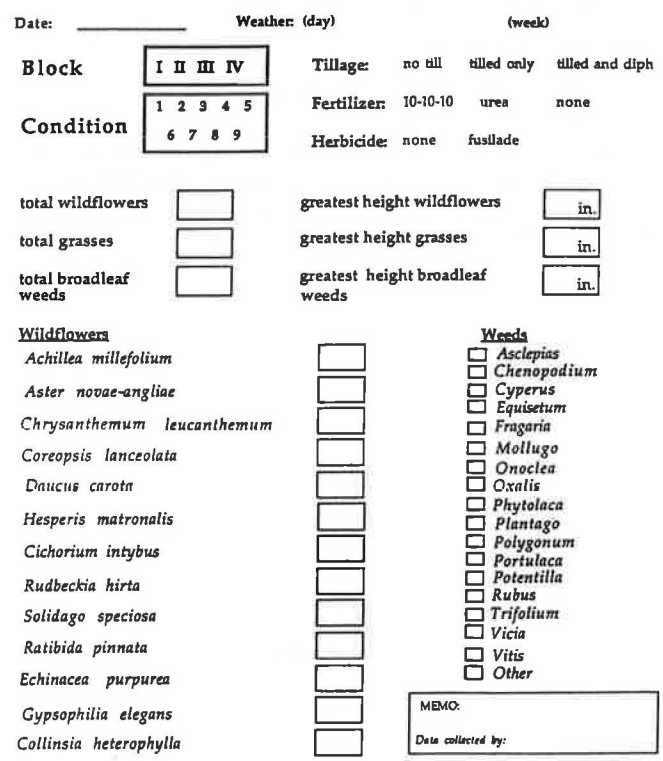

FIGURE 4 Data collection format.

TABLE 2 WILDFLOWER POPULATION DENSITIES PER SQUARE METER AVERAGED ACROSS JUNE, JULY, AND AUGUST 1990

NO FUSILADE	NO FERT	10-10-10	UREA	AVERAGE
TILL	90	66	59	72
TILL/HERB	98	111	66	92
NO TILL	56	87	109	84
AVERAGE	81	88	78	82
FUSILADE				
TILL	95	87	80	87
TILL/HERB	99	76	73	83
NO TILL	94	99	147	113
AVERAGE	96	87	100	94

STATISTICS (LSD 0.05)

FUSILADE = 6
FERTILIZERS = NS
TILLAGE = NS
ALL INTERACTIONS = NS

TABLE 4 BROADLEAVED WEED POPULATION DENSITIES PER SQUARE METER AVERAGED ACROSS JUNE, JULY, AND AUGUST 1990

NO FUSILADE	NO FERT	10-10-10	UREA	AVERAGE
TILL	96	87	89	89
TILL/HERB	110	75	83	89
NO TILL	58	27	44	43
AVERAGE	88	63	71	74
FUSILADE				
TILL	121	122	99	114
TILL/HERB	113	108	78	100
NO TILL	93	62	66	74
AVERAGE	109	97	81	96

STATISTICS (LSD 0.05)

FUSILADE ($p \leq 0.10$) = 20
FERTILIZERS = NS
TILLAGE = 15
ALL INTERACTIONS = NS

grasses, but it will also reduce the noninvasive grasses that are recommended for wildflower meadows.

Tillage Effects

Wildflower performance was less vigorous in the no-till treatment (Table 2). The tilled-only treatment and the tilled-followed-by-preemergent-herbicide treatment showed similar numbers of wildflowers present. In the no-till treatment there were many more grasses in subplots that were and that were not treated with Fusilade (Table 3). There were fewer grasses in the subplots that were tilled then treated with preemergent herbicide, particularly when it interacted with the postemergent herbicide Fusilade.

TABLE 3 GRASS POPULATION DENSITIES PER SQUARE METER AVERAGED ACROSS JUNE, JULY, AND AUGUST 1990

NO FUSILADE	NO FERT	10-10-10	UREA	AVERAGE
TILL	114	124	115	118
TILL/HERB	65	70	63	65
NO TILL	148	200	92	147
AVERAGE	109	131	90	110
FUSILADE				
TILL	27	23	33	28
TILL/HERB	17	20	21	19
NO TILL	53	26	40	40
AVERAGE	32	23	31	29

STATISTICS (LSD 0.05)

FUSILADE (H) = 32
FERTILIZERS (F) = NS
TILLAGE = (T) = 29

H X F = 26
H X T = 30
F X T = 26
H X F X T = 37

MANAGEMENT

Once a wildflower meadow has been successfully established, management is relatively straightforward. Most species in the meadows are annuals or perennials with life expectancies of one to several years. They all can reproduce through vegetative growth or seed germination. The meadow can thus be seen as a constantly changing mosaic of herbaceous forbs and grasses. If a highway meadow in New England is not maintained, however, it is likely to succeed to an old field or young forest in 5 to 10 years. To prevent this natural tendency, interventions are needed to stabilize the meadow community and arrest succession. There are three principal ways of achieving this stabilization: mowing, grazing, and burning. Only mowing is considered appropriate in most highway applications, but grazing and burning are worth consideration (*14*).

Mowing selectively favors herbaceous plants over woody species, because woody plants invest more in producing aboveground biomass that is easily removed by mowing. The timing of mowing can be controlled to determine which species will persist in a meadow (*15*). Mowing plants just before the flowers mature will often exhaust their stored energy and prevent them from setting seed. This technique can be used to control invasive species such as Canadian goldenrod (*Solidago canadensis*). The management objective in highway meadow maintenance is usually achieved by an annual mowing. The optimal time to mow is late fall after the seeds have matured; delaying until early spring produces the same control but provides a standing dormant cover for visual interest throughout winter.

Managing the edges of highway meadows presents challenges of a different kind. The matrix of turfgrass that typically surrounds meadows is usually mowed six times a year. Over the course of the growing season, an unnaturally abrupt mowed edge is produced that often dominates the view of the meadow from the highway (Figure 5). In Massachusetts an alternative

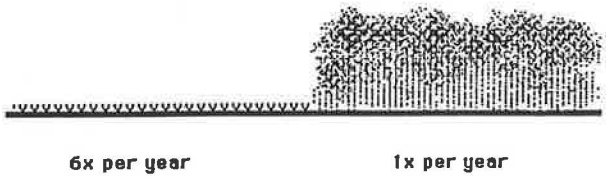

FIGURE 5 Present mowing scheme.

stepped mowing scheme has been designed to resolve this problem. Under this method, each time the turf is cut the mow-line is sequentially moved away from the meadow, producing a stepped or graded edge by the end of the season (Figure 6). This method has been found to be an effective way to allow existing wildflower plantings to increase incrementally in size without any additional cost or effort. It is particularly suited to median applications where wildflower meadows are highly visible from both directions and where mowing is often more dangerous (Figure 7).

CONCLUSIONS

Preparation of the soil by tilling permitted better performance and seedling establishment of wildflower plants than the treatments in which tilling was not used. This enhanced performance of wildflowers in tilled plots was due in part to the reduced number of grasses in these plots. Wildflower growth and establishment was more successful when the competition for light, space, water, and nutrients from invasive grasses was reduced. This competition is further evidenced by the comparison between the subplots that were treated with Fusilade and the subplots that were not. The Fusilade subplots showed a significant decrease in the number of grasses and an increase in the number of wildflowers across all tillage treatments. Wildflower establishment was most successful in the treatments, tilled and Fusilade-treated, in which the numbers of grasses were reduced.

Fertilization did not appear to improve the growth of wildflowers, grasses, or broadleaved weeds. This is not surprising, because the fertilizer treatments had been applied more than a year earlier and their effect had probably diminished. However, it appears that the plots that were not fertilized had more wildflowers. Weeds are opportunistic species that can use sudden influxes of nutrients, water, and light. The application of fertilizer to the meadow during the first year was more effective in aiding the establishment of broadleaved weeds and invasive grasses.

The presence of grasses was an important factor in the attractiveness of the wildflower site. In June, when the oxeye daisies (*Chrysanthemum leucanthemum*) were in full bloom,

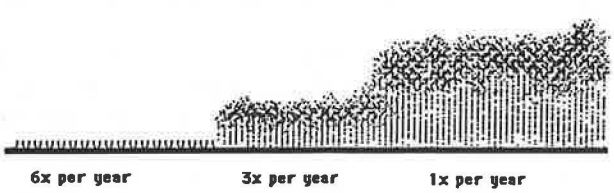

FIGURE 6 Alternative mowing scheme.

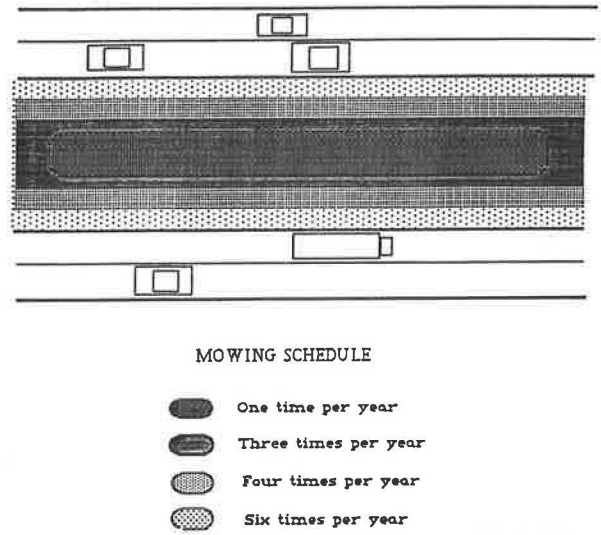

FIGURE 7 Alternative mowing scheme for median wildflower meadow.

the grasses were shorter than the wildflowers and did not interfere with their display. By August the grasses had reached 3 to 4 ft, thus obscuring the bloom of the black-eyed Susans (*Rudbeckia hirta*) and the purple coneflowers (*Echinacea purpurea*). It appears that it is necessary to control the growth of opportunistic grasses or to encourage shorter clump-forming native grasses to produce an attractive wildflower site. Using a postemergent herbicide such as Fusilade and preparing the site by tilling are effective means for controlling grasses.

These conclusions are useful for modifying future wildflower planting and establishment procedures used by the Massachusetts Department of Public Works. Starting with the plantings done in 1990, the seed mix was expanded to include four species of native grasses in the interest of establishing a more stable herbaceous plant community. As this research has documented, the primary obstacle to successful wildflower establishment is the spread of opportunistic grasses and broadleaved weeds.

The stepped-edge mowing method maintains a more attractive visible edge and can be applied to allow meadows to expand and create a more attractive visible edge. More recent research initiated in 1990 involved establishing no-mow zones to evaluate the potential for native herbaceous vegetation to become reestablished in existing turfed areas without any cultivation or supplemental planting. These natural revegetation areas are located in highly visible locations in public rights-of-way and marked with large signs to provoke public response—which has been overwhelmingly positive. The edges of mowed areas were modified to complement the topography and visual context of the highway. The success of this program is causing fundamental landscape management policies in highway rights-of-way to be reconsidered in hopes of increasing the benefits of wildflower meadows.

ACKNOWLEDGMENTS

The authors wish to express their gratitude for the support of this research by Commissioner Jane Garvey and Associate

Commissioner Esther H. Francis of the Massachusetts Department of Public Works. Research assistants also involved with the project are Douglas Evans, Donna Butz, Betsy Corner, Michelle Hiltzik, Sara Donald, and Barbara Wilson; thanks to all of them for their excellent work and tremendous enthusiasm for the project.

REFERENCES

1. J. Ahern. The Establishment and Maintenance of Wildflowers and Native Woody Plants in the Highway Landscape. *Proc., 4th Symposium on Environmental Concerns in Right-of-Way Management* (R. W. Byrnes and H. Holt, eds.), Purdue University, West Lafayette, Ind., 1988. pp. 99–104.
2. National Wildflower Research Center. *Wildflower Handbook*. Texas Monthly Press, Austin, 1989.
3. L. C. Martin. *The Wildflower Meadow Book*. Fast and McMillan, Charlotte, N.C., 1986.
4. J. G. Fabos. *Land Use Planning: From Global to Local Challenge*. Chapman and Hall, New York, N.Y., 1985.
5. A. W. Spirn. *The Granite Garden*. Basic Books, New York, N.Y., 1984.
6. L. B. Leopold and T. Dunne. *Water in Environmental Planning*. W. H. Freeman and Company, New York, N.Y., 1978.
7. R. Kaplan. Dominant and Variant Values in Environmental Preference. *Proc., Symposium on Environmental Preference and Landscape Maintenance*, New London, Conn., Oct. 1983. pp. 8–11.
8. E. L. Blake, Jr. Translating the Beauty: Idealized Nature in an Urban Context. *Wildflower*, Vol. 3, No. 1, 1990, pp. 14–23.
9. J. Ahern. Preparation and Establishment Techniques for Meadow Gardens. *Meadows and Meadow Gardening*, Vol. 5, No. 1, 1990, pp. 14–20.
10. H. W. Art. *The Wildflower Gardener's Guide*. Storey Communications, Inc., Pownal, Vt., 1987.
11. W. E. Brumback and D. R. Longland. *Garden in the Woods: Cultivation Guide*. New England Wildflower Society, Framingham, Mass., 1986.
12. H. R. Phillips. *Growing and Propagating Wildflowers*. University of North Carolina Press, Chapel Hill, 1985.
13. D. R. Longland. Lawns, Meadows or Both? *Wild Flower Notes*, Vol. 1, 1985, pp. 11–18.
14. B. Andersen. Using Prescribed Burns as a Prairie Management Tool. *Wildflower*, Vol. 3, No. 2, 1990, pp. 27–33.
15. B. H. Emerson. Meadow Management. *Meadows and Meadow Gardening*, Vol. 5, No. 1, 1990, pp. 29–32.

Publication of this paper sponsored by Committee on Roadside Maintenance.